

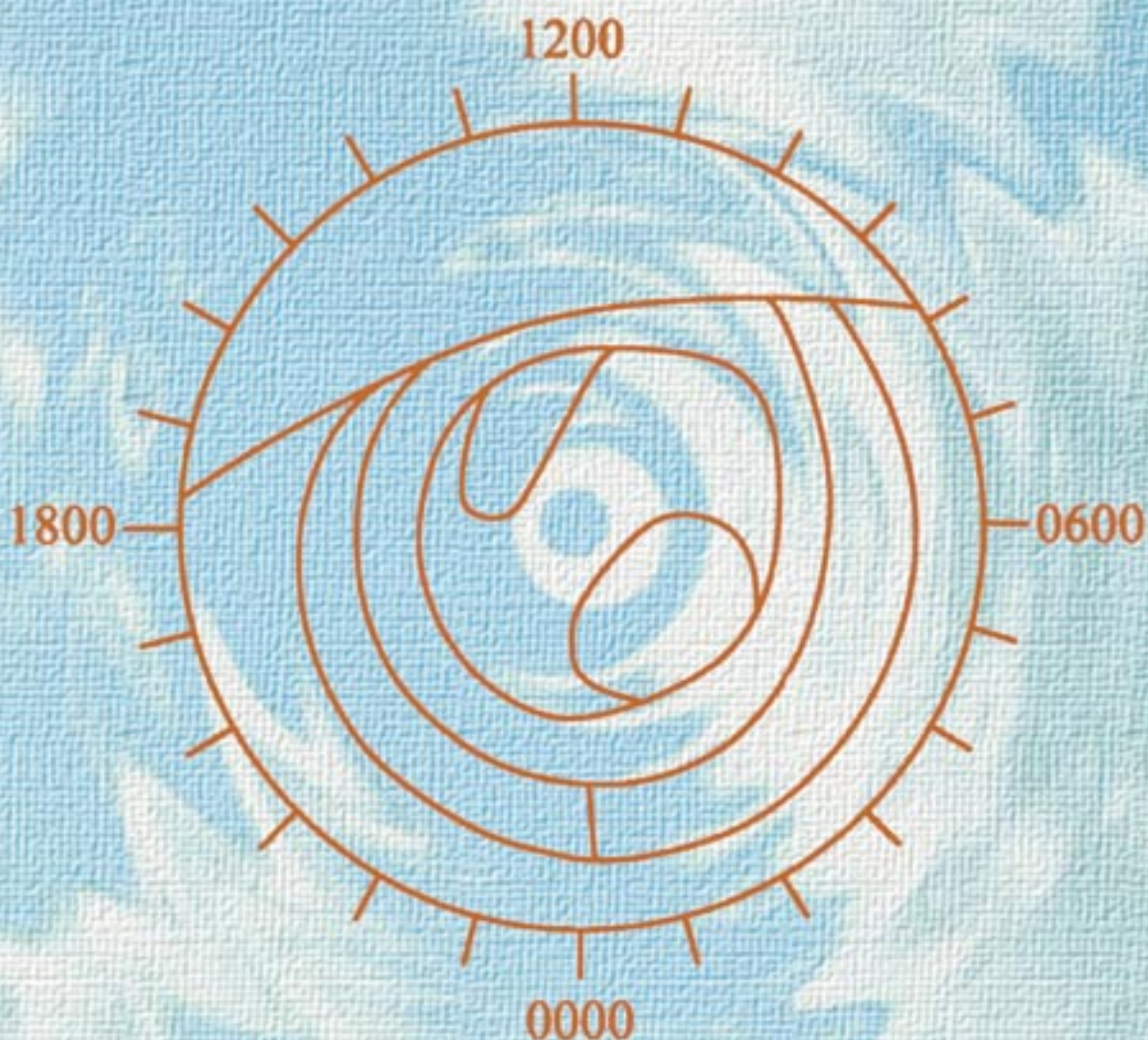


INTERNATIONAL TELECOMMUNICATION UNION

HANDBOOK

THE IONOSPHERE AND ITS EFFECTS ON RADIOWAVE PROPAGATION

A guide with background to ITU-R procedures
for radioplanners and users



1998

Radiocommunication Bureau

HANDBOOK

THE IONOSPHERE AND ITS EFFECTS ON RADIOWAVE PROPAGATION

A guide with background to ITU-R procedures for radio
planners and users

CONTENTS

	Page
CHAPTER 1 - INTRODUCTION	1
1.1 RELATIONSHIP OF THIS HANDBOOK TO ITU-R RECOMMENDATIONS	1
1.2 APPLICATION OF THE HANDBOOK.....	1
CHAPTER 2 - IONOSPHERIC PROPERTIES	3
2.1 THE IONOSPHERE.....	3
2.2 IONOSPHERIC PROFILES AND STRUCTURAL FEATURES.....	4
2.2.1 Physical processes of the ionosphere.....	4
2.2.1.1 Ionization production and loss.....	4
2.2.1.2 Electron collision frequency.....	5
2.2.2 D region (50-90 km).....	5
2.2.3 E region (90-130 km).....	5
2.2.4 Sporadic E (Es).....	5
2.2.4.1 Mid-latitude Es.....	5
2.2.4.2 Equatorial Es.....	6
2.2.4.3 Auroral Es.....	6
2.2.5 F region (130-500 km).....	6
2.2.6 F region irregularities (Spread F).....	7
2.2.7 Topside ionosphere.....	7
2.3 GEOGRAPHICAL FEATURES.....	8
2.3.1 Ionospheric control points.....	8
2.3.2 High latitudes.....	8
2.3.2.1 Relationship to magnetic and solar activity.....	10
2.3.2.2 The auroral oval.....	10
2.3.2.3 The outer precipitation zone.....	13
2.3.2.4 Storms and substorms.....	14
2.3.2.5 Ionization increases after geomagnetic storms (the post-storm effect).....	14

	Page
2.3.2.6 Polar cap events	15
2.3.2.7 High-latitude trough.....	15
2.3.2.8 High latitude irregularities	16
2.3.2.9 High-latitude F region.....	16
2.3.3 Mid-latitudes	16
2.3.4 Equatorial latitudes	17
2.3.4.1 Equatorial anomaly	17
2.3.4.2 Equatorial irregularities	19
2.4 SOLAR CYCLE EFFECTS ON PROPAGATION.....	20
2.4.1 Solar cycle.....	20
2.4.2 Annual cycle	20
2.4.3 Diurnal cycle.....	20
2.5 MODELLING OF IONOSPHERIC PROPERTIES.....	20
2.5.1 Empirical models	20
2.5.2 Physical models	21
2.5.3 Hybrid models	22
2.6 IONOSPHERIC VARIABILITY AND DISTURBANCES	22
2.6.1 Solar-induced disturbances	22
2.6.1.1 Ionospheric storms.....	24
2.6.1.2 Sudden ionospheric disturbances (SIDs).....	24
2.6.2 Disturbances of atmospheric origin	25
2.6.2.1 Winter variability of D-region ionization	25
2.6.2.2 Travelling ionospheric disturbances (TIDs)	25
References for Chapter 2	26
Bibliography	28
CHAPTER 3 - IONOSPHERIC PROPAGATION	29
3.1 WAVEGUIDE PROPAGATION.....	30
3.2 SKY-WAVE PROPAGATION.....	30
3.3 TRANS-IONOSPHERIC PROPAGATION	31
Bibliography	31

CHAPTER 4 - PROPAGATION AT VERY LOW FREQUENCIES BELOW ABOUT 500 kHz	33
4.1 ELF, VLF AND LF PROPAGATION	33
4.2 PROPAGATION CHARACTERISTICS.....	34
4.2.1 The waveguide mode propagation of VLF waves to great distances	34
4.2.2 Normal diurnal variations of phase and amplitude at middle and low latitudes	35
4.2.3 Phase stability	36
4.2.4 Fading of the waves	38
4.2.4.1 Daytime fading	38
4.2.4.2 Night-time fading.....	38
4.2.5 Variations during ionospheric disturbances.....	39
4.2.5.1 Sudden ionospheric Disturbance (SID's) associated with solar X-ray events.....	39
4.2.6 High latitudes	40
4.3 CALCULATING FIELD STRENGTH: EARLY APPROACHES	40
4.4 ITU-R METHOD OF CALCULATING FIELD STRENGTH AT VLF AND LF....	43
4.4.1 The Wave-Hop method.....	44
4.4.2 The Waveguide Mode method.....	44
4.5 RELIABILITY OF THE WAVE-HOP METHOD	44
References for Chapter 4	46
CHAPTER 5 - PROPAGATION AT FREQUENCIES BETWEEN 150 kHz AND 1 700 kHz	49
5.1 FIELD STRENGTH MEASUREMENTS AND ANALYSIS	49
5.1.1 Field strengths at distances of less than 300 km.....	49
5.1.2 Field strengths at distances between 300 and 3 500 km.....	49
5.1.2.1 Region 1	49
5.1.2.2 Region 2.....	50
5.1.2.3 Region 3.....	50
5.1.3 Field strengths at distances greater than 3 500 km	50

5.2	VARIATIONS OF FIELD STRENGTHS AND FACTORS AFFECTING PROPAGATION.....	50
5.2.1	Fading rate	50
5.2.2	Amplitude distribution	50
5.2.3	Diurnal variations.....	51
5.2.4	Variation with season.....	51
	5.2.4.1 LF band	51
	5.2.4.2 MF band.....	51
5.2.5	Variation with solar and magnetic activity	53
5.2.6	Influence of the ground on radiation towards the ionosphere.....	53
5.2.7	Excess polarization coupling loss, L_p	56
5.2.8	Field strengths exceeded for different percentages of time	58
5.3	DISCUSSION ON PREDICTION METHODS	59
5.3.1	Sky-wave prediction methods in use at LF and MF	59
5.3.2	Comparison of predicted field strengths with measured data.....	60
	5.3.2.1 Region 1	60
	5.3.2.2 Region 2.....	60
	5.3.2.3 Asia	60
5.3.3	Comparison of prediction methods	61
	5.3.3.1 The Cairo North-South curve.....	61
	5.3.3.2 Region 2 method	61
	5.3.3.3 Recommendation ITU-R P.1147.....	61
	5.3.3.4 Modified FCC method	62
5.4	LF/MF SKYWAVE PROPAGATION AT DAYTIME	62
5.4.1	Seasonal variation	62
5.4.2	Effects of latitude	62
5.4.3	Effects of solar activity	62
5.4.4	Statistical distribution of field strengths	62
5.4.5	Daytime sky-wave field strength and interference levels.....	63
	5.4.5.1 MF annual median value.....	63
	5.4.5.2 MF upper decile value	63
	5.4.5.3 MF top-percentile value.....	63
	5.4.5.4 LF cases	63
	References for Chapter 5	64

CHAPTER 6 - HF PROPAGATION	67
6.1 HF CIRCUIT DESIGN.....	67
6.2 REQUIREMENT FOR PREDICTIONS	68
6.3 DEVELOPMENT OF PREDICTION TECHNIQUES.....	68
6.4 NOISE AND INTERFERENCE	69
6.5 VARIATIONS OF FIELD STRENGTH AND PROPAGATION FEATURES.....	70
6.5.1 HF signal characteristics - multipath	70
6.5.1.1 Time delay	71
6.5.1.2 Amplitude fading	71
6.5.2 Absorption.....	72
6.5.3 Fading	72
6.5.3.1 Causes of fading.....	72
6.5.3.2 Characteristics of amplitude fading	73
6.5.3.3 Fading allowances for service planning	74
6.5.4 Regional anomalies	75
6.5.4.1 Features of fading encountered in the Tropical Zone.....	75
6.5.4.2 High latitude effects.....	76
6.6 RELIABILITY OF HF RADIO SYSTEMS.....	77
6.6.1 Basic circuit, reception and service reliability (BCR, BRR, BSR).....	77
6.6.2 Overall circuit, reception and service reliability (OCR, ORR, OSR).....	77
6.6.3 Basic path and communications reliabilities (BPR, R).....	78
6.6.4 Computation of compatibility	78
6.7 SERVICE NEEDS.....	78
6.8 THE HF RADIO SKY-WAVE PROPAGATION MODEL	79
6.8.1 Path lengths up to 7 000 km.....	79
6.8.1.1 Monthly median path basic MUF and operational MUF.....	79
6.8.1.2 E-layer basic MUF.....	80
6.8.1.3 F2-layer basic MUF	80
6.8.1.4 Oblique ray paths	81
6.8.1.5 Field strength	82
6.8.1.6 Transmission losses	82

6.8.1.7	Median available receiver power.....	82
6.8.2	Path lengths beyond 9 000 km.....	83
6.8.2.1	Introduction.....	83
6.8.2.2	Monthly median path basic MUF.....	83
6.8.2.3	Field strength.....	83
6.8.2.4	Median available receiver power.....	83
6.8.3	Paths between 7 000 and 9 000 km.....	83
6.8.4	System performance parameters.....	83
6.9	ANTENNA CONSIDERATIONS.....	84
6.9.1	Antenna characteristics.....	84
6.9.2	Gain.....	84
6.9.3	Radiation pattern.....	85
6.9.4	Polarization.....	86
6.9.5	Ground effects.....	86
6.9.6	Radiated power.....	86
6.10	APPLICATION OF PREDICTION TO HF SYSTEM PLANNING AND DESIGN...	87
6.11	OPERATIONAL CONSTRAINTS.....	87
6.11.1	Available frequencies (bands).....	87
6.11.2	Interference.....	92
6.11.3	Digital systems.....	96
6.11.3.1	Signal-to-noise ratio.....	97
6.11.3.2	Time dispersion.....	98
6.11.3.3	Frequency dispersion.....	100
6.12	SELECTION OF SYSTEM PARAMETERS.....	102
6.12.1	Selection of frequencies.....	102
6.12.2	Selection of antennas.....	103
6.12.3	Selection of transmitter power.....	108
6.12.4	Location of terminals.....	109
6.13	OVERVIEW OF COMPUTER PROGRAMS.....	111
	References and Bibliography for Chapter 6.....	119

	Page
CHAPTER 7 - 7PROPAGATION AT VHF AND ABOVE - EARTH-SPACE	121
7.1 EARTH-SPACE PROPAGATION	121
7.2 TOTAL ELECTRON CONTENT (TEC).....	121
7.3 EFFECTS DUE TO BACKGROUND IONIZATION.....	121
7.3.1 Faraday rotation	121
7.3.2 Group delay.....	122
7.3.3 Dispersion	124
7.3.4 Doppler frequency shift	125
7.3.5 Direction of arrival of the ray	125
7.3.6 Absorption.....	125
7.3.6.1 Auroral absorption	126
7.3.6.2 Polar cap absorption.....	126
7.4 EFFECTS DUE TO IONIZATION IRREGULARITIES	127
7.4.1 Scintillation effects	126
7.4.2 Geographic, seasonal and solar dependence.....	128
7.4.3 Scintillation models	129
7.5 SUMMARY.....	131
References for Chapter 7	132
CHAPTER 8 - PROPAGATION AT VHF AND ABOVE - TERRESTRIAL	135
8.1 IONIZED PROPAGATION AT VHF AND ABOVE	135
8.1.1 Normal F-region propagation at VHF.....	135
8.1.2 Trans-equatorial propagation (TEP)	135
8.1.3 Sporadic-E propagation	136
8.1.4 Meteor-trail ionization	136
8.1.5 Auroral ionization	141
8.1.6 Ionospheric scatter propagation	141
8.1.7 Summary	141
References for Chapter 8	143
Bibliography	143

	Page
CHAPTER 9 - GLOSSARY	145
9.1 IONOSPHERE AND WAVES	145
9.2 SIGNALS, NOISE AND INTERFERENCE.....	147
9.3 ANTENNAS AND RADIATION	148
9.4 RADIOWAVE PROPAGATION.....	149
9.5 FADING AND LOSS	151
9.6 RELIABILITY AND COMPATIBILITY.....	152

PREFACE

This Handbook has been developed by experts of Working Party 3L (HF propagation) of the ITU-R Study Group 3 (Radiowave propagation), under the Chairmanships of Mr. P. A. Bradley (U.K.) and Dr R. Hanbaba (France), and edited by Dr D. G. Cole (Australia).

Major contributors to the Handbook were:

Prof.	Les Barclay
Dr.	Jack Belrose
Mr.	Peter Bradley
Dr.	David Cole
Mr.	Ian Davey
Mr.	Mike Dick
Dr.	Rudi Hanbaba
Dr.	Juergen Hortenbach
Dr.	Kevin Hughes
Dr.	Patrick Lassudrie-Duchesne
Dr.	Tadahiko Ogawa
Mr.	Don Ross
Dr.	Haim Soicher
Prof.	Noboru Wakai
Mr.	John Wang
Dr.	Bruce Ward

CHAPTER 1

INTRODUCTION

1.1 Relationship of this Handbook to ITU-R Recommendations

This Handbook on ionospheric properties and propagation supplies background and supplementary information on radiowave propagation effects, and serves as a companion volume and guide to the Recommendations that are maintained by Study Group 3 (SG 3) (Radiowave Propagation) of the International Telecommunication Union, Radiocommunication Sector (ITU-R), to assist in the design of radio communication systems.

This Handbook is intended to be used in conjunction with the published SG 3 Recommendations to assist the user in the application of the Recommendations. The Recommendations, listed below, contain the ionospheric radio propagation prediction methods and engineering advice for the fixed, broadcasting, satellite and mobile (maritime, land and aeronautical) services in the VLF/LF/MF/HF and VHF/UHF bands. A glossary of terms is provided at the end of the Handbook.

- ITU-R P.684-1: Prediction of field strength at frequencies below about 500 kHz
- ITU-R P.1147: Prediction of sky-wave field strength at frequencies between about 150 and 1 700 kHz
- ITU-R P.533-5: HF propagation prediction method
- ITU-R P.531-4: Ionospheric propagation data and prediction methods required for the design of satellite services and systems

This Handbook follows the order of the above Recommendations. Duplication of propagation data from the Recommendations is intentionally minimal, and the detailed prediction methods are found in the Recommendations. Where applicable, reference is made in the text to ITU-R Recommendations and Reports simply by their numbers, e.g. Recommendation P.533. The latest version of the Recommendations (e.g. 533-5) should be used for system calculations.

1.2 Application of the Handbook

Accurate propagation information is required to support the design, implementation and operation of most modern communication systems. The propagation behaviour of radiowaves, in and through the ionosphere or upon reflection from the Earth's surface, is of concern to radiocommunication systems that use the ionospheric propagation channel for the transmission of electromagnetic energy between antennas in the system. Signal degradation that occurs with sufficient frequency and intensity to affect the performance and availability objectives must be estimated and accounted for in the system design. Methods are thus required to predict the magnitude and occurrence of relevant propagation characteristics with sufficient accuracy for engineering applications.

The Handbook provides background on the physical causes for the variations in propagation and path impairments, the bases for the prediction methods that are found in the Recommendations, and additional information deemed useful for engineering applications, including data and models that are yet inadequate for ITU-R Recommendation status. As far as possible, the prediction methods are evaluated by testing with measured data from the data banks of SG 3, and the results are used to indicate the accuracy of the prediction methods and the variability of the measured data. This Handbook addresses propagation characteristics for systems operating from about 30 kHz to above 10 GHz; this including the VLF, LF, MF, HF, and trans-ionospheric satellite frequency bands.

The effect of particular ionospheric conditions on an ionospheric or trans-ionospheric telecommunication system depends on wave frequency and polarization; path geometry (e.g., elevation angle of the path); the system performance objectives; achievable performance margins; details of the system configuration; and local ionospheric features.

CHAPTER 2

IONOSPHERIC PROPERTIES

2.1 The ionosphere

The ionized region in the Earth's atmosphere extending from about 50 km to roughly 2 000 km above the surface is called the ionosphere; above that it is called the magnetosphere. For reasons related to the historical development of ionosphere research, the ionosphere is divided into three regions designated D, E and F, respectively, in order of increasing altitude (see Fig. 2.1). Subdivisions of these regions may exist under certain conditions; for example, F1 and F2 layers during daylight hours.

Radiowaves in the low frequency to high frequency bands are receivable over long distances because they can be reflected by the ionized regions of the atmosphere. From the viewpoint of HF propagation, the E and F regions act principally as radiowave reflectors, and permit long range propagation between terrestrial terminals. The D region acts principally as an absorber, causing signal attenuation in the HF range, although VLF and ELF waves are reflected at D-region altitudes. The transition between reflection at D-region altitudes and E-region altitudes occurs in the medium frequency range (<3MHz). The ionosphere is also an important factor in space communications at VHF and higher frequencies, since the signal is modified and degraded to varying degrees in passing through the ionosphere.

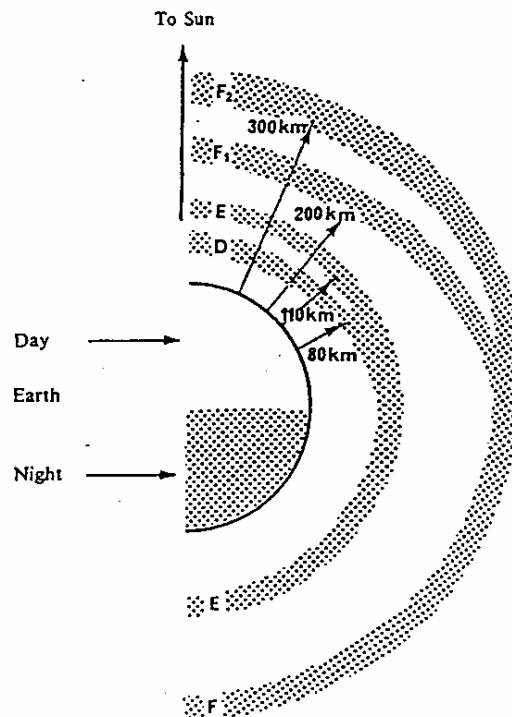


FIGURE 2.1

Ionospheric regions as a function of height above the Earth's surface

The transmission channel for radiowave propagation at LF to HF includes much of the Earth's atmosphere between the circuit terminals (transmitter and receiver). In particular, the varying ionization in the upper atmosphere is the major cause of changes in the transmission channel and therefore in the path loss. These variations in ionization are due to a number of causes, all related to the solar influence on the Earth's atmosphere. The regular variations may be classified according to period: multi-years, year and day. Annual and diurnal variations are a function of geographic location.

2.2 Ionospheric profiles and structural features

2.2.1 Physical processes of the ionosphere

2.2.1.1 Ionization production and loss

The most important ionospheric parameter, from the point of view of radiowave propagation, is the electron density. The density at any given point in space and time is a function of three competing physical processes; production, loss and transport. These three "processes" in practice involve a multitude of complex photochemical and electrodynamic processes which are influenced by a variety of external conditions within the atmosphere and magnetosphere.

The principal source of ionization in the ionosphere is electromagnetic radiation from the Sun extending over the ultra-violet and X-ray portions of the spectrum. Other sources of ionization are, however, important, such as energetic charged particles of solar and magnetospheric origin and galactic cosmic rays. The ionization rate at various altitudes depends upon the intensity of the solar radiation as a function of wavelength and the ionization efficiency of the neutral atmospheric gases. Since the Sun's radiation is progressively absorbed in passing through the atmosphere, its residual ionizing ability depends upon the length of the atmospheric path, and consequently upon the solar zenith angle (χ). The maximum ionization rate occurs when the Sun is overhead ($\chi = 0$), but geographic, diurnal and seasonal variations in the ionization density are found.

The production of free ionization by solar radiation (and charged particles) is counter-balanced by ionization loss processes, principally the collisional recombination of electrons and positive ions, and the attachment of electrons to neutral gas atoms and molecules. It is possible to determine, from physical principles, a reasonably realistic mathematical description of the altitude distribution of ionization, based on estimates of the solar ionizing flux, the vertical distribution of neutral atmospheric constituents and their absorption efficiency, and the solar zenith angle. This was first done by Chapman [1931] for a single constituent, isothermal atmosphere ionized by monochromatic solar radiation. This model (Chapman model) is a good approximation for the E and F1 regions where photoionization and collisional recombination are the dominant physical processes but is a poorer representation in the D and F2 regions where other processes are also important.

At the height of the F2 layer the transport of ionization is important. This movement can be caused by diffusion, neutral atmospheric winds and electromagnetic drift.

Plasma diffusion occurs along magnetic field lines and is therefore greatest at the magnetic poles where the electrons and ions can move nearly vertically along the field lines. The effect on ionization distribution is not as strong as the effect of neutral winds that are driven from the hotter dayside to the cooler nightside of the Earth. The winds move the ionization through neutral-ion collisions and thence the electrons by Coulomb attraction.

In the F2 region electromagnetic drift ($E \times B$), caused by interaction of ionized particles with the Earth's magnetic field (B) and electric fields (E) in the ionosphere, is important because it accounts for ionization moving across magnetic field lines. Electric fields are important near the equator causing vertical drifts and in the auroral zones and polar caps causing horizontal drifts [Rishbeth, 1989].

2.2.1.2 Electron collision frequency

Collisions between electrons and neutral particles are important in the attenuation of radiowaves. The collision frequency within the 50-90 km region, derived from laboratory experiments, rocket-borne measurements and analysis of radiowave propagation data, has been found to be as high as 2×10^6 per second at 75 km. The collision frequency in this region changes with season, latitude, and on some occasions, with solar activity. The variability from day to day is especially marked at high latitudes in winter.

Collision frequency versus height profiles in the height range 100 to 200 km have been derived from both radiowave propagation data and rocket probe measurements. Daytime results show an exponential decrease in electron collision frequency with height, to about 140 km, and above that height the collision frequency decreases more slowly with height due to electron-ion collisions [Davies 1990 p 24]. At night the collision frequency increases by six to seven times in summer and by three to four times in winter over daytime values.

2.2.2 D region (50-90 km)

The electron density in the D region increases rapidly with altitude and exhibits a marked diurnal variation, with peak densities shortly after local noon (typically 10^8 to 10^9 electrons/m³) and very small values at night. There is a pronounced seasonal variation with maximum densities in summer.

The diurnal, seasonal and solar cycle dependence of the D region electron density varies with altitude, reflecting a change in the source of ionization with altitude. Solar ultra-violet radiation and X-rays are the dominant sources in the range 70-90 km whereas galactic cosmic rays are the major contributor in the altitude range 50-70 km. The solar cycle dependence of D region electron density directly reflects this change in ionization source. In the 70-90 km range maximum densities occur at the peak of the solar cycle, mirroring the solar cycle variation. Below 70 km maximum densities are found at solar minimum as a result of reduced interplanetary scattering of galactic cosmic rays.

The principal effect of the D region on MF/HF radiowave propagation is absorption. This arises from the high collision frequency between the electrons and neutral particles at these altitudes. At VLF/LF the region reflects radio waves.

2.2.3 E region (90-130 km)

The E region conforms closely to the Chapman model with a maximum density near noon and a seasonal maximum in summer. The maximum density (approximately 10^{11} electrons/m³) occurs near 110 km although this height varies with local time. At night only a small residual level of ionization remains. The E region also exhibits a solar cycle dependence with maximum densities occurring at solar maximum. The variation in daytime E-region plasma frequency is about 30% over the solar cycle at a given location.

2.2.4 Sporadic E (Es)

Embedded within the E region is an anomalous form of ionization, known as sporadic E, which has little direct relationship with solar ionizing radiation. The properties of this ionization vary considerably with both location and time but can be differentiated into three principal types:

2.2.4.1 Mid-latitude Es

Dense, thin layers of ionization are formed by the combined effect of wind shear and the geomagnetic field on long-lived metal ions. The ionization is compressed into patches ranging in spatial extent from several kilometres to 1 000 km and with thickness typically 500 to 2 000 m.

Es layers may be found in the height range 95 to 135 km with the most probable height being 110 km. The peak density may often reach a value many times that of the ambient E region.

The occurrence of mid-latitude Es layers is quasi-random although there are well defined diurnal and seasonal variations. The diurnal variation exhibits maxima in the mid-morning hours and near sunset, lagging the growth and decay of the regular E region. The seasonal variation is complex and possibly related to the upper atmosphere winds. Seasonal maximum occurrence is during the months of local summer. The seasonal minimum is usually near midwinter or the spring equinox.

Mid-latitude Es can have significant effects on HF radio waves. It can support propagation in its own right, often of unwanted signals, and can impose large losses on F mode propagation.

2.2.4.2 Equatorial Es

A dense band of irregularities is formed within 6 degrees of the geomagnetic equator by the high electron drift velocity in the daytime equatorial electrojet. This equatorial Es is usually observed during daylight, is highly transparent and gives high vertical incidence critical frequencies (frequently up to 10 MHz).

2.2.4.3 Auroral Es

The auroral E region is characterized by several phenomena produced by auroral particle ionization and occurring almost continuously around the auroral oval. A relatively regular thick layer of ionization resembling the normal E region, referred to as auroral E, exists primarily at night and is of significance since it reflects radio waves. Other auroral E-region phenomena, referred to as auroral Es, may be thin and patchy and are positively correlated with the presence of visible aurora. Auroral sporadic E can cause rapid fading and multipath problems on HF communications.

Sporadic E within the polar cap exhibits a different character from auroral Es, being substantially weaker and exhibiting a negative correlation with magnetic activity. It extends in bands across the polar cap, roughly in the direction of the Sun, and may be associated with weak sub-visual auroral optical emissions.

2.2.5 F region (130-500 km)

The lower part of the F region (130 to 200 km) displays different behaviour to the upper part and for this reason the terms F1 and F2 are applied to these layers in daytime. The F1 layer, like the E region, is under strong solar control and possesses Chapman-like features although it exhibits a different solar zenith angle dependence to that of the E region. The distinction between the F1 and F2 layers is not maintained at night.

The F2 layer is the most prominent layer in the ionosphere. It is the highest layer, generally exhibits the greatest electron densities and is the only layer which persists to any significant degree during the night. The F2 layer is not well represented by the Chapman formulation since it is strongly influenced by neutral winds, ambipolar diffusion and other electrodynamic effects. The relationship between the direction of the geomagnetic field and the direction of the neutral winds and electrodynamic drifts plays a major role in the structure of the F2 layer. It is the plasma response to the dynamic processes in the presence of the geomagnetic field that gives rise to the observed geographical and temporal variations in the F2 layer.

The maximum density generally occurs well after local noon, sometimes in the evening. The height of the maximum ranges from 250 to 350 km at mid-latitudes to 350 to 500 km at equatorial latitudes. At mid-latitudes the height of the maximum electron density is higher at night than in the daytime but the opposite behaviour occurs in the equatorial regions.

In the early days of ionospheric research, when the Chapman model was believed to be valid, various significant departures from expected behaviour were termed "anomalies". Although this description is no longer valid the following terms remain in popular use:

The "diurnal anomaly" refers to the fact that the maximum F2-layer electron density often occurs at times other than solar noon. The maximum typically occurs in the range 1300 to 1500 local time, with a semi-diurnal component which produces secondary maxima at approximately 1000-1100 and 2200-2300 local time. The shape of the day/night variations of electron density and height are largely due to the effect of neutral winds and, to a lesser extent, electric fields.

The "seasonal anomaly" is the observed tendency for maximum F2-layer densities, at around 1200 local time in winter, to exceed the corresponding summer values. This is thought to be attributable to seasonal changes in the O/N₂ ratio of the neutral atmosphere.

The "equatorial anomaly" refers to the marked departure from solar zenith angle dependence of F2-layer densities within 20 to 30 degrees either side of the geomagnetic equator. This anomaly is produced by dynamo electric fields which cause a drift of ionization vertically up and away from the equator.

At high latitudes a variety of anomalous features are observed, some of which are associated with charged particle precipitation. The F-region "trough" is a pronounced depression in the F2-layer electron density resulting from magnetospheric convection. The trough extends from about 2 to 10 degrees equatorward from the auroral oval in the late afternoon and night-time ionosphere.

2.2.6 F region irregularities (Spread F)

Ionization irregularities in the F region occur mostly at equatorial and high latitudes. They are responsible for high flutter fading rates at HF and VHF, and scintillation in satellite propagation.

Within 20 degrees of the magnetic equator the irregularities are a night-time phenomenon and tend to develop in the evening about one hour after local sunset with scale-sizes from about 3 m to more than 10 km. The irregularities are embedded in the F region at heights up to 1 000 km and tend to be aligned along the Earth's magnetic field lines. Equatorial spread F is associated with magnetically aligned bubbles in the ionospheric plasma that rise through the ionosphere after sunset.

At geomagnetic latitudes greater than about 40 degrees high latitude spread F develops and its occurrence increases with increasing latitude. Again the irregularities develop in the evening and night-time.

In general the occurrence of spread-F irregularities is highest in the equinoxes with a sub-maximum at the summer solstice. However, F-region ionization irregularities display significant longitudinal variability in addition to latitudinal and temporal dependencies. Details of these findings as well as the effect of equatorial irregularities on the performance of transionospheric propagation systems can be found in the review by Aarons [1977].

2.2.7 Topside ionosphere

Observations of electron density at altitudes above the height of maximum density determined from incoherent scatter radars, rockets and satellite-borne sounders indicate that the electron density decays approximately exponentially with height. The electron density is typically between 10⁹ and 10¹⁰ electrons/m³ at 1 000 km height, and about 10⁹ electrons/m³ at 5 000 km. Observations of electron densities reveal that the equatorial anomaly can extend well beyond 500 km in altitude. In addition, these measurements show that the mid- and high-latitude F-region trough of depressed electron density in the night-time ionosphere is also a predominant feature of the topside ionosphere.

2.3 Geographical features

Ionospheric properties are largely governed by the location of the Sun (the ionizing source), the Earth's magnetic field and atmospheric winds that can move the ionization and charged particles between hemispheres. In general terms the effects of these dependencies result in three regions of geographic characteristics (beside the temporal), high-latitude, low-latitude and mid-latitude. The geographic regions of ionospheric behaviour are approximately defined in Table 2.1.

TABLE 2.1

Geographic regions of ionospheric behaviour

Geographic Region	Geomagnetic Latitude λ (degrees)
High Latitude	$90 > \lambda > 60$
Mid Latitude	$60 > \lambda > 20$
Low Latitude	$0 > \lambda > 20$

2.3.1 Ionospheric control points

When planning or managing a radiocommunications circuit that involves propagation via the ionosphere, one needs to take account of that part of the ionosphere that is relevant to the circuit. Thus in a simple ionospheric link using a single reflection from the ionosphere it is the ionospheric properties at the mid-point of the circuit that are important, in an Earth-satellite path it is the sub-ionospheric point, the region where the Earth-satellite path passes through the ionosphere and in a multiple hop ionospheric path it is the mid-points of the hops at each end of the circuit (control points) that control the propagation.

The above assumes that the propagation mechanism is one of sky-wave hops. In the case of very long waves (frequencies below 60 kHz), where the propagation mechanism is one of waveguide modes in the Earth-ionosphere waveguide, the conductivity of the ionosphere and the ground along the whole of the transmission path must be considered.

2.3.2 High latitudes

The high-latitude F region is an extremely variable and dynamic region as exhibited by several quasi-permanent features. The most prominent feature is an area of severely depressed night-time F-region electron densities referred to as the F-region trough equatorward of the auroral oval (see Fig. 2.2). The maximum electron density may be reduced by as much as an order of magnitude. Enhanced electron densities are observed on the dayside region immediately poleward of the auroral oval (see Fig. 2.3). The region in the vicinity of the magnetic pole is one of depleted electron density, sometimes referred to as the "polar cavity".

A review of high-latitude phenomenology and morphology affecting propagation has been summarized in Belrose [1988].

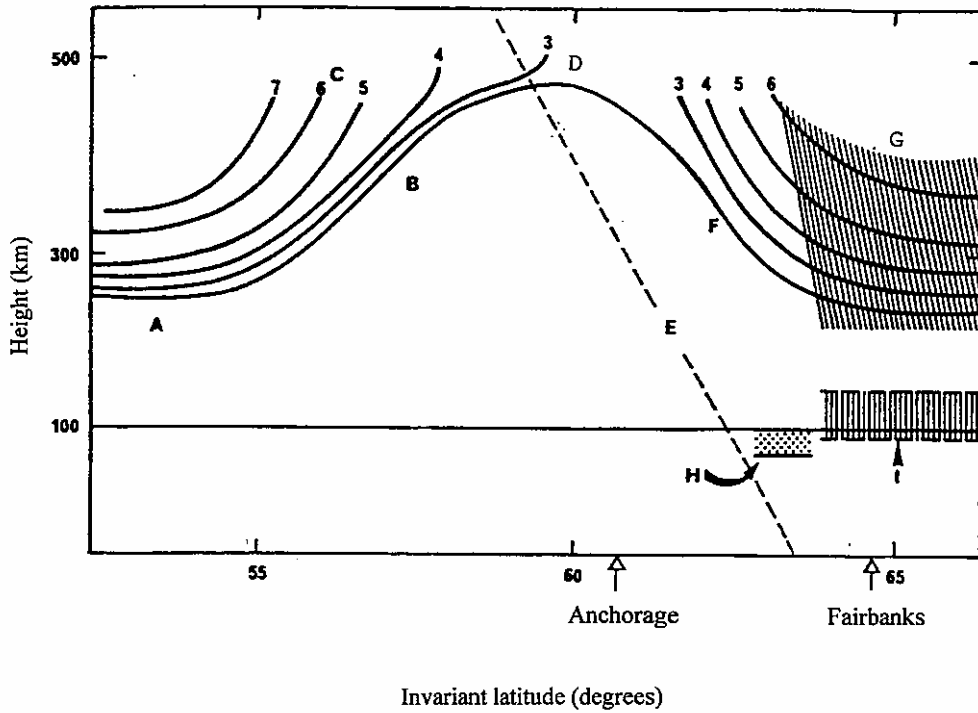
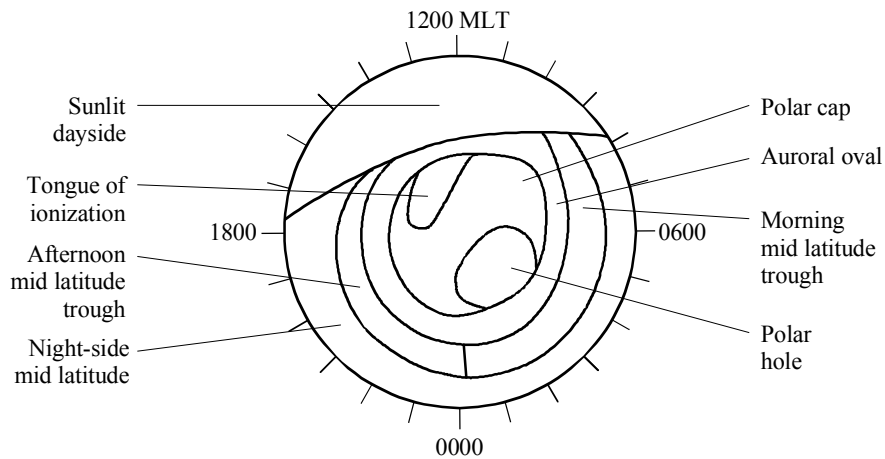


FIGURE 2.2
Idealized sketch of plasma frequencies (MHz) in the vertical north-south plane through Fairbanks and Anchorage, Alaska.

The salient ionospheric features which affect MF/HF sky-wave propagation are illustrated

- | | |
|-------------------------------|---------------------------------|
| A: equatorward of trough | F: poleward edge of trough |
| B: equatorward edge of trough | G: F-region blobs |
| C: plasma frequency (MHz) | H: enhanced D-region absorption |
| D: trough minimum | I: E-region irregularities |
| E: plasmapause field line | |



MLT : magnetic latitude local time

FIGURE 2.3

A schematic diagram of the basic morphological regions of the polar ionosphere [URSI, 1993] (MLT : Magnetic latitude local time)

2.3.2.1 Relationship to magnetic and solar activity

Since the morphology of the high-latitude ionosphere is controlled to a great extent by the magnetic field, its properties are best described in terms of magnetic coordinates. The most useful orthogonal coordinate is local magnetic time, which is similar to ordinary local time, except that it is based on the geomagnetic pole rather than the geographic pole. For points well away from the region between the geographic and magnetic poles, the two types of local time are approximately equal. In each hemisphere, a "magnetic latitude local time" frame of reference is fixed with respect to a line from the magnetic pole to the Sun. In this reference frame, the observer on Earth is on a moving platform that passes underneath phenomena that are stationary in space. One important exception is the solar terminator (the sunrise/sunset line), which is fixed with respect to the geographic pole, at a given time of year. In the magnetic coordinates just described, the solar terminator moves diurnally towards and away from the Sun.

There are several definitions of latitude connected with the geomagnetic field [Chapman, 1963]. The "dipole" latitude which is based on an approximation to a centred-dipole magnetic field, was used for ionospheric work and is adequate, provided that high precision is not required. "Corrected" geomagnetic latitude represents the real geomagnetic field more accurately, and is widely used in auroral studies. Conversion tables are given by Hakura [1965] and Gustafsson [1970]. Corrected geomagnetic latitude lines in the high-latitude regions are displayed on Figs. 2.4 and 2.5. A corresponding magnetic local time is defined, and the complete coordinate system is commonly referred to as CGLT (corrected geomagnetic-local time). "Invariant" latitude is another coordinate system [McIlwain, 1966], which is used primarily for studies of energetic trapped particles. At the Earth's surface, in high-latitude regions, it is almost identical to corrected geomagnetic latitude.

2.3.2.2 The auroral oval

There are two kinds of aurora: visual aurora and radio aurora which can be further classified as discrete or diffuse. Discrete visual aurora and discrete radio aurora are believed to be closely correlated. No such temporal correlation is evident between diffuse visual aurora and diffuse radio

aurora. The auroral oval [Feldstein and Starkov, 1967], defined in the CGLT system, has been widely used as a reference domain for describing many high-latitude phenomena. It is an annular region in which the frequency of occurrence of visible discrete aurora is high. The oval for moderate magnetic activity is indicated in Fig. 2.3. The oval is eccentric with respect to the geomagnetic pole, being displaced about 4° toward the night side of the Earth. Therefore, an observer under the oval at midnight will be equatorward of it at noon. The polar cap is usually defined as the region poleward of the high-latitude boundary of the auroral oval. A method for determining the location of the oval as a function of space and time was developed by Whalen [1970], and a mathematical representation is given by Holzworth and Meng [1975].

The concept of an "auroral oval" as a band of luminosity encircling each of the geomagnetic poles was first deduced statistically. However, satellite imaging photometry clearly confirmed the omnipresence of auroral zone particle precipitation. In these images, the entire auroral oval is observed in visible and ultraviolet wavelength bands, permitting analysis of auroral features such as the growth, expansion and recovery phases of substorms. The patterns of particle precipitation that produce the aurora are seen to be dynamic functions of location. Multispectral imaging allows extraction of the energy deposition rate and the characteristic energy of the precipitation over the entire auroral region at low spatial resolution. Alternatively, statistical models of ionospheric parameters have been deduced from local measurements of electron precipitation by lower-altitude polar-orbiting satellites, averaged over long periods of time [Fuller-Rowell and Evans, 1987; Hardy *et al.*, 1985].

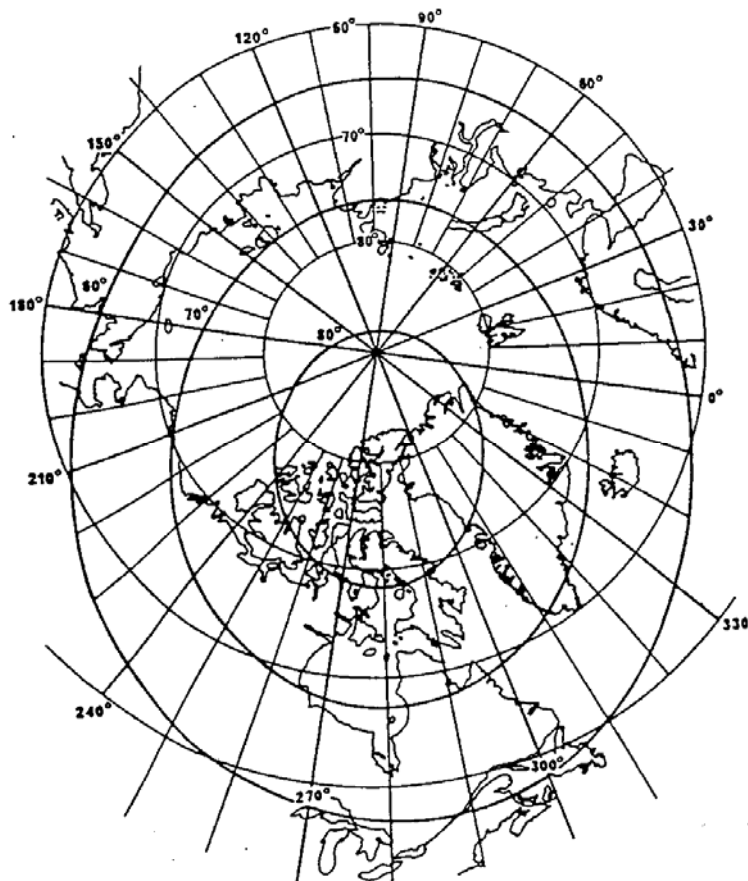


FIGURE 2.4

**Corrected geomagnetic latitude in the northern hemisphere
(Geographic latitude and longitude are also displayed for reference)**

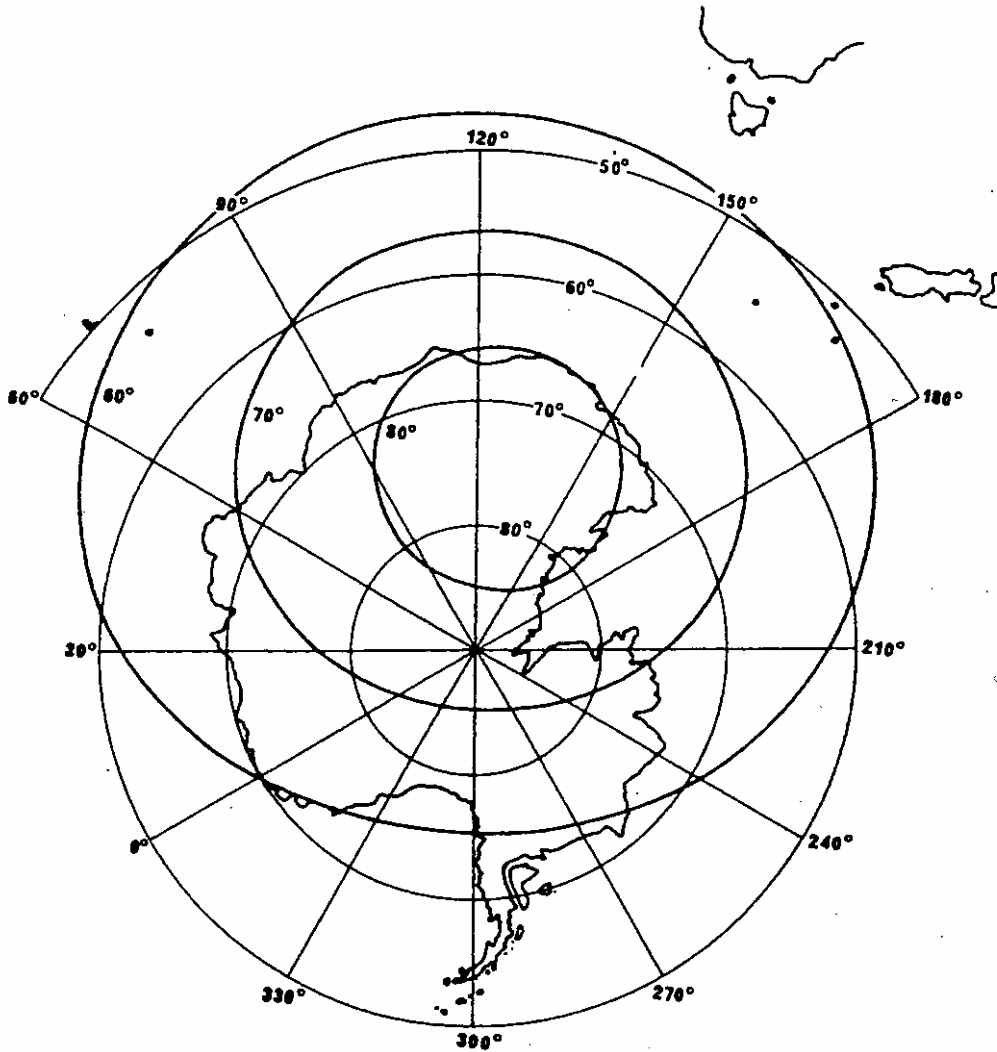


FIGURE 2.5

Corrected geomagnetic latitude in the southern hemisphere

2.3.2.2.1 Magnetic activity and the size of the auroral oval

Feldstein labelled the ovals with a "Q" index of magnetic activity. There is a rough correspondence between Q and geomagnetic K_p index, which is widely available, although it is a planetary index, rather than an auroral one. An auroral electrojet (AE) index has been defined as a measure of substorm activity. The AE index is a widely accepted measure of global auroral electrojet activity based on 2.5 min readings of the H magnetic component trace from a ring of observatories located between 65° and 70° magnetic latitude.

Electron precipitation data from hundreds of polar passes of U.S. Defence Meteorological Satellite Programme (DMSP) satellites have determined the average locations of the equatorward and poleward boundaries of the precipitation region as a function of the hourly AE index of geomagnetic activity. It was found that for quiet conditions ($AE < 150$ nT), the poleward boundary of the low-energy electron precipitation (< 500 eV) is located at about 80° to 82° corrected geomagnetic latitude in both the evening and morning sectors, and the equatorward boundary of the

high-energy precipitation (> 500 eV) is located at 61° to 71° in the evening sector and 67° to 69° in the morning sector. The transition boundary between the high- and low-energy regions is at about 73° to 75° in both the evening and morning sectors. During magnetically disturbed periods ($AE > 400$ nT) the poleward boundary is located at about 73° to 75° in the evening sector and 76° to 77° in the morning sector; the transition and equatorward boundaries are located at about 70° to 72° and 64° to 66° respectively, in both the evening and morning sectors. Thus the extent of the polar cap varies from an equivalent latitude of approximately 84° during quiet conditions to further than 65° equivalent latitude during geomagnetic storms. In general, as geomagnetic activity increases, the size of the polar cap increases, the width of the low-energy auroral electron precipitation region decreases, and the width of the high-energy auroral electron precipitation region increases.

2.3.2.3 The outer precipitation zone

Equatorward of the oval, there is a zone of precipitation that does not produce discrete aurora. This zone is more circular than the oval and occupies the latitude range 60° to 70° geomagnetic. Phenomena related to the more energetic electron precipitation, such as diffuse aurora, auroral radio absorption, and X-rays, appear most strongly equatorward of the oval in the outer zone. Absorption in this zone is shown in Figs. 2.6 and 2.7.

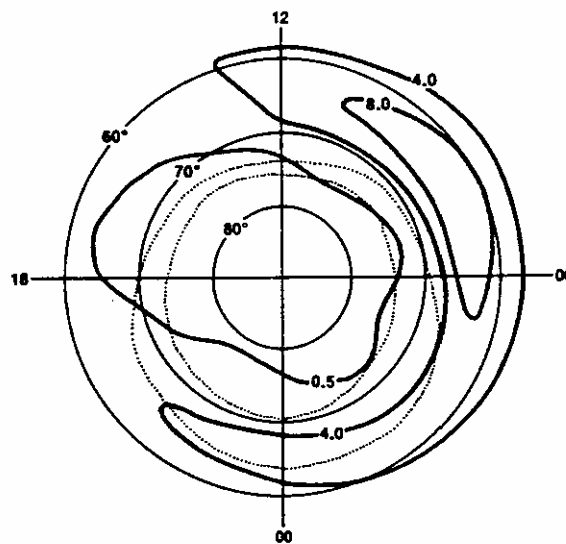


FIGURE 2.6

Percentage of time for which auroral absorption was at least 1 dB. Coordinates are geomagnetic latitude and time. The boundaries of the auroral oval ($Q = 3$) are shown as dotted lines

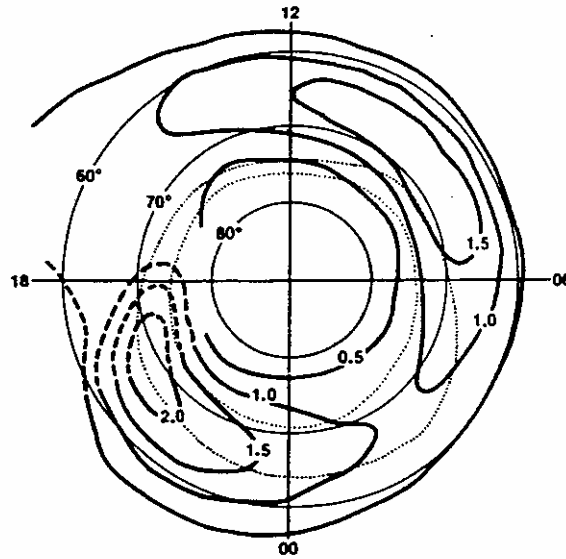


FIGURE 2.7

Median intensity of auroral absorption events in dB. Coordinates are geomagnetic latitude and time. The boundaries of the auroral oval ($Q = 3$) are shown as dotted lines

2.3.2.4 Storms and substorms

Our understanding of the visual auroral event as a substorm has evolved to include a variety of associated physical signatures that denote complex magnetospheric processes. Briefly, a magnetospheric substorm is a transient process during which a significant amount of energy, derived from the interaction between the solar wind and the Earth's magnetic field, is deposited in the auroral ionosphere and magnetosphere. Isolated substorms last about an hour, but they may occur in rapid succession, especially during major geomagnetic storms. Substorms are accompanied by intense charged particle precipitation, enhanced auroral electrojets, and heating of the neutral atmosphere. All radio propagation parameters for high latitude paths may vary rapidly under the influence of an auroral substorm; those variations most frequently noted are found in D-region absorption (Auroral Zone Absorption, AZA) and sporadic E. Total electron content can be significantly affected.

2.3.2.5 Ionization increases after geomagnetic storms (the post-storm effect)

Increased D-region absorption is observed regularly after geomagnetic storms from sub-auroral latitudes to mid-latitudes. The increased absorption in this belt is distinct from the auroral absorption zone and is caused by precipitation of energetic electrons from the radiation belt.

The zone of increased absorption starts to develop shortly after the main phase of the storm and exists during the whole recovery phase, i.e. up to ten days or more. The amplitude and duration of the absorption increase are closely correlated with the Dst index but also depend on the polarity of

the interplanetary magnetic field. At the beginning of the recovery phase after a geomagnetic storm, the poleward boundary of the belt is found around 55-58° invariant latitude in Europe; it moves slowly poleward reaching about 62° invariant latitude at the end of the recovery phase. A notable feature of the post-storm events is the large spread in the deduced effective electron-loss rates, which is greater at 80 km than at higher or lower heights.

2.3.2.6 Polar cap events

Sporadic E within the polar cap exhibits a different character from auroral Es, although the same current-driven plasma instability is active in both regions. In general, it is substantially weaker and displays a negative correlation with geomagnetic activity related to auroral substorms. Polar cap sporadic E extends in bands or ribbons across the polar cap, roughly in the direction of the Sun and may be associated with weak sub-visual auroral optical emissions.

Polar cap absorption (PCA) events which are often called solar proton events (SPE), are caused by the eruption of solar X-ray flares that emit energetic (MeV) protons which reach the Earth. The absorption occurs between about 45 and 75 km altitude. At HF, attenuation can be greater than 100 dB. The occurrence of such a flare may be announced by a Sudden Ionospheric Disturbance (a brief absorption event) on the sunlit side of the Earth, at all latitudes, caused by X-rays from the flare. The PCA event can occur from 15 minutes to several hours later. The delay time represents the travel time of the protons from the Sun to the vicinity of the Earth.

Whereas it is not possible to predict the occurrence of a sudden ionospheric disturbance, once a flare has been observed there is a good chance of forecasting the occurrence, time of arrival, and severity of a PCA event [Cliver *et al.*, 1978; Akinyan *et al.*, 1980]. Unlike X-rays, the protons are guided by the Earth's magnetic field, and appear only above about 60° magnetic latitude, whether sunlit or not. (Note that the area covered by "Polar Cap Absorption" is usually larger than the "polar cap".) However, absorption in the sunlit part of the polar cap is about four times stronger (at 30 MHz) than in the dark part, where many of the electrons are immobilized by attachment to air molecules to form negative ions. Depending on the phase of the sunspot cycle there may be from 0 to 14 PCA events per year. The average duration of a PCA event is about two days, but it may be as long as four days. A survey of PCA events from 1952 to 1973 [Larsen, 1974] suggests that the number N of hours of PCA per year is given approximately by $N = -70 + 4.4R$ where R is the mean smoothed sunspot number. For the worst year in the survey, this is 780 hours, representing about 9% of the year. Since absorption is greatly reduced during dark hours, any given circuit will be blacked out for a smaller fraction of the time than this.

Magnetic storms may occur from 20 to 60 hours after a major flare. If the PCA still exists when a storm commences, the absorption can spread to lower latitudes, to about 55°, due to the distortion of the geomagnetic field. It has been observed that the PCA absorption increases at about the time of the beginning of a storm, then decreases for an hour or more.

2.3.2.7 High-latitude trough

Equatorward of the auroral oval, a trough is found in the electron density of the night-time F region [Muldrew, 1965]. The density can become low because ionization is not supplied by anti-sunward drifting or by precipitation or by the storage effect of permanently closed magnetic field lines. The trough exists initially in the afternoon at high magnetic latitudes (about 70°) where it is only a few degrees wide. With increasing local time it shifts gradually to about 57° magnetic latitude (for

moderate K_p) near local midnight when it can be about 10° or more in width. It may swing a few degrees poleward of this before disappearing near sunrise. The centre of the trough moves equatorward approximately $1.8^\circ \pm 0.4^\circ$ per unit increase in K_p .

Very large latitudinal gradients of electron density exist at the equatorward and poleward edges of the ionospheric trough. These latitudinal gradients are even more strongly pronounced on the topside of the ionosphere, where the poleward boundary has been described as a "wall" of ionization. The latitudinal gradients at the low latitude boundary of the ionospheric trough are not as large as those at its high latitude boundary (the auroral oval edge) but are nevertheless often considerably larger than the gradients encountered at mid-latitudes. The ratio of densities inside and outside the trough can vary between less than 0.1 to almost 1, but there is no known dependence on magnetic activity. A model of the trough has been given by Halcrow and Nisbet [1977].

2.3.2.8 High latitude irregularities

Irregularities are found more or less continuously throughout the high latitude region starting at about 60° corrected geomagnetic latitude. Associated with the auroral oval is an "irregularity zone" in the bottomside of the F layer.

Sun-aligned polar cap F-layer auroral arcs drifting from dawn to dusk have been observed in the winter polar cap. During years of enhanced solar activity they constitute substantial (5 to 8 fold) enhancements above a nominal 10^{11} electrons/ m^3 , background density (foF2 approx 3 MHz) and occupy the polar cap mainly during quiet geomagnetic conditions. Near solar minimum the density enhancements are rarely more than a factor of 2 above the background. During more disturbed conditions ($K_p > 4$), large, structured electron density patches are observed moving at high speed in the anti-sunward direction. The occurrence of these patches is under strong UT control. There is also evidence for solar cycle dependence of the maximum densities within the patches. The diameter of these patches is greater than 1 000 km and they can therefore affect HF communications on circuits with reflection points in the polar cap.

2.3.2.9 High-latitude F region

The F region in the auroral night-time ionosphere very often displays substantially lower electron densities than the E region, and is virtually always irregular in nature. Very large latitudinal gradients occur frequently at the equatorward and poleward edges of the auroral zone.

Poleward of the auroral oval at magnetic noon, irregular F-region ionization of relatively high intensity is almost always observed. The irregularities in the structure of the high latitude ionosphere are reviewed in [Hunsucker and Greenwald, 1983].

2.3.3 Mid-latitudes

Of the geographic regions the mid-latitude region exhibits the least extreme behaviour. At mid-latitudes the magnetic field is neither close to vertical nor horizontal with the consequence that field aligned behaviour is not found as frequently as at other latitudes. On their poleward edge the mid-latitudes are defined by the auroral zones, these being the zones where the Earth's magnetic field lines are open to the vagaries of solar-induced events.

One of the most important features of the normal mid-latitude ionosphere is the seasonal anomaly in the F region, in that the maximum F2 layer densities at around 1200 hours (local time) in winter tend to exceed the corresponding summer values.

2.3.4 Equatorial latitudes

At the geomagnetic equator the Earth's magnetic field is horizontal. The equator is also at the juncture of the hemispheric winds in the atmosphere. Electric fields become important near the equator causing vertical drifts of ionization. As a consequence, the equatorial ionosphere is higher in altitude than at mid-latitudes with anomalous peaks in electron density either side of the equator. The equatorial ionosphere suffers from irregularities in electron density that can cause scintillation in radiowave propagation. During ionospheric storms, an ionospheric current system can form along the equator during the period of the storm.

2.3.4.1 Equatorial anomaly

It is well known from both ground-based and satellite observations that significant latitudinal gradients exist in the F-layer ionization at low latitudes and that the form of the trans-equatorial distribution of foF2 changes markedly with local time. Around sunrise a single maximum of ionization exists near the magnetic equator. Shortly thereafter, the latitudinal distribution of ionization changes sharply with the appearance of two crests separated by a narrow trough 2 to 5 degrees wide centred on the magnetic equator. By late morning the latitudinal separation of the crests has increased and the crests have increased in ionization density. Except in the northern winter, the northern crest is farther from the dip equator than is the southern, and in northern summer, the northern crest can reach its maximum latitude excursion several hours earlier than the southern crest. The time at which the crests are farthest from the magnetic equator varies with solar activity occurring in the early afternoon during solar minimum and in the early evening during solar maximum. Later the crests move equatorward, finally merging together to form a maximum of ionization above the equator.

It is now well established that the crest formation is explained by an "equatorial fountain" mechanism, connected with Hall drift, which is upwards when the electric field of the equatorial electrojet is in the eastward direction. Considerable day-to-day variability is seen in the time of onset, decay and maximum development of the anomaly. Marked differences can occur between the latitudinal distributions of foF2 observed on a particular day at the same local time, but separated in longitude by only 30°.

The latitudinal variation of foF2 across the equator is often asymmetrical; that is the critical frequencies at the two crests are appreciably different. This asymmetry appears to be due to thermospheric winds blowing across the equator from the sub-solar latitude; in general, the crest which lies farther from the sub-solar latitude will be the greater. In the topside ionosphere, however, the situation is reversed with the crest of the anomaly being more pronounced in the summer hemisphere.

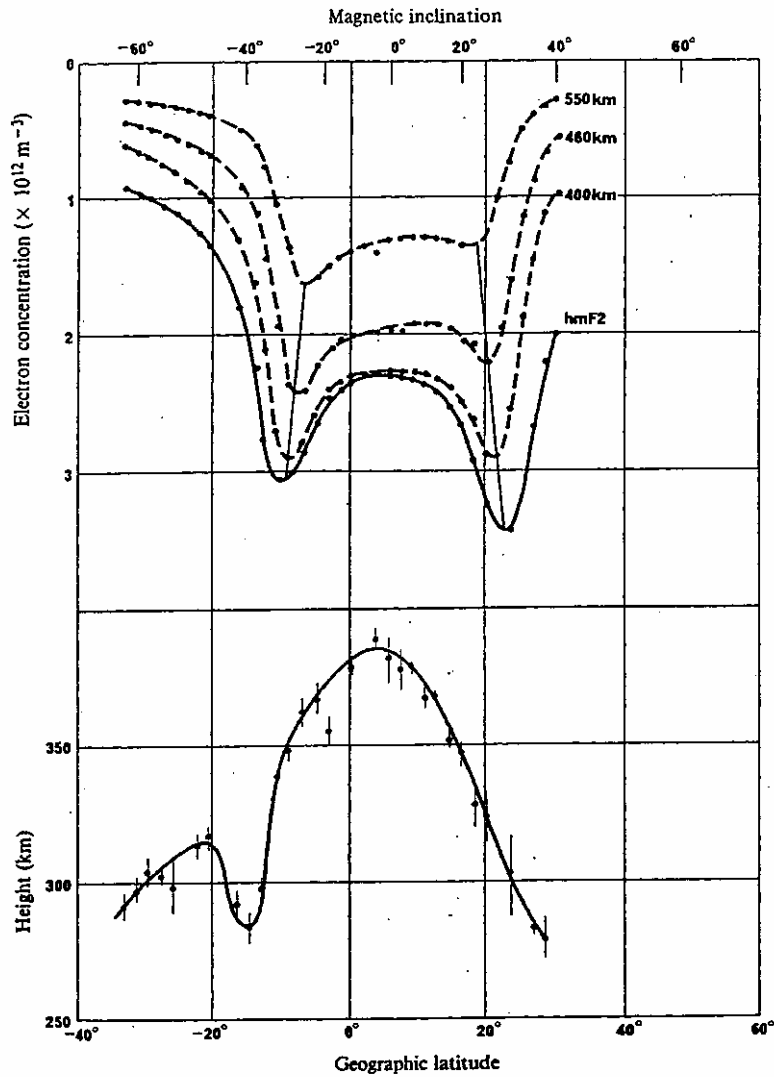


FIGURE 2.8

Data obtained from ISIS-I ionograms recorded on 27 October, 1969, at 160° E longitude, 1505 LMT. (*Upper section: latitudinal variations of NmF2 (continuous curve) and electron concentration at fixed heights in the topside ionosphere (broken curves). The thin lines join points which lie on a magnetic field line. Lower section: the corresponding variation of hmF2*)

Figure 2.8 shows an example of the structure of the topside ionosphere when the anomaly exists, together with the corresponding latitudinal variations of the F2 maximum electron density and height. The anomaly crests occur at the two points where a magnetically field aligned arch of enhanced ionization intersects the peak of the layer; this arch extends into the topside ionosphere to altitudes of the order of 1 000 km. The height of the layer peak is greatest (approximately 400 km) above the magnetic equator and decreases rapidly on either side to about 300 km near the location of the crests. During the development phase of the anomaly, the arch of enhanced ionisation moves

to higher magnetic field lines such that its top extends to greater altitudes and the crests move away from the equator. During the decay phase, there is evidence which suggests that the top of the arch decreases in altitude and the crests move back towards the equator. The time at which the anomaly develops and decays in different longitude sectors varies appreciably. The equatorial anomaly factor (the ratio of the mean foF2 at the two maxima north and south of the magnetic equator to foF2 at the magnetic equator) shows a longitude-dependent diurnal variation which appears as a difference between eastern hemisphere (60° E-150° W) and western hemisphere (120° W-30° E).

On magnetically disturbed days the anomaly crests are usually closer to the magnetic equator and the anomaly is not as well-developed as it is on quiet days. When the planetary magnetic index $K_p > 5$, the anomaly is absent.

2.3.4.2 Equatorial irregularities

Ionization irregularities in the F region tend to develop in the evening about one hour or so after local sunset and possess scale-sizes from about 3 m to more than 10 km. The irregularities appear to be associated with the change in the height of F layer above the dip equator during the evening. Generally the irregularities are more widespread in the equinoxes but may be different in different longitudes. Topside soundings carried out during sunspot maximum revealed that equatorial spread-F activity is high at longitudes from 45°W to 135°W in northern winter months and from 45°E to 135°E in northern summer months, while it tends to be widespread in the equinoxes. The occurrence probability of topside spread F shows two night-time peaks; one at post-sunset and the other pre-sunrise in the low latitude region. The occurrence frequency of intense spread ("bubbles") maximizes near 2300 hours local time. The occurrence of irregularities in the equatorial F region appears to decrease during times of geomagnetic disturbance.

The irregularities tend to be field-aligned with axial ratios of the order of 20 to 1. Satellite data suggest patch sizes of 100 to 2 000 km in the N-S direction and 500 to 3 000 km in the E-W direction. On the other hand, HF back-scatter data indicate patch sizes of 30 to 400 km, with a mean value of 100 km, in the E-W direction.

These earlier results have been corroborated and elaborated upon by the use of data from more detailed in situ satellite-borne measurements and ground-based scintillation observations. With the use of these data it has become fully appreciated that F-region ionization irregularities display significant longitudinal variability in addition to latitudinal and temporal dependencies. Details of these findings as well as the effect of equatorial irregularities on the performance of trans-ionospheric propagation systems can be found in the review by Aarons [1977].

Equatorial irregularities were found to extend up to about 600-1 000 km height in the topside ionosphere and that radio waves were ducted by small-scale field aligned irregularities (approximately 1 km length) which existed within large-scale field-aligned irregularity patches or bubbles (approximately 100 km extent). The electron density distribution within the ducts was not symmetrical with respect to the equator. When such regions are traversed by a probing radiowave, the associated Faraday rotation shows depletions of the electron content. Experimental evidence indicates that average depletions are of the order of 1.5 to 3.0×10^{16} electrons/m². Further, the amplitude scintillation rate may increase suddenly when these bubbles either form along or drift across the propagation path. There is evidence that there are also isolated enhancements in the ambient electron content, and these are accompanied by simultaneous decrease in fading rate, scintillation index, and the signal's average amplitude level [Tyagi *et al.*, 1982]. The generation of a

large-scale bubble can be very localized and the resulting large-scale irregularity patches may exist for several hours. The irregularities maximize in the June solstice at Asian longitudes and in the December solstice at American longitudes.

2.4 Solar cycle effects on propagation

2.4.1 Solar cycle

The longest-period variation in the energy emitted by the Sun is a cycle averaging eleven years in length, corresponding to the time between reversals in the solar magnetic polarity. The intensity of the solar emission is generally quantified by the sunspot number or Wolf number R , which has been recorded since the seventeenth century. For system studies a year or more ahead, a prediction of the 12-month running average R_{12} is used (Recommendation P.371). R_{12} is used for F2-layer critical frequency predictions up to one year, and the index Φ_{12} (Φ is the monthly mean of the daily values of solar radio noise flux at 10 cm wavelength, in units of $10^{-22} \text{ W m}^{-2} \text{ Hz}^{-1}$) is used for E and F1-layer predictions up to one year ahead ($\Phi_{12} = 63.7 + 0.728R_{12} + 8.9 \times 10^{-4} (R_{12})^2$). The F region reacts slowly to changes in the background solar activity, so that daily values of indices are of limited use.

R_{12} varies from a minimum of about 10 to a maximum generally of 100 to 150. Solar cycle predictions for more than a few years in the future can be in error by many months in the date of the minimum, and ± 20 in sunspot number, which is usually adequate for system studies. Note that ionospheric effects tend to saturate for R_{12} greater than about 150.

2.4.2 Annual cycle

There is an annual cycle of ionization in the upper ionosphere analogous to the seasonal variation in temperature at the Earth. In general, this results in less ionization in winter than in summer, with corresponding variation in propagation. However, at mid latitudes, maximum usable frequencies are higher in winter than in summer; the winter anomaly effect in the F2 layer.

2.4.3 Diurnal cycle

The effect of solar radiation during the day is to increase the ionization at all altitudes. The result is that propagation is improved during the day, but there is also increased absorption at low altitudes, particularly in the MF band and at the lower frequencies in the HF band.

2.5 Modelling of ionospheric properties

In designing and engineering ionospheric radio circuits it is often necessary to have a knowledge of the ionospheric properties in the region of radiocommunications application. These can be modelled mathematically in time and space and may then be used to calculate the appropriate propagation parameters to ensure optimum operation of radiocommunications systems. The types of models that are simplest and most used are those based on empirical data; the most complex are the physical models that calculate the ionospheric characteristics from first principles (e.g. continuity and momentum equations for the ionized species) [Anderson, 1993]. There are also hybrid, or semi-empirical, models that take elements of both types to try to achieve realistic results within reasonable limits of computation time and data requirements.

2.5.1 Empirical models

Empirical models are based on statistical descriptions of the ionosphere derived from large databases of measured data. As a general rule, an empirical model consists of a mean parametric model complemented by an electron density profile model. The purpose of the mean parametric model is to predict the mean (or median) value of a few basic ionospheric parameters, such as the

critical frequencies and heights of the layers, from a limited number of inputs (e.g. location, time, date, expected index of solar activity). The density profile model is then used to derive the whole vertical distribution of the electron density at the time and place of interest.

In one of the most widespread mean parametric models, spherical harmonic analysis is used to describe the spatial variations of the F-layer parameters. The model consists of a set of solar index dependent coefficients from which the monthly median values of the parameters can be computed for any location and time. The data set used to build the model was composed of ionosonde data measured at about a hundred locations in the world during periods of various solar activity. Two very similar sets of coefficients, known as "CCIR Oslo-66" and "URSI-90" coefficients, are currently in use.

Although a number of electron density profile models have been proposed for various applications, only three of them, which are of extensive use, will be mentioned here: the Bradley-Dudeney model [Bradley and Dudeney, 1973], the Bent model [Llewellyn and Bent, 1973] and the International Reference Ionosphere (IRI) [Rawer *et al.*, 1981]. The former model was intended for HF propagation prediction applications. Hence, only the bottom side profile is computed by making use of the parabolic approximation. In the Bent model, an analytic profile is fitted to the F2-layer critical frequency f_oF2 . The data used to build the model originated from both ground-based and satellite-based ionosondes. This model is particularly appropriate for applications to Earth-space systems when the Total Electron Content (TEC) is of prime importance. However, one limitation of the model arises from the absence of data during periods of high solar activity. In addition, the modelled profile does not account for the detailed shape of the layers, especially during the day. The latter problem has been given much attention in the IRI in which continuous profiles, accounting for the E, F1 and F2 layers are computed up to 1000 km of height. The IRI continues to be upgraded by incorporating the results of modelling efforts [Bilitza, 1990]. Models of the equivalent thickness of the ionosphere can also be included in this category [Klobuchar and Allen, 1970].

2.5.2 Physical models

Physical or first-principle models attempt to model the complex physical and chemical processes which occur within the ionosphere. These models permit investigation of the mechanisms which control the behaviour of the ionosphere. Although they have reached a state of development which permits advanced climatological studies to be undertaken they have not reached a state where they are suitable for routine operational use.

The ionosphere is immersed in the neutral atmosphere and geomagnetic field and is bounded above by the magnetosphere. This magnetospheric-ionospheric-atmospheric system is strongly coupled due to the influence of thermal flow, frictional interaction, electric and magnetic fields, and particle precipitation. Because of the extremely complicated nature of the complete system the principal emphasis of research effort has been on the development of realistic models of individual regions of the ionosphere. Although it is recognised that there is coupling between regions this coupling is frequently ignored, the effects of other regions being parameterized and used as inputs.

Existing models cover a wide variety of regions including the equatorial F region, mid-latitude F region, low and mid-latitude E region, high-latitude F region [Anderson, 1993] and coupled thermospheric-ionospheric models [Fuller-Rowell and Evans, 1987; Roble *et al.*, 1988; AGARD, 1989] using interplanetary parameters as input.

2.5.3 Hybrid models

One serious drawback of physical ionospheric models is their computational requirements. In addition, most of these models require input parameters that are not routinely measured. The recent development of hybrid models is directed towards providing the physical realism of first-principle models with the computational speed of empirical models. A hybrid model is constructed by running a physical model for a variety of conditions and parameterizing the resulting electron density profiles. These profiles can then be reconstructed for required conditions without the need for the user to run a full physical model.

Empirical models are notably deficient in their description of the low-latitude region. In an effort to improve this situation Anderson *et al.*, [1987] developed a semi-empirical low-latitude ionospheric model (SLIM) which calculates F-region O⁺ density profiles from 180 to 1 000 km between $\pm 25^\circ$ dip latitude. SLIM consists of a database of coefficients which reproduces profiles produced by a physical model of the equatorial F region for a variety of conditions. A subsequent development (FAIM or Fully Analytic Ionospheric Model) [Anderson *et al.*, 1989] extended this capability by integrating an analytic model of the low-latitude F region with the widely used Chiu empirical model [Chiu, 1975].

More recently, a global hybrid model (PRISM) has been developed [Daniell, 1991]. PRISM combines a parameterized ionospheric model (PIM) with a capability for near-real-time updates using data from ground-based and satellite-based sensors. PIM consists of databases created from a low-latitude F-region model, mid-latitude F-region model, low- and mid-latitude E-region model and a high-latitude (E/F) model.

2.6 Ionospheric variability and disturbances

The ionosphere varies in electron density distribution with time, season, location, and solar activity in a well defined way. However, overlaid on this behaviour is a much more sporadic and not well defined variability. In effect the ionosphere becomes disturbed beyond the regular variations. The nature of the variability is such that some causes can be distinguished and taken into account as distinct predictable events while others can only be described statistically. When designing radio systems, margins for fading caused by the day-to-day variability should be taken into account (Recommendation F.339). When operating a radio system, account should be taken of the discrete events as predicted and observed.

The causes of these disturbances have their origin in either the Sun or the Earth's atmosphere. They are classed as solar-induced and atmospheric disturbances. Because of the delay between the solar cause and the terrestrial effect, some of the solar-induced disturbances can be forecast and the expected effects anticipated and allowed for. On the other hand the disturbances of atmospheric origin are more difficult to predict and hence are usually allowed for by means of statistical expectations of their effects.

2.6.1 Solar-induced disturbances

Of the solar-induced effects on the ionosphere and radio propagation, ionospheric storms are the most significant in terms of duration (days). They also stand the greatest chance of being forecast and taken into account by changing frequency to match the changing ionosphere. SID, Sudden Ionospheric Disturbances, are sharp and short (minutes) disturbances that are difficult to foresee except in terms of probability of occurrence.

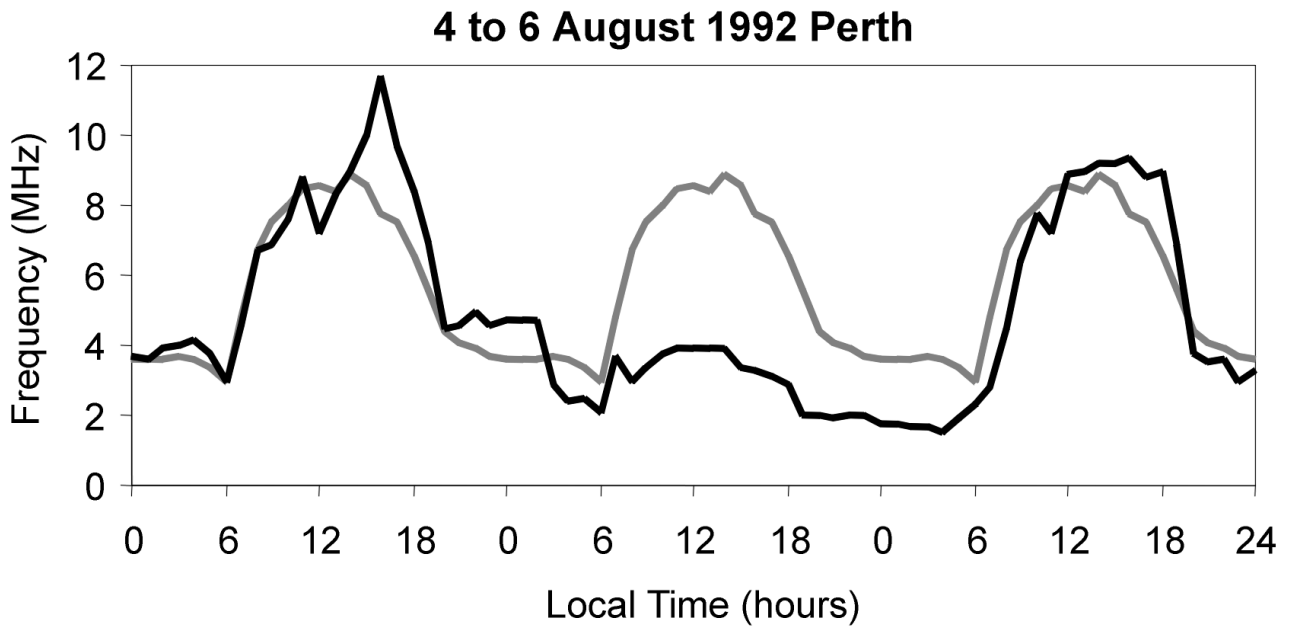


FIGURE 2.9

The effects of an ionospheric storm on F2-layer critical frequencies (broken line shows monthly median values)

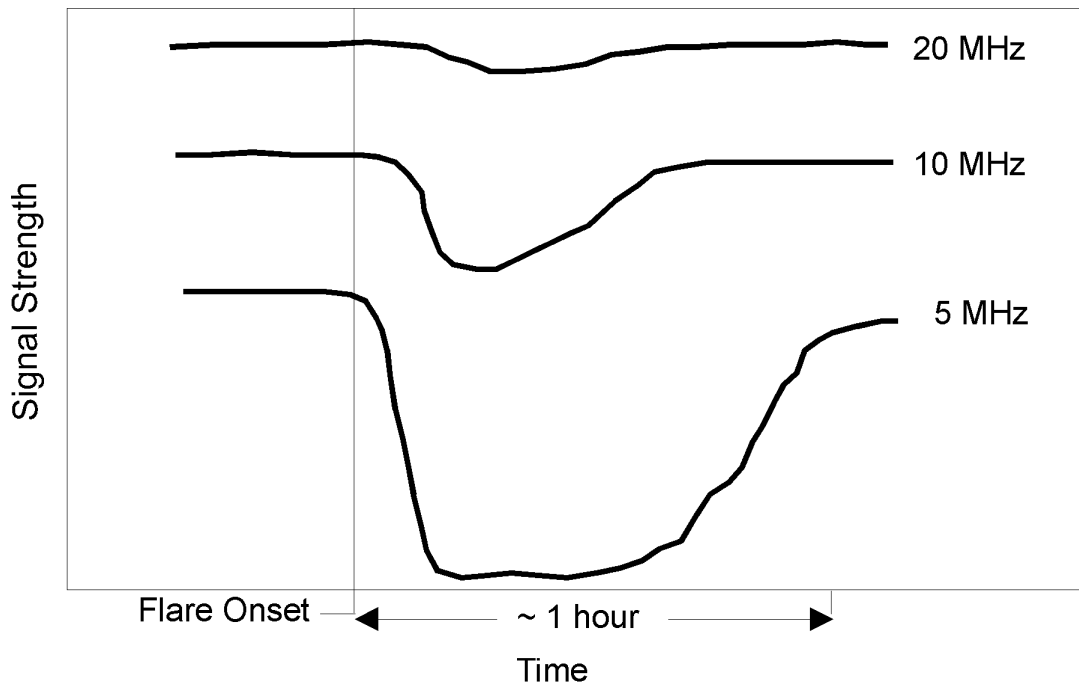


FIGURE 2.10

The effect of a short-wave fadeout

2.6.1.1 Ionospheric storms

The electron density of the ionosphere and its height distribution are sensitive to changes in the Sun's output that interacts with the Earth's upper atmosphere. Solar flares and other symptoms of solar emission can give rise to both enhanced and depressed electron density, and hence F2 critical frequencies, depending on the geographic location and time within the disturbance cycle. The average model of an ionospheric storm in terms of F2-layer critical frequencies is shown in Fig. 2.9. On average there is a positive enhanced phase followed by a negative phase of depressed critical frequencies. The amplitude of the positive phase is dependent on geomagnetic latitude. The magnitude of the positive phase increases towards the equator; at latitudes greater than about 35 degrees there is often very little evidence of such a positive phase to the storm.

The length of the storm, and the length of the positive phase, vary with the strength of the solar input and with the state of the ionosphere at the time of input, that is, the season and time of day at which the ionosphere is disturbed. However, the effect on the expected maximum frequencies varies during the daily regular progress of the build-up and decay of the ionospheric F layer.

Because it is the F2 layer that is most affected by the ionospheric storm, one of the common phenomena of the storm is the prominence of the F1 layer as the F2 layer is depressed. Once the F2-layer density has decreased below that of the F1 layer, the F1 layer will become the layer that carries the HF propagation and radio frequencies can be chosen to take account of this fact.

2.6.1.2 Sudden ionospheric disturbances (SIDs)

Sudden ionospheric disturbances are caused by X-ray emission from the Sun. As such the propagation time from Sun to Earth is the same as radio and light waves, and thus the cause cannot be seen before the SID event. The only forecast of such events is as a probability of occurrence based on the likelihood of an active region on the Sun erupting and producing an X-ray emission. Because of the nature of the cause, SIDs occur only in the sunlit zones of the Earth.

Once arrived at the Earth's upper atmosphere the X-rays cause increased electron production in most ionospheric layers. The penetration depends on the amplitude of the X-ray emission and the energy of the X-rays. The effect of the enhanced ionospheric density on the radio system in use depends on the frequency of operation. For example, at HF the greater density in the absorbing D layer causes increased signal attenuation and possibly complete loss of signal during the SID. At other frequency ranges, such as VLF, which use the D layer as a reflecting boundary, the signal intensity can be enhanced during the event.

The model of the Short Wave Fadeout (SWF) is typical of each event (Fig. 2.10), the build up to maximum absorption being shorter than the decay back to normal propagation. The duration of each SWF is dependent on its maximum amplitude. The effect on radio propagation is felt at the lower

frequencies first, proceeding towards the higher frequencies. Inversely, the return to normal starts from the higher frequency end and moves toward the lower frequencies, so that the lower frequencies suffer the longest SWF. The highest frequency affected depends on the intensity of the SWF maximum.

In the event of an SWF, or where an SWF is expected, the radio operator should, where possible, consider moving to higher frequency operation during the SWF.

2.6.2 Disturbances of atmospheric origin

The ionosphere is ionized and it is part of the upper atmosphere. It is therefore governed by both the Earth's magnetic field and any bulk changes in the atmosphere. Winds and waves in the neutral atmosphere affect the distribution of the ionization, and hence the refractive and reflective properties of the ionosphere.

2.6.2.1 Winter variability of D-region ionization

On some days in winter marked increases in ionization densities are observed throughout the D region. This phenomenon has been extensively studied in Europe and Canada, and is believed to be due to meteorological effects in the lower ionosphere.

The enhanced electron densities are attributed to increases in the number densities of normal ionizable constituents, and to decreases in electron loss rates. However, high energy particle electron drizzle associated with post-storm effects may dominate the winter variability of absorption at high latitudes. It is now clear that both "post-storm" effects and "meteorological" changes affect ionization densities, and that these phenomena can occur together [Belrose, 1981].

2.6.2.2 Travelling ionospheric disturbances (TIDs)

Gravity waves in the atmosphere cause travelling waves in the ionosphere that appear to a radiowave as a rippled surface of electron density, the wavelength of the ripple being related to the atmospheric wave. The effect of this on radio propagation is to defocus the wave if the beamwidth covers more than a full wavelength of the TID or to periodically focus and defocus the signal if the beamwidth covers less than the TID wavelength. Therefore TIDs can give rise to fading in radio systems and in the case of radiolocation systems, can give faulty measurement if not corrected.

The average period of TIDs is 20 minutes, that is to say the rise and fall of the height of an isofrequency level in the ionosphere follows a 20 minute cycle. Since TIDs are caused by the atmospheric dynamics, they are regional in their characteristics but many of the major TIDs are caused by sudden heating in the auroral regions which propagate toward the equator.

REFERENCES
FOR CHAPTER 2

- AARONS, J. [1977]. Equatorial scintillations: A review., *IEEE Trans. Ant. Prop.*, 25, 729-736.
- AGARD [1989] Ionospheric structure and variability on a global scale and interactions with the atmosphere, *AGARD Conf. Proc.*, CP441.
- AKINYAN, S.T., CHERTOK, I.M. and ZHULINA, E.M. [1980]. Determination of PCA value from the characteristics of solar radio bursts. *Solar Terrestrial Predictions Proc.* Vol. III, Ed. R.F. Donnelly, D27 to D33, US Govt. Printing Office, Stock No. 003-017-00473-2, Washington, DC 20402.
- ANDERSON, D.N [1993]. Global ionospheric modelling, *Modern Radio Science 1993*, Ed Hiroshi Matsumoto, Oxford University, Press, Oxford, 159-188.
- ANDERSON, D.N., M. MENDILLO and B. HERNITER [1987]. A semi-empirical low-latitude ionospheric model, *Radio Science.* 22, 292-306.
- ANDERSON, D.N., J.M. FORBES and M. CODRESCU [1989]. A fully analytic low and middle latitude ionospheric model. *J. Geophys. Res.*, 94, 1520-1524.
- BELROSE, J.S. [1981] The Propagation Medium: An Overview. *AGARD Conf. Proc. No. 305* on Medium, Long and Very Long Wave Propagation (at Frequencies less than 3 000 kHz), pp. 1.1 - 1.18. Ed. J.S. Belrose. Avail: NTIS (Ref. NASA Access. No. N82-27513).
- BELROSE, J.S. [1988] HF communications and remote sensing in the high-latitude region, *AGARD LS No. 162* Media Effects on Electronic Systems in the high-Latitude Regions, ISBN 92 835-0478-X.
- BILITZA, D. [1990] International Reference Ionosphere, Rep. NSSDC/WDC-A-R/90-22, Lanham, Maryland.
- BRADLEY, P.A. and DUDENEY, J.R. [1973] A simple model of the vertical distribution of electron concentration in the ionosphere, *J. Atmos. Terr. Phys.*, 35, 2131-2146.
- CHAPMAN, S. [1931]. The absorption and dissociative or ionizing effect of monochromatic radiation in an atmosphere on a rotating earth. *Proc. Roy. Soc.* 43, 26.
- CHAPMAN, S. [1963] Geomagnetic nomenclature. *J. Geophys. Res.*, 68, 1174.
- CHIU, Y.T. [1975]. An improved phenomenological model of ionospheric density. *J. Atmos. Terr. Phys.*, 37, 1563-1570.
- CLIVER, E.W., SECAN, J.A., BEARD, E.D. and MANLEY, J.A. [1978]. Prediction of solar proton events at the Air Force Global Weather; Space Environment Forecasting Facility. *Effect of the Ionosphere on Space and Terrestrial Systems.* Ed, John M. Goodman, US Govt. Printing Office 0-277-182, 393-400 Washington, DC 20402.
- DANIELL, R.E. [1991]. Parameterised real-time ionospheric specification model: PRISM Version 1.0, Tech. Rep. PL-TR-91-2299, Phillips Lab., Hanscom AFB, Mass. 01731.

- DAVIES, K. [1990]. *Ionospheric radio*, IEE electromagnetic wave series 31, Peregrinus Press, London.
- FELDSTEIN, Y.I. and STARKOV, G.V. [1967]. Dynamics of auroral belt and polar geomagnetic disturbances. *Planet and Space Sci.*, Vol. 15, 209-229.
- FULLER-ROWELL, T.J. and D.S. EVANS [1987]. Height-integrated Pedersen and Hall conductivity patterns inferred from the TIROS-NOAA satellite data. *J. Geophys. Res.*, 92, 7606-7618.
- GUSTAFSSON, G. [1970]. A revised corrected geomagnetic coordinate system. *Arkiv for Geophysic.*, 5, 595-617.
- HAKURA, Y. [1965]. Tables and maps of geomagnetic coordinates corrected by the higher order spherical harmonic terms. *Rep. Ion. and Space Res. Japan*, Vol. 19, 121-157.
- HALCROW, B.W. and NISBET, J.S. [1977]. A model of F2 peak electron densities in the main trough region of the ionosphere. *Radio Sci.*, Vol. 12, 815-820.
- HARDY, D.A., GUSSENHOVEN, M.S. and HOLEMAN, E. [1985] - A statistical Model of Auroral Electron Precipitation. *J. Geophys. Res.*, Vol. 90, A5, 4229-4248.
- HOLZWORTH, R.H. and C.-I. MENG [1975]. Mathematical representation of the auroral oval. *Geophys. Res. Letters*, 2, 377-380.
- HUNSUCKER, R.D. and GREENWALD, R.A. (Guest Eds.) [1983]. Including special papers: radio probing of the high latitude ionosphere and atmosphere: new techniques and new results. *Radio Sci.*, Vol. 18, 6.
- LARSEN, T.R. [1974]. Irregular variations in the high latitude ionosphere and their effects on propagation. *ELF-VLF Radio Wave Propagation*, 171-185, Ed. J.A. Holter, D. Reidel Publishing Co., Dordrecht, Netherlands.
- LLEWELLYN, S.K. and BENT, R.B. [1973] Documentation and description of the Bent ionospheric model, Rep. AFCRL-TR-73-0657, Indialantic, Florida, USA.
- KLOBUCHAR, J.A. and ALLEN, R.S. [1970] A first-order model of total electron content group path delay for a midlatitude ionosphere, Rep. AFCL-TR-70-0403, Bedford, Mass, USA.
- McILWAIN, C.E. [1966]. Magnetic coordinates. *Space Sci. Rev.*, 5, 585-598.
- MULDREW, D. F. [1965] F-layer ionization trough deduced from Alouette data, *J. Geophys. Res.*, 70, 2635-2650.
- RAWER, K., LINCOLN, J.V., CONKRIGHT, R.O. [1981] International Reference Ionosphere 79, Rep. UAG 82, WDC-A, Boulder, Colorado, USA.
- RISHBETH, H. [1989] F-region storms and thermospheric circulation, in *Electromagnetic Coupling Polar Clefts and Caps*, Proc. of the NATO Advanced Research Workshop, Lillehammer, September 20-24, 1988, Dordrecht, pp. 393-406.
- ROBLE, R.G., E.G. RIDLEY, A.D. RICHMOND and R.E. DICKINSON [1988]. A coupled thermosphere/ionosphere general circulation model. *Geophys. Res. Letters*, 15, 1325.
- TYAGI, T.R., YEH, K.C., TAURIANEN, A. and SOICHER, H. [1982]. The electron content and its variation at Natal, Brazil. *J. Geophys. Res.*, Vol. 87, 2525-2532.

- URSI [1993]. *Review of Radio Science 1990-1992*, Ed. W. Ross Stone, Oxford University Press, Oxford, p 507.
- WHALEN, J.A. [1970]. Auroral oval plotter and monograph for determining corrected geomagnetic local time, latitude and longitude for high latitudes in the Northern Hemisphere, Air Force Cambridge Research Laboratories, Report No. QAFCL-70-0422, Environment Research Paper, No. 327, AD 713170.

BIBLIOGRAPHY

- AKASOFU, S-I and CHAPMAN, S. [1972]. *Solar-terrestrial physics*, Oxford University Press, Oxford.
- FRANKE, S.J. [1993]. A review of recent progress in ionospheric propagation modeling. *Review of Radio Science 1990-1992*. Ed. W. Ross Stone, Oxford University Press, Oxford, 523-553.
- GOODMAN, J.M. [1992]. *HF Communication: Science and Technology*, Van Nostrand Reinhold, New York.
- MAURITS, S.A. and IVANOV-KHOLODNY, G.S. [1993]. Ionospheric structure and modelling. *Review of Radio Science 1990-1992*, Ed. W. Ross Stone, Oxford University Press, Oxford, 491-521.
- McNAMARA, L.F. [1991]. *The ionosphere: communication, surveillance, and direction finding*, Krieger Publishing Company, Malabar, Florida.

CHAPTER 3

IONOSPHERIC PROPAGATION

All radiocommunication is by means of electromagnetic waves having frequencies less than 3 000 GHz (by definition), although frequencies above 300 GHz are rarely used. Radiowave propagation varies greatly with the frequency of the radiowave and with the medium used to carry the wave (troposphere, ionosphere or space), and the techniques used for radiocommunication vary accordingly. Near the Earth, radiowaves having frequencies less than 30 MHz (i.e. wavelengths greater than 10 metres) are affected mainly by the characteristics of the Earth's surface and the ionosphere, but very little by the troposphere.

TABLE 3.1

The radio spectrum

Band	Frequency range	Wavelength	Principal propagation mode
ELF	< 3 kHz	>100 km	Waveguide/Groundwave
VLF	3 - 30 kHz	100 - 10 km	Waveguide/Groundwave
LF	30 - 300 kHz	10 - 1 km	Waveguide/Sky-wave/Groundwave
MF	300 - 3 000 kHz	1 000 - 100 m	Sky-wave/Groundwave
HF	3 - 30 MHz	100 - 10 m	Sky-wave
VHF	30 - 300 MHz	10 - 1 m	Line of sight
UHF	300 - 3 000 MHz	1 000 - 100 mm	Line of sight
SHF	3 - 30 GHz	100 - 10 mm	Line of sight
EHF	30 - 300 GHz	10 - 1 mm	Line of sight
	300 - 3 000 GHz	sub-millimetric	

In the VLF and LF bands at frequencies below about 100 kHz (wavelengths greater than 3 km), propagation is by wave-guide mode, that is the radiowave propagates through a channel bounded by the ground and the lower ionosphere at about 70 to 90 km height.

Higher frequency radiowaves in the LF, MF and HF bands, up to about 30 MHz, can travel either directly along the Earth's surface (ground-wave propagation) or by successive reflections between the Earth and the ionosphere (sky-wave propagation). Although the ground-wave is employed by services such as radionavigation and broadcasting, it has limited range at the higher frequencies and over land, and is not considered in this Handbook. On the other hand, sky-wave propagation can provide medium- to long-range communication at MF and HF. In the ionosphere, a major factor is the frequency of the wave compared with the critical frequency of the ionospheric layers although other factors such as absorption and noise are significant.

At frequencies above 30 MHz, radiowaves travel directly from point to point, and can pass through the ionosphere. They are therefore used for both terrestrial and Earth-space communication. In the VHF and UHF bands the effects of the terrain and the troposphere predominate, and are taken into account in system design. The ionosphere can cause interference to terrestrial services due to unwanted propagation modes. Sky-wave propagation above 30 MHz can be caused by higher-than-normal ionospheric ionization due to sporadic-E, meteor-trail or auroral ionization. At UHF and higher frequencies, the Earth-space services must cope with additional ionospheric effects. These effects are due to the total electron content along the path, leading to absorption, depolarization, group delay, dispersion and scintillation of the signal.

3.1 Waveguide propagation

In the frequency bands ELF (< 3 kHz), VLF (3 - 30 kHz), and LF (30 - 300 kHz) propagation takes place within the concentric sphere duct between the ionosphere and the ground. Only at LF (above about 100 kHz) does the sky-wave become distinguishable from the ground-wave. At all the lower frequencies the ground-wave fills the duct and its characteristics are governed by the height and shape of the ionospheric-ground waveguide, in the same way as microwaves propagate through waveguides.

The boundaries of the waveguide are dependent on the conductivity profiles of the waveguide. Thus at ELF and VLF frequencies the wave can propagate many tens of metres below the Earth or sea. The upper boundary at these frequencies is formed by the D region of the ionosphere, the height of which changes with day and night and is reduced by intense solar activity.

The distance separating the boundaries is less than the wavelength of radiowaves at ELF and VLF and consequently the waves propagate as a pattern of electric fields.

3.2 Sky-wave propagation

Sky-wave propagation may be represented by rays reflected between ground and ionosphere. In the ionosphere, the radiowaves experience dispersion (both velocity and refraction vary with frequency) and changes in polarization. The propagation is affected by the operating frequency, the electron density, ground conductivity and elevation angle.

Radiowaves in the ionosphere undergo continuous refraction (bending of the ray path). At any given point, refraction is less at lower electron densities, for higher frequencies (since the wavelength is shorter) and for higher elevation angles. For any given elevation angle, there will exist a certain frequency below which the rays will be reflected back to Earth. Also, for a given frequency, a ray launched with an elevation angle greater than the "critical angle" will not be reflected. At a higher frequency or at a greater elevation angle, the refraction is too low for the ray to be returned to Earth.

Waves launched vertically may be reflected, if their frequency is below the "critical frequency" as determined by the maximum electron density of the ionospheric layer. As the frequency is increased beyond this, the ray will penetrate the layer.

The apparent height of reflection varies between about 100 and 300 km depending on the operating frequency relative to the critical frequency of the ionospheric layers. Radiowaves that are launched more obliquely in most cases travel to greater range. The maximum range attained after one ionospheric reflection (one hop) arises for rays launched at Earth-grazing incidence. For typical E, F1 and F2 layers, it is respectively 2 000, 3 400 and 4 000 km.

At frequencies above the critical frequency there is an area surrounding the transmitter defined by the "skip distance" in which the sky-wave cannot be received because the elevation angle is too high and the wave passes through the ionospheric layer. The skip distance increases as the wave frequency increases. The maximum usable frequency (MUF) may be considered to be the frequency that makes the distance from the transmitter to a given reception point equal to the skip distance.

Some sky-wave propagation into the skip zone is possible in reality because energy is scattered from the ground back towards the transmitter site (ground back scatter). In addition, some energy is scattered into the skip zone by ionospheric irregularities.

The MUF increases with the path length and decreases with the height of the ionospheric layer. The Earth's magnetic field causes the radiowave to be split in two polarized components, the ordinary (O) and extraordinary (X). These ordinary and extraordinary waves travel along different ionospheric paths. The O wave is refracted less than the X wave and is reflected from a greater height and so has a lower critical frequency and MUF. For propagation between a pair of fixed terminals the path MUF is the greatest of the individual MUFs for reflection from the different layers.

3.3 Trans-ionospheric propagation

At frequencies that pass through the ionosphere (VHF and above) the trans-ionospheric paths are characterized by the properties of the ionosphere through which they have passed. These effects may be realized as fluctuations in amplitude (scintillation), in direction, in time delays and phase variability. Any irregularity in the path will have a corresponding effect on the received signal. These irregularities in ionospheric density are most prevalent near the magnetic equator and the polar regions.

BIBLIOGRAPHY

Hall, M. P. M., Barclay, L. W., and HEWITT, M. T. (Eds) [1996]. *Propagation of Radio Waves*, Institution of Electrical Engineers, London.

CHAPTER 4

PROPAGATION AT VERY LOW FREQUENCIES BELOW ABOUT 500 kHz

4.1 ELF, VLF and LF propagation

The LF band (30 - 300 kHz) provides for navigation and communications to intermediate distances, shorter than the global distances afforded by VLF (3 - 30 kHz) but longer than ground-wave distances characteristic of the MF broadcasting band (535 - 1705 kHz), although MF sky-wave signals propagate to great distances with relatively low loss at night. The use of frequencies in the LF band is limited by the available bandwidth and certain practical considerations discussed below. In this frequency range, at distances where the surface wave becomes too weak to be useful (a distance of the order of 500 to 1 500 km which depends on frequency, time of day, season, epoch of the solar cycle, and Earth surface condition), propagation, particularly at LF and below, continues between the Earth and the lower boundary of the ionosphere to great distances and is characterized by good reliability and stability. For a given radiated power, increased field strength is obtained with decreasing frequency, down to frequencies of 10 to 20 kHz [Watt, 1967] and the diurnal, seasonal and solar cycle variations become smaller. The maximum in the absorption of ionospheric radiowaves lies in the frequency range 100 kHz to 1 000 kHz. Owing to the long wavelengths involved, fading is characterized by spatial variations as the waves or modes add vectorially. Comprehensive reviews of propagation in the VLF/LF range are given by Belrose [1982, 1990].

Marine communications often use LF and VLF, which can also be used for point-to-point communications at times of severe ionospheric disturbances to HF circuits, since the lower frequencies are not in general adversely affected, an exception being solar proton events affecting long range transpolar VLF circuits which traverse arctic or Antarctic ice caps. Communication to points under the sea or beneath the ground can be achieved on these frequencies. Propagation has been assumed to be essentially by way of vertical polarization, which at long distances is well preserved. A limitation is the need for large transmitting antenna installations and high transmitter powers. Another limiting factor is the increasing level of atmospheric noise with decreasing frequency (noise generated in the Earth's ionosphere can also become important at the lowest frequencies on some occasions in high latitudes), and thus, apart from the small total bandwidth available, services generally use a fairly narrow bandwidth and hence low communication rates. Because of the stability of propagation (amplitude and phase), frequencies in the VLF/LF range are useful not only for communication but also for standard frequency and time broadcasts [Blair *et al.*, 1967], as well as navigation systems employing CW phase comparison or direction-finding techniques.

The ELF band (< 3 000 Hz) has deficiencies when compared with conventional radiocommunication bands. Its restricted bandwidth implies very low data rates, and because of the very large wavelength, transmitting antennas are inefficient, as measured by radiated power. However, for specific applications where part of the propagation path involves lossy media such as rock, soil and water, ELF offers the possibility of communicating whereas conventional bands offer none. Even at VLF (3 to 30 kHz) where the wavelength is one to two orders of magnitude smaller, efficient transmitting antennas must be large costly structures with high transmitting power if global communications are desired, particularly to points under the sea or ground.

In describing propagation, it will be found useful to consider whether the transmission is by way of a once-reflected sky-wave together with the surface wave, or whether waves reflected more than once from the ionosphere contribute to the received field strength. These considerations depend on frequency, distance, Earth surface conditions, and ionospheric conditions [Wait, 1962].

The mode theory, which is used extensively at VLF and may be used efficiently at LF up to at least 60 kHz, is a full wave theory that includes diffraction and surface wave propagation. The waves are considered to propagate between the Earth and the ionosphere as normal modes, analogous to microwave propagation in a lossy waveguide [Budden, 1985]. For frequencies above about 30 kHz the waveguide is many wavelengths high and for short distances many propagating modes must be considered but at VLF and distances greater than 1 000 km only a few modes need be considered. While the physical picture of waveguide mode theory is less easy to visualize compared with ray-paths it provides a better explanation of certain features of VLF propagation which are not readily explicable on ray-path/wave-hop theory.

4.2 Propagation characteristics

In the Earth-ionosphere waveguide the phase of the VLF field may display short-term variations caused by the irregular nature of the boundaries of the waveguide, in addition to long-term variations associated with diurnal and seasonal changes in the ionosphere. Superimposed on these regular variations are phase changes due to ionospheric disturbances caused by solar X-ray flares, and by energetic particle precipitation into the D region, associated with geomagnetic and auroral storms, and with solar proton events. All of these phenomena affect VLF transmission phase, and they are associated with different time and space scales.

4.2.1 The waveguide mode propagation of VLF waves to great distances

The propagation of VLF over very great distances is usually described in terms of waveguide modes where the electromagnetic waves are guided between the two reflecting boundaries, the finitely conducting curved Earth and the imperfectly conducting anisotropic curved ionosphere with dipping magnetic field.

The approximate electric field patterns within the Earth-ionosphere waveguide are illustrated in Fig. 4.1. For distances out to the first major null (distances of about 700 km) the E field patterns are rather complex. Several modes contribute to the total field: the TM (transverse magnetic) mode is the primary contributor to the fields at VLF and modes 1 to 3 have been considered. Usually after the first major null (which in the wave-hop concept is due to the ground and total sky-wave being in antiphase), the first mode becomes dominant and the patterns for greater distances become appreciably more regular. The figure illustrates also the waveguide field changes due to changing solar illumination (day-to-night transition), and due to a change of the Earth conductivity (land-to-sea boundary).

Because of the effect of the Earth's magnetic field there is strong non-reciprocity between east-west and west-east propagation; the attenuation is markedly less for propagation from west-to-east [Hanselman, *et. al.*, 1964]. Propagation in north-south directions give intermediate attenuation rates. At the magnetic equator there is little dependence of the phase velocity on direction of propagation.

VLF and LF transmitters in common use radiate a vertically polarized field. Although the ionosphere and terrestrial magnetic field may, in principle, introduce a horizontally polarized component, there is no experimental evidence which demonstrates that such fields are significant at great distances. Theoretical calculations [Foley *et al.*, 1973] suggest, however, that at night in low latitudes there may be considerable horizontal polarization.

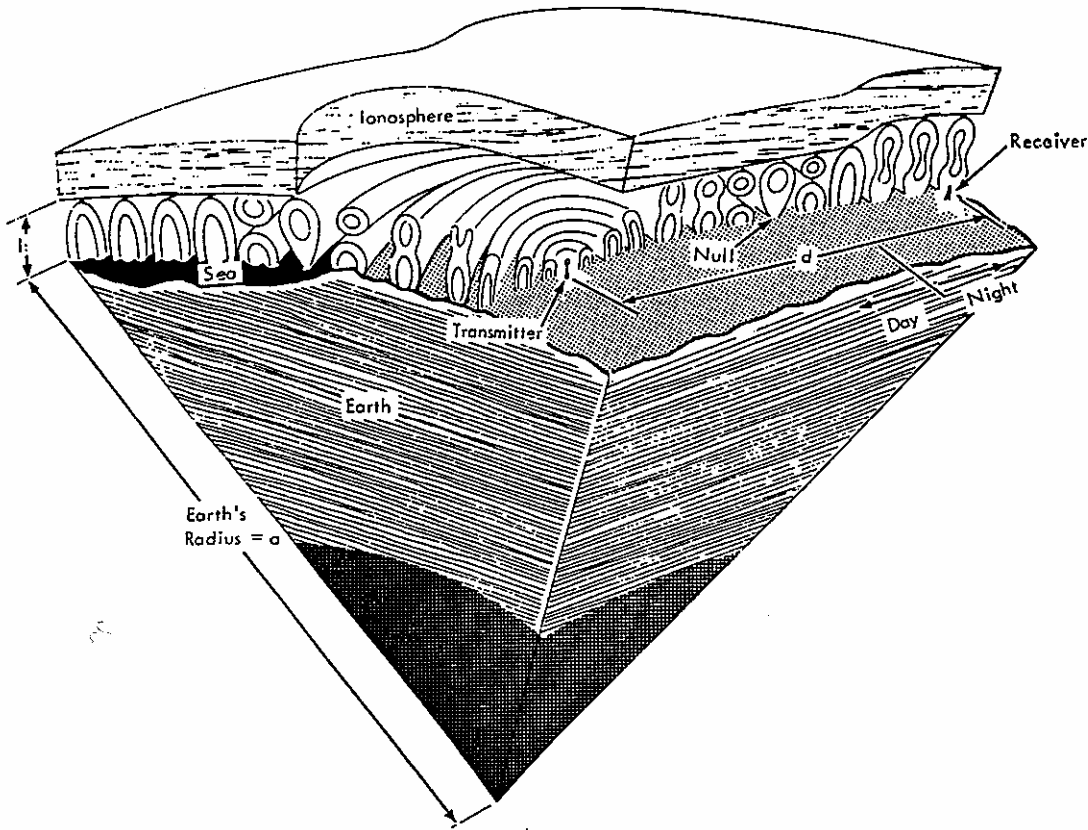


FIGURE 4.1

Schematic electric field modes within the Earth-Ionosphere waveguide

4.2.2 Normal diurnal variations of phase and amplitude at middle and low latitudes

There are marked changes in both amplitude and phase at dawn and dusk. These and the differences between propagation at night and day, are explained by a change in waveguide modes due to a lowering of the base of the ionosphere during daylight and a change of its conductivity (Fig. 4.2). For propagation over shorter paths, less than 3 000 km, more waveguide modes must be taken into account, the number of nodes required to explain propagation increases as the distance decreases. For distances less than 1000 km it is more practical to use the wave-hop concept of propagation rather than waveguide propagation, although both interpretations give the same result.

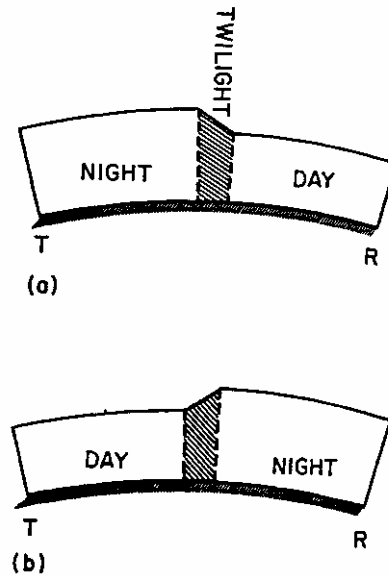


FIGURE 4.2

Schematic model of the ionospheric waveguide height at sunrise/sunset

4.2.3 Phase stability

VLF transmission phase stability is an important parameter which must be considered for such applications as VLF navigation, frequency comparison and time synchronization. For such applications, if the user has a choice of transmission paths, as for example was possible with the Omega navigation system, those which are dominantly single mode should be employed. When two or more modes are present, the phase stability of the total field will vary with distance in a complex oscillatory manner and will clearly be worse for some ranges of distance. The use, for example, of VLF transmissions over distances less than 1,000 km should be avoided, since it is in this distance range that the first major minimum is found. This minimum in field strength is associated with an anti-phase relation between two components, a ground- and a sky-wave of almost equal amplitude. In this distance range the diurnal variation of phase can be unpredictably asymmetrical, since the direction of rotation of the phase of the resultant depends on which component is stronger at the time.

While multi-mode propagation is particularly severe at short distances, it can be a problem at all distances. The magnitude of the effect is a function of frequency, distance, time-of-day and ground conductivity. Phase stability is clearly worse in the vicinity of field strength minima (Figs. 4.3).

The regular variations of VLF phase, and the changes associated with ionospheric disturbance have been studied by many researchers, and there is a great deal of information available in the literature [Belrose, 1982]. However, there are few statistical studies that are useful for the design of systems. Watt [1967] has summarized data available at that time, and has shown how the standard deviation of phase varies as a function of frequency (for the 10 - 20 kHz band), distance (for paths $d > 1,000$ km) and time-of-day (day and night conditions). Pan and Tian [1988] have published results of a study in China of 12.5 kHz phase stability for 500 - 3,000 km north-south paths under night-time conditions and have developed a mathematical expression for the standard deviation of phase that takes into account multi-mode effects.

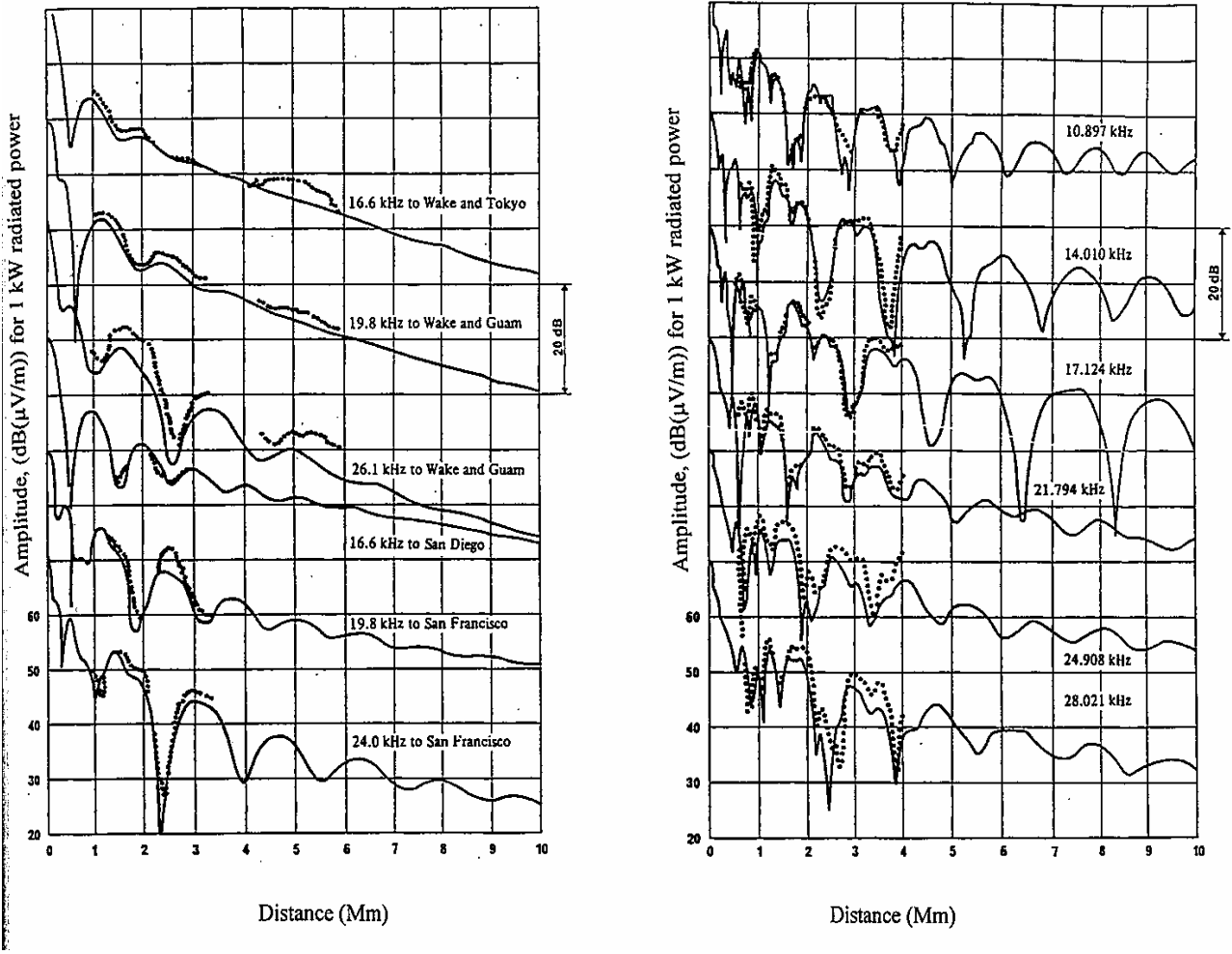


FIGURE 4.3

Propagation (full line - predictions; dotted line - observations) over the Pacific Ocean from Hawaii (a- daytime, summer; b- night-time winter)

Measurements of 100 kHz signals, transmitted from Y station of the north-west Pacific chain of the Loran-C navigation system (Okinawa, Japan) and received at Lintong, China (distance 2 006 km), have been conducted continuously during 1980-1988 and they show that the phase delay and the field strength of a 100 kHz one-hop sky-wave vary with the solar cycle, the season and the time of day. For instance, the monthly mean value of the hourly delay for noon in winter is about 2.5 μs greater than that in summer for the same year. As for the same season in different years, the delay at solar minimum is about 1 μs greater than that at solar maximum. The increments in the monthly mean value of the hourly delay corresponding to the period from 0880 hours to 1200 hours local time are about 4.5, 3.5 and 2.5 μs for winter, spring or autumn, and summer respectively, showing regularity of variation with the solar zenith angle [Pan *et al.*, 1988]

4.2.4 Fading of the waves

The simplest parameters to measure are the fading speed (number of maxima/hour) and the depth of fading; both depend on frequency, transmission distance, time of day and ionospheric conditions (normal, abnormal).

When the amplitude and phase of VLF/LF signals are observed as a function of time, the gross diurnal changes in both amplitude and phase are readily apparent. Apart from these regular changes, there are random variations which may result from changes in the height of the ionospheric reflection, changes in reflection coefficients, focusing or defocusing of the wave by the ionosphere, interference between the various waves which may reach the receiver. In considering the reflection of waves from the ionosphere, the fading of the signals and the effects of small local changes in ionospheric properties, it must be realised that the wave energy that reaches a receiver does not come from a point in the ionosphere, but from an elliptical area in the ionosphere, centred on path midpoint, defined as the Fresnel zone. Calculations have shown that the Fresnel zone at LF can be quite large, e.g., in the case of 100 kHz waves propagated over paths of length 1 000, 1 500 and 2 000 km the minor and major axis of the first Fresnel zone are 55 and 290 km, 72 and 600 km, and 76 and 1 110 km respectively. The Fresnel zone is proportionally larger at VLF. Since the ionospheric parameters over dimensions approaching a Fresnel zone are irregular and non-stationary, fading results.

4.2.4.1 Daytime fading

The daytime sky-wave appears to be dominantly a “specular like” reflection from a “rather smooth” reflecting layer, especially at oblique incidence and at the lower frequencies; since the amplitude is substantially constant, and the phase changes in a regular way, the phase changes being due almost entirely to bodily movements of the reflection height. The sky-wave amplitude becomes less regular at frequencies near the upper end of the LF band. While the amplitude does fade in a somewhat irregular manner, the phase fading is always appreciably less, and for transmissions on different frequencies over paths which are closely the same there is often a noticeable correlation, confirming that even at night, and especially by day, the dominant phase change is due to reflection height changes.

4.2.4.2 Night-time fading

The sky-wave field is less regular during the night-time. The phase fluctuations contain a random component superimposed on the component due to bodily movement of the reflection height. The probability distribution of amplitudes has been found to be more nearly log-normal than Rayleigh. This implies that the amplitude assumes large values more often than would be expected on a Rayleigh distribution.

The fading of VLF/LF signals seems to be made up of two components, with quite different amplitudes and fading speeds. The fading of the dominant component, which is relatively independent of frequency, has a substantially constant quasi-period of about 7 minutes. This component is readily recognised at steep incidence, but difficult to recognise at oblique incidence, and at the lower frequencies. Superimposed on this slow fade is a smaller component whose fading speed is more rapid. The fading speed of this component varies somewhat from time to time, but when simultaneous observations are made at a number of frequencies, it varies directly with the equivalent frequency, $f \cos i$ (angle of incidence at the ionosphere). During magnetic storms the amplitude and speed of this faster component increases, and it can, in fact, become the dominant component.

4.2.5 Variations during ionospheric disturbances

The ionospheric disturbances which severely affect long range VLF propagation are those resulting from or associated with solar flares, solar proton events, magnetic storms and high altitude nuclear detonations.

Solar flares normally cause sudden increase in phase, that is a decrease in phase lag (sudden phase anomaly), and an increase in signal level for frequencies above about 16 kHz, when the path is sunlit. These two effects can be interpreted as resulting from increased ionisation below the normal D region, caused by solar X-rays, together with an increase in the height gradient of the ionisation at the lower boundary. The change in effective height of reflection may be as much as 10 km. The effects usually last from some tens of minutes to an hour or so, with the onset being much more rapid (2-10 minutes) than the recovery (0.3-3 hours). There seems to be little relationship between the size of the phase perturbation and the optical classification of the flare. In general the magnitude of the phase perturbation increases with the length of the sunlit path, but this proportionality depends on the zenith angle of the Sun, (χ).

Polar cap disturbances follow a few hours after certain solar flares. They are caused by extra ionisation in the D region. The duration of the disturbance depends on the magnitude of the solar proton event, and is also a function of latitude. For large events the disturbance lasts for periods up to a few hours at mid-latitudes, to days (10-20 days) for high latitude trans-polar VLF paths. The associated phase lag and amplitude decreases for VLF signals propagating across the Greenland icecap are consistently larger than those for transmission paths which do not cross Greenland, thus such paths are very sensitive for the detection of proton events. Practical VLF circuits between Europe and North America which traverse Greenland over the short great-circle route also traverse Antarctica over the long great-circle route, and, since protons affect both polar caps the increased attenuation over the long path is even greater than over the short path. Since attenuation rates change from 1.3 to 22 dB/1 000 km during the course of the normal night-to-day change for signals which traverse the Greenland icecap, and since the excess ionisation associated with the proton event results in a further enhancement of the daytime ionisation levels, it is reasonable to anticipate a further increase in attenuation rate.

Magnetic storms and associated auroral phenomena at high latitudes, which are believed to be due to precipitation of energetic electrons into the lower ionosphere resulting in abnormal ionisation densities in the D region, also affect VLF propagation over long paths. Unlike solar flare effects and polar cap events which affect a wide region simultaneously, electron precipitation events are more localised in space and time. Their effect on VLF propagation over long paths is particularly evident at night, when both phase and amplitude of the signal may be severely disturbed. The disturbance takes the form of irregular variations having quasi-periods of the order of tens of minutes, superimposed on the normal diurnal variation. While the electron precipitation is strongest at auroral latitudes (60-70°), VLF effects can be detected at lower latitudes, ($\leq 50^\circ$), and at these latitudes an "after-effect" has been noted following certain magnetic storms. This after-effect is a maximum 2-4 days after the storm and can last for 10-14 days, the effect being mainly one of an abnormal daily variation and increased attenuation and depressed reflection height during the night.

4.2.5.1 Sudden ionospheric Disturbance (SID's) associated with solar X-ray events

One type of ionospheric disturbance which has long been known to be caused by the enhanced solar X-rays accompanying certain solar flares is called sudden ionospheric disturbance, SID. SID covers a range of effects seen in propagation and caused by a solar flare X-ray event (SXR) (e.g., sudden

phase anomaly (SPA), sudden field anomaly (SFA), sudden enhancement of atmospherics (SEA)). The ionisation increase in the lower ionosphere caused by solar flare X-rays, begins at the time of the visible flare, and affects the whole sunlit half of the Earth, up to $\chi \approx 85^\circ$ or so.

Sudden phase anomalies (SPA) are associated with SXR events and the total field intensity of long waves received from a distant transmitter undergoes characteristic changes. These sudden field anomalies (SFA's) take on different forms, depending on frequency and transmission path by supposing that the oscillations are the result of changes in the phase difference between ground- and sky-waves. The turning points on the record correspond to times when the sky- and ground-waves are in phase, or in anti-phase, and the amplitude at the turning points determines the amplitudes of the two waves. It is thus possible to follow in outline, the variation of both the phase and the amplitude of the sky-wave during the progress of the disturbance effect.

The assumption is made that, during the first part of the disturbance there is a decrease in apparent height and an increase during the second part, and that before the disturbance starts reflection is from the height normally determined. The resulting anomaly in phase height, usually referred to as sudden phase anomaly (SPA), is deduced from analysis of SFA. It is therefore concluded that during an SPA the apparent height of reflection of long and very long waves, transmitted over a wide variety of distances, and over a range of frequencies, all exhibit approximately the same change of apparent height. The reflection heights decrease in 2-10 minutes, and return to normal within a few minutes to 1 to 3 hours depending on the magnitude of the SXR event. Class 3 and 3+ solar flares drop the apparent reflection height to 60 km, but not lower.

When the oscillations on the total field record are used to determine the amplitude of the SID effect, it is found that the form of the variation depends on the amplitude prior to the SXR event and so depends on the season of the year.

4.2.6 High latitudes

The shadowing effect of the polar ice caps is important. Attenuation rates for signals propagating across the Greenland ice cap are 1.3 dB/1 000 km by night and 22 dB/1 000 km by day. Since daytime solar proton disturbances result in a further lowering of the ionospheric reflecting boundary, this results in attenuation rates that are still markedly greater, to such an extent that signal reception is no longer possible. Estimates of field strength agree well with observed results at middle latitudes provided the effects of the poorly conducting ground are properly taken into account. However, at high latitudes there may be significant dependence on seasonal and solar cycle changes in ionospheric reflectivity.

4.3 Calculating field strength: early approaches

The field strength, E , from a transmitter at a distance d km, on the ground, can be calculated [Wait, 1962]:

$$E = \frac{300\sqrt{p}}{\sqrt{a \sin d / a}} \cdot \frac{\sqrt{\lambda}}{h} e^{-i(kd + \pi/4)} \sum_n \Lambda_n e^{-ikS_n d} \quad \text{mV/m} \quad (4.1)$$

where

- p : radiated power (kW),
- a : radius of the Earth (km),
- λ : free space wavelength (km),

k : $2\pi/\lambda$,

Λ_n : excitation factor for the n th mode,

kS_n : propagation constant,

h : height of ionosphere (70 km-day; 90 km-night).

In general, the terms Λ_n and S_n are complex. The excitation factor Λ_n gives the relative amplitude and phase of each mode of order n excited in the Earth-ionosphere waveguide by the source. The real part of the propagation constant kS_n contains the phase information for each mode while the imaginary part determines the attenuation rate. In order to obtain the field strength the contributions of each mode must be summed giving proper attention to the relative phases of the terms. Modification is required near the antipode when $d/a \approx \pi$.

The field strength for mode n is:

$$E_n = \frac{300\sqrt{p}}{\sqrt{a \sin d / a}} \cdot \frac{\sqrt{\lambda}}{h} |\Lambda_n| e^{-\alpha_n d} e^{i(\Phi_n - kd \operatorname{Re} S_n)} \quad \text{mV/m} \quad (4.2)$$

where:

$$\Lambda_n \text{ (excitation factor)} = |\Lambda_n| e^{i\Phi_n}$$

$$\alpha_n \text{ (attenuation factor)} = \frac{2\pi}{\lambda} \operatorname{Im} S_n = -8.68 \frac{2\pi}{\lambda} \operatorname{Im} S_n \quad \text{dB/km}$$

$\operatorname{Im} S_n$ and $\operatorname{Re} S_n$ denote the imaginary and real parts of S_n respectively. The phase velocity $V_n = c/\operatorname{Re} S_n$, where c is the free space velocity.

In most cases, it is practical to derive field strength versus distance curves [Watt, 1967]. The recommended method is to start with appropriate values of Λ_n and S_n and perform the calculations in equation (4.1). In some cases (e.g., for VLF propagation during daytime from a ground-based transmitter), it is unnecessary to consider more than three modes; however more modes are needed for night-time propagation at the higher VLF [Snyder and Pappert, 1969; Pappert and Bickel, 1970].

The field strength due to each mode n depends on Λ_n and S_n . These factors depend on wavelength, ionosphere height, the ground electrical properties, and the spherical reflection coefficient of the ionosphere. The ionosphere reflection coefficients depend on the vertical distribution of electron density and collision frequency, the direction and magnitude of the Earth's magnetic field, the frequency, and angle of incidence. The electron density distribution is a function of latitude, season, solar cycle, time of day and whether or not ionospheric disturbances are present.

The influences of these various parameters can be broadly summarized in the following way:

- Ground conductivity: In general the effect of reducing the ground conductivity is to increase the attenuation rate of all modes. For moderate conductivities the magnitude of the excitation factor for the first order mode usually increases somewhat as the conductivity is reduced. Furthermore, as the conductivity is reduced, the phase velocity of each mode is also reduced.
- Direction of propagation with respect to the Earth's magnetic field: VLF model parameters show little variation with latitude or direction of propagation in the daytime. At night, there is little latitudinal variation for propagation to the magnetic east. For propagation to the

magnetic west, all VLF propagation parameters show a strong latitudinal variation as the magnetic equator is approached. In particular, attenuation is greater for propagation to the west than to the east.

Experimentally, observations of trans-equatorial anomalies over westerly trans-equatorial paths have been reported which suggest that the major variation occurs within some 15° of the magnetic equator. At Omega navigational frequencies, the diurnal phase shift on the east-to-west trans-equatorial path is 35% less than the average value at mid-latitudes [Lynn, 1975]. Anomalous interference caused by a long-path signal takes place around the geomagnetic equator, indicating a large east-west asymmetry in the attenuation of propagation [Kikuchi and Ohtani, 1984].

- Use of conductivity parameter: Wait and Spies [1965] showed that useful calculations of waveguide mode propagation can be performed by assuming the height variation of a conductivity parameter $\omega_r(z)$ to be:

$$\omega_r(z) = \omega_r(h) \exp [\beta (z - h)] \quad (4.3)$$

where $\omega_r = \omega_0^2/\nu$ for $\nu \gg \omega$; ω , ν and ω_0 are the wave angular frequency, the collision frequency, and plasma angular frequency respectively; z is the height, h is a reference height at which $\omega_r \approx 2.5 \times 10^5 \text{ s}^{-1}$. The term β gives the vertical gradient of ω_r . Under daytime conditions, h is about 70 km and $\beta \approx 0.3$, while at night h is around 90 km and $\beta \approx 0.5$. These two parameters, h and β , provide a convenient, but approximate, means of describing the ionosphere for use in VLF calculations. An extensive summary of specific values of the β and h parameters needed to simulate daytime and night-time VLF and LF propagated fields is given by Morfitt [1977] and by Davis and Berry [1977].

Calculating field strength in a non-homogeneous guide:

The above calculations refer to conditions where the path properties are independent of distance. When the electron density distribution with height along the path is constant but the ground conductivity or magnetic field angle changes, it is approximately correct to use average values of the attenuation rate and phase velocity in performing the computation. The amplitude and phase of a single mode change smoothly in a non-oscillatory manner with distance. When two or more modes with different phase velocities are present, the field strength changes in an oscillatory manner as the various modes go in and out of phase.

Such an approximate approach appears to account for the gross diurnal changes which are observed on long paths (approximately 10 000 km) at frequencies below about 18 kHz. The total phase delay is the sum of the phase delays along the sunlit and dark portions of the path. As the terminator (i.e. the sunrise or sunset line) moves along the path, the phase in this simple single mode model changes in proportion to the length of path in darkness giving rise to the well known trapezoidal diurnal variation.

At higher frequencies or on shorter paths, however, this approach is no longer adequate since it is found that the diurnal changes of phase may almost disappear, or even be reversed (i.e. phase delays are greater during the day than at night) or that the changes at sunrise and sunset may be in the same direction. However, when two or more modes are included in equation (4.1) and the calculations of phase delay are made for appropriate daytime and night-time parameters the observed patterns are obtained.

Mode parameter values are best derived by fitting equation (4.1) to measurements of field strength versus distance taken during day and night conditions over a wide variety of paths [Bickel *et al.*, 1970].

Considerable progress has been made in developing models which more correctly partition the radio energy into propagating modes through regions of rapid changes in the medium [Wait, 1970]. These mode conversion procedures are required for calculating the diurnal field strength changes when signals are transmitted across the daytime - night-time terminator region. Mode conversion procedures are also important when the medium changes along the propagation path (e.g., anomalous solar effects on the ionosphere or large changes in the ground conductivity).

The modal interference spacing (the distance over which the phase difference between two propagation modes changes by one phase cycle (2π)) is a theoretically calculable parameter which can be measured with great accuracy. Experimental determinations for the two most significant modes have been given as a function of frequency for day or night conditions [Steele and Crombie, 1967; Rawles and Burgess, 1967] and for a range of latitudes [Lynn, 1977]. Modal interference spacings determine the location of signal minima observed in aircraft flights, the timing of signal minima and of the steps in phase during sunrise and sunset, and the regular variations in diurnal phase magnitude and day-to-night signal levels with distance [Kaiser, 1969] and frequency [Araki, 1973; Lynn, 1978].

4.4 ITU-R Method of calculating field strength at VLF and LF

The theory of radiowave propagation at VLF and LF, necessary to estimate field strengths, is now fairly well understood and two ITU-R methods are available (Recommendation P.684) for theoretically calculating field strengths. The wave-hop treatment for frequencies above about 60 kHz is based on a statistical analysis of field strength measurements in the band 16 kHz to about 1 000 kHz. The waveguide mode method for frequencies below about 60 kHz is based on a theoretical model of the Earth and the ionosphere, employing ionospheric model parameters determined from propagation data.

The waveguide mode theory seems to describe better certain features of VLF propagation, e.g. the phase steps at dawn which are observed on long east-to-west transmissions, than does the ray-path wave-hop theory. The calculation of field strengths can be simpler using the waveguide mode theory than the wave-hop method for many cases.

The solutions obtained from the wave-hop theory are generally most suitable for short distances and the higher (LF) frequencies, while the waveguide mode theory is most suitable for longer distances and the lower (VLF) frequencies. More precise mode field calculations require inclusion of transverse electric (TE) as well as transverse magnetic (TM) modes and the conversion between these types of modes. The inclusion of both mode polarizations is important for the computation of both horizontal and vertical fields between elevated transmitters and receivers.

The wave-hop theory describes the propagation using terms that correspond to physically real quantities that the radio engineer can easily visualize. The method estimates the amplitude of the sky-wave alone and therefore, for comparison, the ground wave field strength should also be included.

Electron density distributions which may also be useful as models under specified conditions can be found in several papers [Bain, 1981; Mechtly *et al.*, 1972; Montbriand and Belrose, 1979; Rowe *et al.*, 1974; Thomas and Harrison, 1970].

4.4.1 The Wave-Hop method

The “*wave-hop*” method is that in which electromagnetic energy paths between a given transmitter and receiver are represented geometrically as is done in the case of HF sky-wave propagation. It is particularly convenient for the long-distance propagation of LF and MF, and in the case of VLF at distances of less than 1 000 km, where the wave-hop theory requires only a limited number of paths.

This method treats radio transmission as taking place along certain paths defined by one or more ionospheric reflections, depending on whether the propagation in question involves one or more “hops”. The total field is then the vectorial resultant of the fields due to each path. In view of the long wavelengths concerned, the diffraction of the waves by the Earth's surface must be taken into account, which is not the case for HF. The wave-hop method may be justified by the fact that, with oblique incidence, the dimensions of the section of altitude in which propagation takes place are equal to or greater than several wavelengths.

With this method it is necessary to know the values of the reflection coefficients of the incident wave on the ionosphere. These vary greatly with frequency, length and geographic and geomagnetic coordinates of the transmission path, time of day, season and epoch of solar cycle. It is also necessary to know the electrical characteristics (conductivity and permittivity) of the ground at the receiving and transmission sites since the finite conductivity of the Earth affects the vertical radiation patterns of the terminal antennas. The theoretical calculation of the reflection coefficients may be carried out in two different ways:

- if the ionosphere is regarded as homogeneous and as having a sharp lower edge, the reflection coefficients on the air-ionosphere interface can be calculated by the theory of rays, taking into account the polarization of the incident wave. One thereby obtains transmission and reflection matrices because, with an incident plane wave, the polarization of the reflected wave is usually elliptical;
- if we wish to use a real ionospheric model, which varies with altitude, the ionosphere must be divided into slices thin enough for the medium to be regarded as homogeneous. Since the thickness of each slice will then be small in comparison with the wavelength, the differential equations obeyed by each component of the electromagnetic field must be written out and solved below the ionosphere, taking account of boundary conditions at high altitude. If the solutions for the up and down paths are separated, the reflection coefficients can be determined.

4.4.2 The Waveguide Mode method

The “*waveguide mode*” method is that in which propagation is analysed as the sum of the waves corresponding to each of the different types of propagation in the Earth-ionosphere waveguide, analogous to a mode as defined for waveguides in the microwave region.

The mode theory is suited to VLF propagation at distances of more than 1000 km since the series of modes converge rapidly and sufficient accuracy can be obtained by adding together only a small number of modes. Propagation at ELF also may be described in terms of a single waveguide mode.

4.5 Reliability of the wave-hop method

In treating the propagation as a series of hops between ground and ionosphere, it is assumed that the ionospheric reflection is dependent on the signal frequency and the angle of incidence at the ionosphere (i.e. $f \cos i$). Fig. 4.4 indicates that the data on which reflection coefficients are modelled,

has a scatter in the measured values of the summer data (by +15 dB to -8 dB for $f \cos i \sim 30$ kHz), and there are few data for $f \cos i > 40$ kHz for long distance propagation. For all oblique incidence data except for one set of observations, ionospheric reflection coefficients have been determined from the interference maxima and minima of sky- and ground-waves.

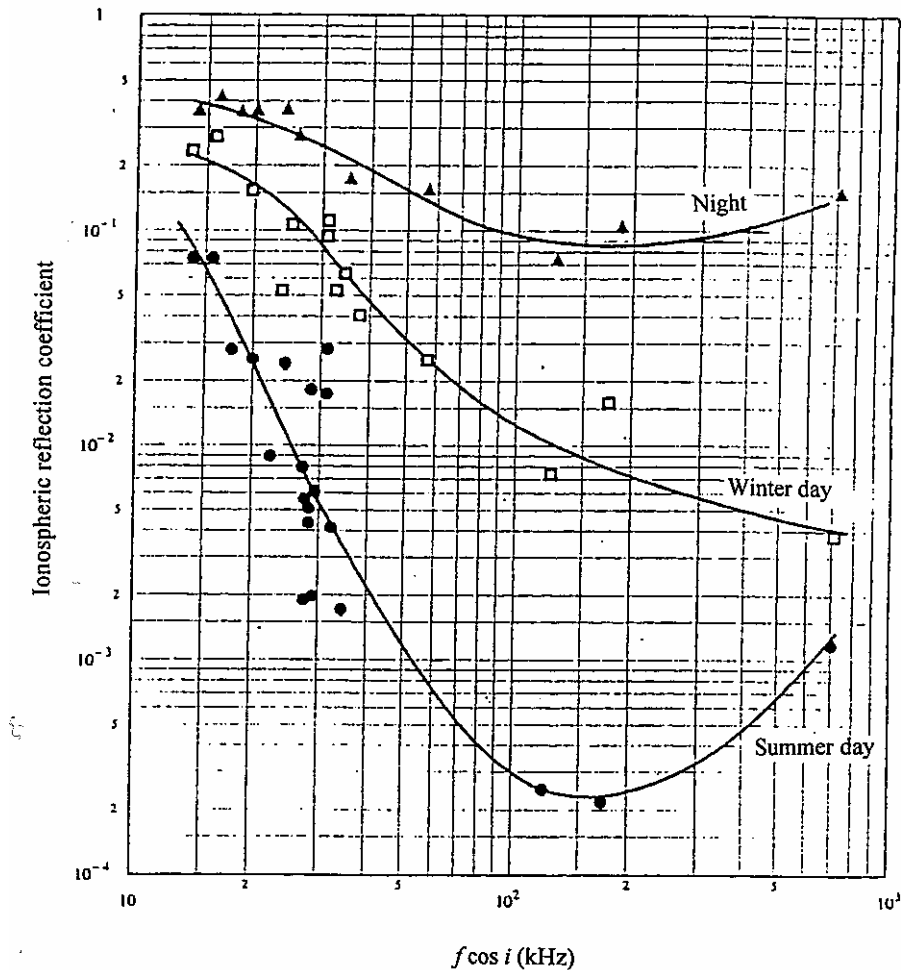


FIGURE 4.4
Ionospheric reflection coefficients under solar minimum conditions

Concerning the reliability of the curves for reflection coefficients, Bell and Knight [1978] have noted that their measured daytime field strengths for Warsaw-Kingswood, 227 kHz/1 370 km ($f \cos i = 31.6$ kHz) and for Tipaza-Kingswood, 251 kHz/1 650 km (30.6 kHz), lie above those predicted by the summer, sunspot minimum curve of Fig. 4.4. But they note that the summer field strengths may be influenced by ground-waves since they measured the total field. On the other hand, field strength measurements made for the paths Rome-Kolberg, 845 kHz/1 143 km (154 kHz) and Monte Carlo-Kolberg, 1 466 kHz/1 050 km (280 kHz) have revealed that the diurnal variation observed in summer is greater than that predicted by the curves [Taumer and Starick, 1969].

Alternative methods to calculate night-time field strengths at LF, 150 to 1 600 kHz, are given in Recommendation P.1147. An intercomparison of results obtained by the methods in Recommendation P.684 with Recommendation P.1147 show good agreement in the overlapping frequency band.

REFERENCES
FOR CHAPTER 4

- ARAKI, T. [1973] Anomalous diurnal changes of transequatorial VLF radio waves, *J. Atmos. Terr. Phys.*, 35 (4), pp 693-703.
- BAIN, W. C. [1981] Models of the ionospheric D region at noon. IEE Conf. Proc. 195, 203-206.
- BELL, C. P. and KNIGHT, P. [1978] Daytime propagation in the LF broadcasting band. *EBU Rev. Tech.* 167, 3-7.
- BELROSE, J. S. [February, 1982] Ed. AGARD Conf. Proc. No. 305, *Medium, long and very long wave propagation (at frequencies less than 3000 kHz)*. NASA Accession No. N82-27613. National Technical Information Service, Springfield, VA 22161, USA.
- BELROSE, J. S. [1990] Long wave propagation. *Radio Wave Propagation, modeling, prediction and assessment*. Ed. Richter, AGARDograph 326, 40-62.
- BICKEL, J. E., FERGUSON, J. A. and STANLEY, G. V. [1970] Experimental observations of magnetic field effects on VLF propagation at night. *Radio Sci.*, Vol. 5, 19-25.
- BLAIR, B. E., CROW, E. L. and MORGAN, A. H. [1967] Five years of VLF world-wide comparison of atomic frequency standards, *Radio Sci.*, Vol. 2, (New Series), 627-636.
- BUDDEN, K. G. [1985] Propagation in radio waves, University Press, Cambridge, U.K.
- DAVIS, R. M. and BERRY, L. A. [1977] A revised model for the electron density in the lower ionosphere. Command and Control Technical Center (DCA), Tech. Rep. 111077, NTIS Accession No. AD17883. National Technical Information Service, Springfield, Va. 22161, USA.
- FOLEY, G., WAND, I. C. and JONES, T. B. [1973] Studies of the modal parameters of VLF radio waves propagated below the night-time ionosphere. *J. Atmos. Terr. Phys.*, Vol. 35, 2111-2122.
- HANSELMAN, J. C., CASSELMAN, C. J., TIBBALS, M. L. and BICKEL, J. E. [1964] Field intensity measurements at 10.2 kHz over reciprocal paths, *Radio Sci. J. of Res.*, 68D, pp 11-18.
- KAISER, A. B. [1969] An explanation of VLF diurnal phase change observations. *Radio Sci.*, Vol. 4, 17-21.
- KIKUCHI, T. and OHTANI, A. [1984] Anomalous interference in Omega VLF wave propagation on east-to-west equatorial paths. *J. Atmos. Terr. Phys.*, Vol. 46, 697-703.
- LYNN, K. J. W. [1975] The transequatorial reception of Omega (13.6 kHz) transmissions. *J. Atmos. Terr. Phys.*, Vol. 37, 1395-1399.
- LYNN, K. J. W. [1977] VLF modal interference over west-east paths. *J. Atmos. Terr. Phys.*, Vol. 39, 347-357.
- LYNN, K. J. W. [1978] Some differences in diurnal phase and amplitude variations for VLF signals, *J. Atmos. Terr. Phys.*, Vol. 40, 145-150.
- MECHTLY, E. A., BOWHILL, S. A. and SMITH, L. G. [1972] Changes of lower ionosphere electron concentration with solar activity. *J. Atmos. Terr. Phys.*, Vol. 34, 1899-1907.

- MONTBRIAND, L. E. and BELROSE, J. S. [1979] Diurnal and seasonal variations of the steady state loss coefficient in the D-region. *J. Geophys. Res.*, **84**, 1921-1929.
- MORFITT, D. G. [1977] Effective electron density distributions which describe VLF/LF propagation data. Naval Ocean Systems Center Tech. Rep. TR141, NTIS Accession No. ADA047508. National Technical Information Service, Springfield, Va. 22161, USA.
- PAN, L. D. LI, D.M., WANG, S. Q. and MA, L. X. [1988] Study on improving the accuracy of time information via LF sky-wave, Proc. of the International Symposium on Radio Propagation, Beijing, China.
- PAN, W. and TIAN, Y. [1988] Multi-mode interference and phase stability of VLF wave propagation, Proc. 1988 International Symposium on Radio Propagation (ISRP-88), Beijing, China.
- PAPPERT, R. A. and BICKEL, J. E. [1970] Vertical and horizontal VLF fields excited by dipoles of arbitrary orientation and elevation. *Radio Sci.*, Vol. 5, 1445-1452.
- RAWLES, A. T. and BURGESS, B. [1967] Results of the two-frequency VLF transmission experiments from Criggion GBZ. *Radio Sci.*, Vol. 2, 1295-1301.
- ROWE, J. N., MITRA, A. P., FERRARO, A. J. and LEE, H. S. [1974] An experimental and theoretical study of the D region - II. A semi-empirical model for mid-latitude D region. *J. Atmos. Terr. Phys.*, Vol. 36, 755-785.
- SNYDER, F. P. and PAPPERT, R. A. [1969] A parametric study of VLF transequatorial propagation anomaly. *Radio Sci.*, Vol. 4, 213-226.
- STEELE, F. K. and CROMBIE, D. D. [1967] Frequency dependence of VLF fading at sunrise. *Radio Sci.*, Vol. 2, (New Series), 547-549.
- TAUMER, F. and STARICK, E. [1969] Jahreszeitliche Feldstärkevariationen im Lang- und Mittwellenbereich (Seasonal variations of field strength in the LF and MF bands). *Techn. Mitt. RFZ*, 13 Jahrgang, Heft 1, 16-19.
- THOMAS, L. and HARRISON, M. D. [1970] The electron density distributions in the D region during the night and pre-sunrise period. *J. Atmos. Terr. Phys.*, Vol. 32, 1-14.
- WAIT, J. R. [1962] *Electromagnetic Waves in Stratified Media*. Pergamon Press, New York, NY, USA.
- WAIT, J. R. [1970] Factorization method applied to electromagnetic wave propagation in a curved waveguide with non-uniform walls, *Radio Sci.* 5, 1059-1068.
- WAIT, J. R. and SPIES, K. P. [1965] Influence of finite ground conductivity on the propagation of VLF radio waves. *NBS J. Res.*, Vol. 69D, 1359-1373.
- WATT, A. D. [1967] *VLF Radio Engineering*. Pergamon Press, New York, NY, USA.

CHAPTER 5

PROPAGATION AT FREQUENCIES BETWEEN 150 kHz AND 1 700 kHz

This chapter summarizes advances made in LF/MF sky-wave propagation studies during the last five decades. Factors affecting sky-wave propagation are discussed. Four major field strength prediction methods are currently used in different regions. Their respective merits and limitations are discussed to guide individual users to select the most appropriate one. The methods are:

- a) Recommendation PI.435 (also known as the method proposed by ex-CCIR IWP 6/4 in 1974);
- b) Cairo North-South curve, which is the official method for the Asian part of ITU Region 3 [ITU, 1975];
- c) Region 2 method (formerly known as the FCC curves) [ITU, 1988];
- d) Wang method which has been adopted by the FCC for applications in the United States (also known as the method developed by IWP 6/4 in 1985 or the modified FCC method) [Wang, 1985; Wang *et al.*, 1993].

5.1 Field strength measurements and analysis

5.1.1 Field strengths at distances of less than 300 km

There are far fewer experimental data for distances less than 300 km than for greater distances, because of the difficulty of separating the sky-wave from the ground-wave. However, a reduction of the ground-wave component can be achieved by using a transversely oriented loop antenna at the transmitting or at the receiving site, or at both sites.

Alternatively, the ground-wave can be separated from the sky-wave by the use of pulse transmissions. Reflections from the E and F regions can be identified by their time delays, as can multiple reflections and their individual amplitudes can be measured.

5.1.2 Field strengths at distances between 300 and 3 500 km

5.1.2.1 Region 1

5.1.2.1.1 Europe

Most of the European measurements were taken before the 1974/75 LF/MF Broadcasting Conference for ITU Regions 1 and 3. The European data have been used to study (among other things) the effect of ground conductivity and sea gain.

5.1.2.1.2 Africa

Measured field strengths on several east-west African paths are significantly lower than expected. This seems to suggest that polarization coupling loss is more severe than expected [Wang *et al.*, 1993].

5.1.2.2 Region 2

The Region 2 method for calculating sky-wave field strengths (formerly known as the FCC curves) was developed solely from North American data. The Wang [1985] method, which has been adopted by the FCC for applications within the United States was developed from the more recent and larger databank.

Data collected in the United States indicate that field strength increases with increasing frequency, in contrast to the frequency term in Recommendation P.1147. This phenomenon is most pronounced at about two hours after sunset. With other factors being near identical, field strength of a signal at 1 530 kHz is typically 5 to 10 dB stronger than that at 700 kHz. At six hours after sunset, the difference is about 3 dB, in favour of the higher-frequency signal [Wang, 1985]. Similar observations have also been made in Brazil (typically, 11 dB between 1 410 kHz and 620 kHz). Data collected in Brazil further indicate that a transmission loss in the east-west direction is about 3.6 dB higher than that in the north-south direction.

5.1.2.3 Region 3

5.1.2.3.1 Australasia

Field strengths collected in this area are generally higher than those measured elsewhere and the variance has been found to be smaller.

5.1.3 Field strengths at distances greater than 3 500 km

An extensive series of measurements over the distance range of about 3 500 to 12 000 km was made from 1935 to 1937 at frequencies of about 1 MHz. These measurements were used to derive the so-called Cairo curves [Knight, 1977a]. The original curves give quasi-maximum field strengths; to enable comparison to be made with other curves and other prediction methods, all values have been reduced by 9 dB to give median field strengths. There are two Cairo curves. The East-West curve was derived from measurements made across the North Atlantic; these measurements may have been affected to some extent by auroral absorption. The North-South curve was derived from measurements mainly between North and South America. These curves are given in Fig. 5.1.

5.2 Variations of field strengths and factors affecting propagation

5.2.1 Fading rate

Sky-wave signals vary continually in strength. The fading rate, defined as the number of times the field strength increases through the median value in a given time, is proportional to frequency and also depends on the angle of incidence at the ionosphere. On long-distance paths, E-layer reflections predominate and the fading rate for a frequency of 1 MHz is about 10 per hour in Europe; fading rates about three times greater have been measured in Japan. This comparatively slow fading is replaced by more rapid fading if F-layer reflections occur or if two propagation modes of comparable strength are received simultaneously.

5.2.2 Amplitude distribution

At the higher frequencies in the MF band, the field strength observed during two or three fading cycles usually obeys the Rayleigh distribution, see Recommendation P.1057. At LF the difference between the quasi-maximum and the median is somewhat less (typically 3 dB at night and 1.7 dB during the day) and the distribution more closely resembles the log-normal.

Median field strengths measured at a given time vary randomly from night to night, with a log-normal distribution. The spread of values, measured over a period of days which is short enough to exclude seasonal and solar-cycle effects, shows no obvious dependence on frequency or path length.

5.2.3 Diurnal variations

LF sky-waves propagating over European paths during winter days are only 10 to 15 dB weaker than at night. Daytime sky-waves are also observed in spring and autumn and during the spring equinox they are almost as strong as in winter. Weak daytime sky-waves are observed in Europe during the summer. In India, however, the difference between summer and winter daytime field strengths is less than 6 dB.

At any given frequency the rates of increase of the field strength at sunset and the decrease at sunrise are almost independent of path length, although there is a slight tendency for the onset of night-time propagation to be progressively delayed as the path length increases. There is also a tendency for the onset of night-time propagation to be delayed at the lower frequencies in the MF band. In temperate latitudes the transition from day to night conditions starts in winter at least an hour before sunset but in summer the transition starts nearer to sunset and takes place more rapidly. The average diurnal variation curve given in Fig. 3 (hourly loss factor) of Recommendation P.1147 is consistent with measurements.

Based on United States data, sky-wave field strength is highly frequency-dependent during transition hours [Wang, 1983]. Consequently, a family of diurnal variation curves for different frequencies has been developed. When compared to the United States data, Fig. 3 of Recommendation P.1147 is most satisfactory for frequencies near 1 000 kHz. Similar results are also quoted in Knight [1977b].

5.2.4 Variation with season

5.2.4.1 LF band

At night, LF sky waves are stronger in solstice months and are weaker in equinoctial months.

In daytime, LF sky waves propagating at temperate latitudes in winter are at least 20 dB stronger than in summer and may be only 10 dB below night-time values.

5.2.4.2 MF band

At night, MF sky-waves propagating at temperate latitudes are strongest in spring and autumn and are weakest in summer and winter, the summer minimum being the more pronounced. The overall variation may be as much as 15 dB at the lower frequencies in the band, decreasing to about 3 dB at the upper end of the band. The variation is much smaller in tropical latitudes.

Night-time MF sky-wave field strengths collected in low- and mid-latitude areas of the Americas show virtually no consistent pattern of any seasonal variation except a slight minimum in the summer. High-latitude field strengths collected in Alaska show a pronounced summer minimum and a consistent maximum in April [Hunsucker *et al.*, 1989]. In a year of minimum sunspot number, night-time monthly median field strength for April is typically 10 to 15 dB greater than the annual median.

In daytime, MF sky waves are strongest in winter months. The seasonal variation may exceed 30 dB.

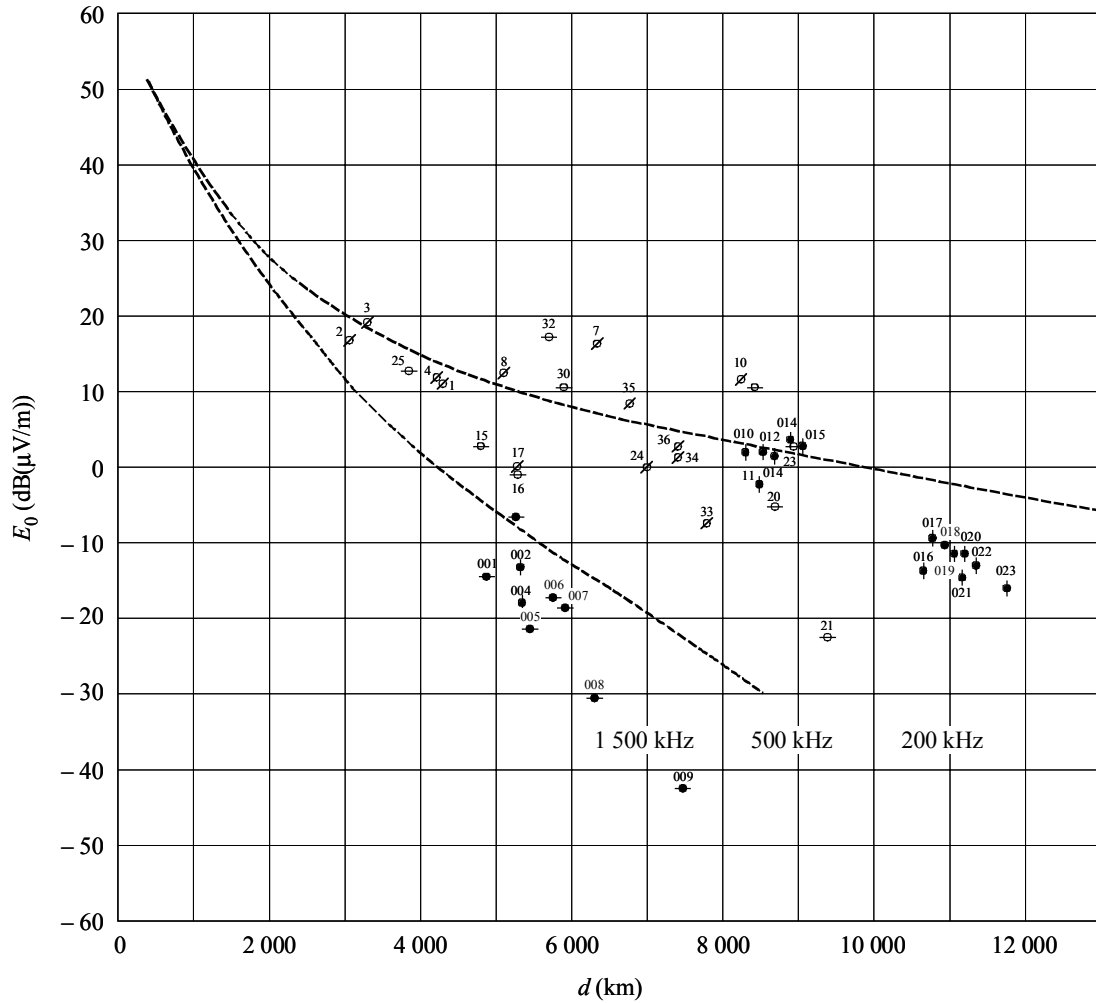


FIGURE 5.1

Sky-wave field strengths measured at distances greater than 3 000 km

A: N-S, Cairo 1938

B: E-W, Cairo

∅N/S	⊕E/W	U.E.R.	◆N/S	◆E/W	U.I.R.	Nov. 1936-Jan. 1937	
1	Riyad-Helsinki	21	Swan Island-Helsinki	001	Northern Ireland-Ottawa	013	Pittsburg-Buenos Aires
2	Batra-Wittsmoor	22	Swan Island-Jurbise	002	Rennes-Ottawa	014	Buenos Aires-Strathburn (CAN)
3	Batra-Helsinki	23	Swan Island-Monza	003	New York-London	015	Buenos Aires-Ottawa
4	Dakar-Limours	24	Fort de France-Jurbise	004	Northern Ireland-Washington	016	Toulouse-Buenos Aires
7	Batra-St-Denis	25	Kuwait-Monza	005	Rennes-New York	017	Rennes-Buenos Aires
8	Harrar-Monza	30	Masirah-Limours	006	New York-Brussels Eindhoven	018	Nice-Buenos Aires
10	Rome-St-Denis	32	Masirah-Leucate	007	Rennes-Washington	019	Buenos Aires-London
15	Sackville-Limours	33	Bangkok-Helsinki	008	New York-Berlin	020	Paris-Buenos Aires
16	Sackville-Châtonnaye	34	Ismaning-Tsumeb	009	New York-Moscow	021	Northern Ireland-Buenos Aires
17	Mocton-Châtonnaye	35	Rome-Tsumeb	010	Buenos Aires-Washington	022	Buenos Aires-Brussels
20	Poro-Helsinki	36	Allouis-Tsumeb	011	Buenos Aires-New York	023	Buenos Aires-Berlin
				012	New York-Buenos Aires		

5.2.5 Variation with solar and magnetic activity

In general, solar activity reduces MF night-time sky-wave field strengths. The reduction is a function of geomagnetic latitude, distance and sunspot number [Wang, 1977]. The reduction increases with increasing latitude. In low latitudes (e.g., lower than about 40°) it is believed to be negligible. The large variation in high latitudes is probably due to excess absorption associated with magnetic storm and post-storm effects [Hagg, 1982]. It has been reported that at MF, the effect of solar activity at two hours after sunset is about twice as great, in terms of dB, than at six hours after sunset. Furthermore, high-latitude data collected in Alaska show that the field strength maximum tends to occur in the year immediately after sunspot minimum [Hunsucker *et al.*, 1989].

Daytime sky-wave field strengths vary with solar activity similar to field strengths at two hours after sunset.

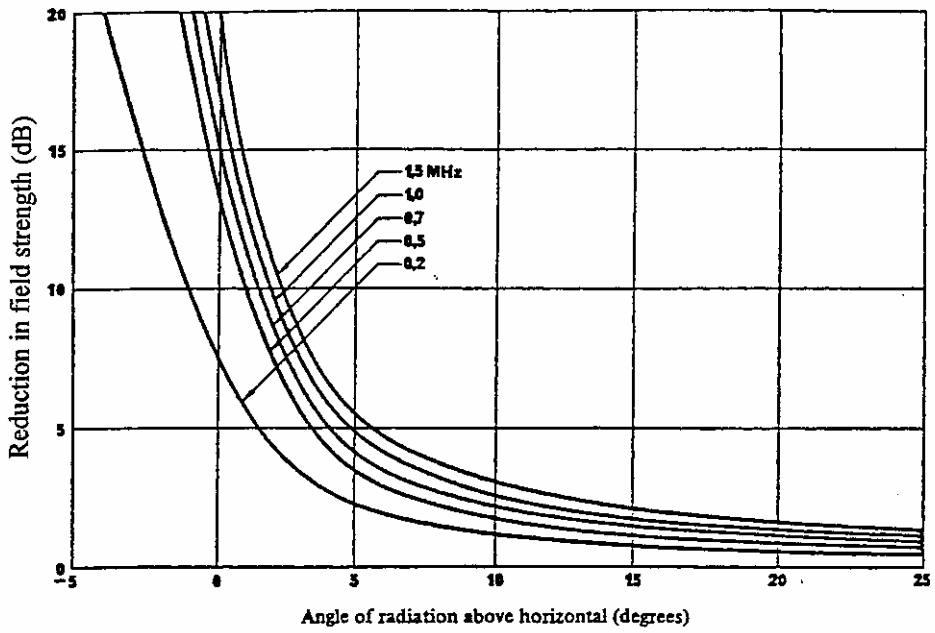
The effects of solar activity at middle latitudes in Europe has an opposite influence on LF propagation (compared with MF). The night-time field strengths increase with solar activity (by 2 to 4 dB over a solar cycle), and the increase in daytime field strength is somewhat greater.

5.2.6 Influence of the ground on radiation towards the ionosphere

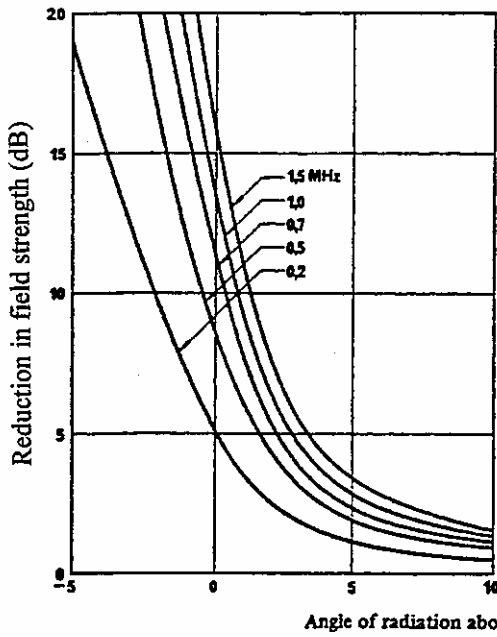
Fig. 5.2 shows the variation of field strength with elevation angle for antennas on an imperfectly conducting curved Earth compared with the case where the antennas are located on flat perfectly conducting ground [Knight, 1973]. Fig. 5.3 gives the effective ground conductivity for various types of terrain. The curves in Fig. 5.2 apply to vertical transmitting antennas up to 0.6λ high. They also extend to negative angles of radiation which apply when waves diffract around the curvature of the Earth (defined as the angular distance between the antenna and the tangent point of the wave, as described in Recommendation P.684).

Recommendation P.1147 was derived from measurements made with transmitting and receiving antennas located on typical imperfectly-conducting ground (3×10^{-3} S/m). Thus the results and predictions implicitly include a ground loss term. For antenna locations near the sea, it is necessary to take account of sea gain. This may be derived from Fig. 5.2 by subtracting field strength reductions for sea water from those for ground of the appropriate conductivity. If the ground conductivity is an order of magnitude smaller than 10 mS/m, it is necessary to take account of the additional ground loss that will occur.

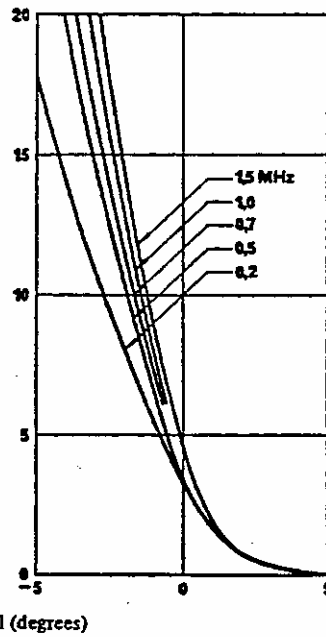
An example which shows the effectiveness of sea gain as a function of the propagation path length for single and multi-hop propagation has been calculated and is shown in Fig. 5.4. A frequency of 1 MHz and E-layer propagation has been assumed.



c) Ground conductivity, 10^{-2} S/m;
Relative permittivity, 20



d) Ground conductivity, 3×10^{-2} S/m;
Relative permittivity, 30



e) Ground conductivity 4 S/m (sea water);
Relative permittivity, 80

FIGURE 5.2

Reduction in field strength for vertical antennas up to 0.6λ high,
including the effect of the curvature of the Earth

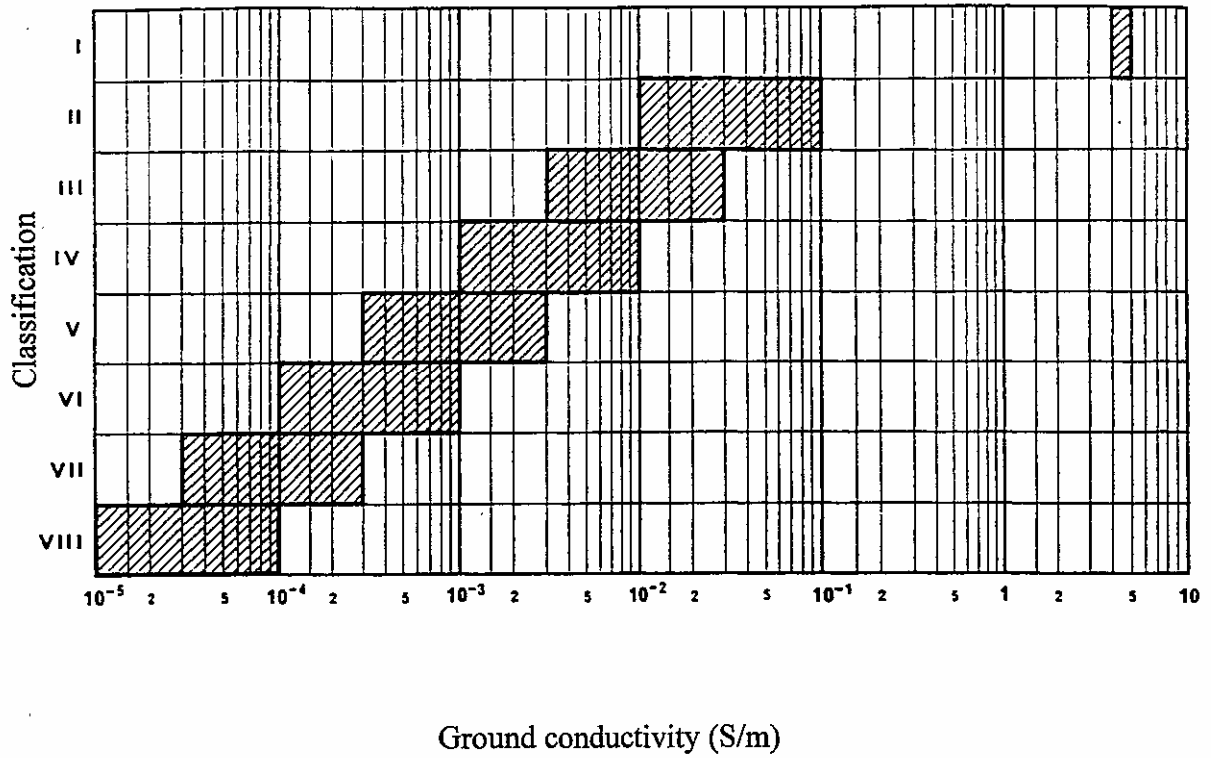


FIGURE 5.3
Expected ranges of effective ground conductivity

Class	Terrain Description	Class	Terrain Description
I	Sea water (in some areas, e.g. the Baltic Sea, sea conductivities can be lower)	V	Medium dry ground; rocks; sand; medium-sized towns
II	Very moist soil; moist cultivated land	VI	Dry ground; desert
III	Marshes (fresh water); cultivated land	VII	Very dry ground; granite mountains in cold regions; industrial areas
IV	Fresh water; sandy loam; hilly country in temperate climates	VIII	Dry glaciers in mountainous areas; permafrost; polar ice; high rocky mountains in temperate and cold climates

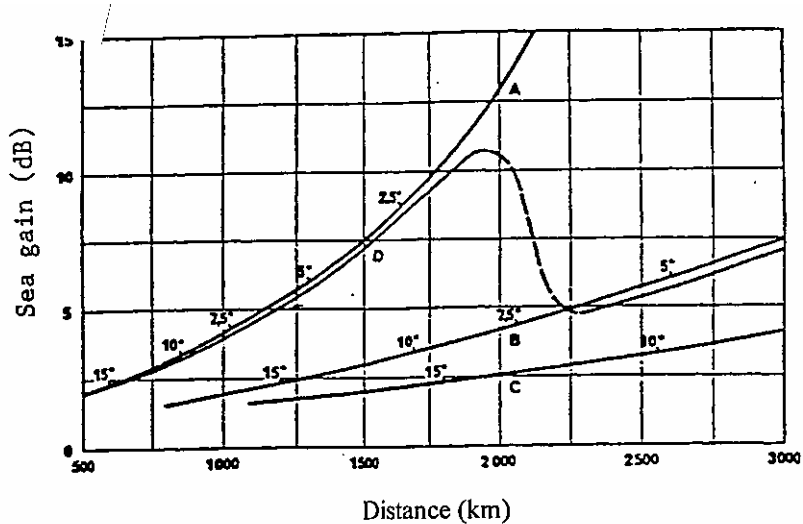


FIGURE 5.4

Sea gain for multi-hop propagation

The curves show the sea gain which occurs when ground of conductivity 5×10^{-3} S/m is replaced by sea water at one end of the path. E-layer reflection (layer height 90 km) is assumed and the numbers against the curves denote angles of radiation.

(Curve A: Single-hop mode B: Two-hop mode C: Three-hop mode D: Effective sea gain for all modes)

5.2.7 Excess polarization coupling loss, L_p

Polarization coupling loss occurs when waves enter the ionosphere, because some of the incident power passes into the extraordinary wave, which is then absorbed. Further loss occurs when the wave leaves the ionosphere, because it is elliptically polarized and only its vertical component normally couples with the receiving antenna [Phillips and Knight, 1965].

Polarization coupling loss is small in temperate latitudes and is included as a constant in propagation curves and formulae. In tropical latitudes, however, it is larger and depends on the direction of propagation relative to that of the Earth's magnetic field. Account must therefore be taken of the amount by which the polarization coupling loss exceeds that occurring in temperate latitudes.

A description of the determination of the excess polarization coupling loss, L_p , is given in Recommendation P.1147.

Manual calculation of this correction is tedious but there are certain simplifying factors:

- The correction is required only between dip latitudes 45° N and 45° S; hence no correction is required for terminals in Europe, North America, Russia, southern Africa, Australia and New Zealand.
- Although it is necessary to estimate the bearing of the great circle path relative to the magnetic meridian rather than the geographic meridian, the difference between these (the magnetic declination) is small over much of the area of Africa, South America and Asia in which the correction must be applied.

Fig. 5.5 represents a map of Regions 1 and 3 using a conic projection based on standard parallels at 28° N and 9° S, i.e. a projection centred approximately on the magnetic dip equator in this area. Great circle paths represented, approximately, by straight lines on this map measured from any one terminal near this dip equator, have bearing errors less than 2° for distances up to 4 000 km.

Although bearing errors become somewhat greater as the distance of the terminal from the dip equator increases, this is associated with a reduction in the value of the predicted polarization coupling loss and, hence, of the possible absolute error in prediction.

Superimposed on Fig. 5.5 is the extent of the area within which errors in coupling loss prediction exceeding 1 dB can result from neglecting magnetic declination. In the remaining part of Africa and the Asian mainland, bearings may be referred to the geographic rather than the magnetic meridian with negligible error.

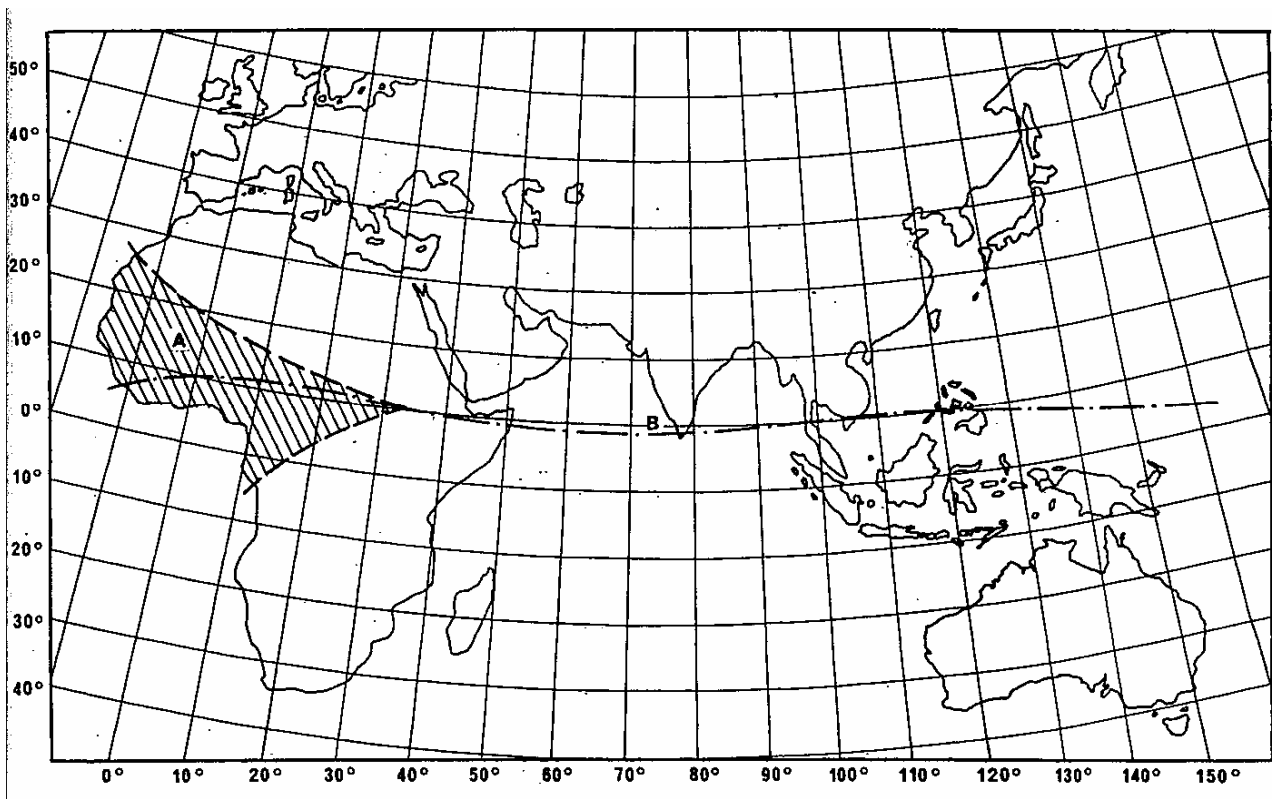


FIGURE 5.5

**Map for facilitating the manual calculation of excess polarization coupling loss
(shaded area A indicates where errors in estimating excess coupling loss
can exceed 1 dB if magnetic declination is neglected;
B is the magnetic dip equator)**

5.2.8 Field strengths exceeded for different percentages of time

Annual median value of sky-wave field strength is generally used to determine a station's sky-wave service area. Field strength exceeded for small percentages of the time is needed to study interference.

Both inter-service and intra-service interference levels must be known in order to achieve orderly utilization of this portion of the spectrum. This means that understanding of field strengths exceeded for small percentages of time is very important.

Field strengths exceeded for 1% and 10% of the time are about 13 dB and 8 dB, respectively, greater than the yearly median value. These figures are typical ones and can be used if simplicity is desired. However, a more accurate approach is shown in Fig. 5.6. At low geomagnetic latitudes, field strength values exceeded for 1% and 10% of the time have been found to be about 11 dB and 6 dB, respectively, stronger than the median value [Wang, 1989a]. At high geomagnetic latitudes, the corresponding differences are about 15 dB and 10 dB [Hunsucker *et al.*, 1989].

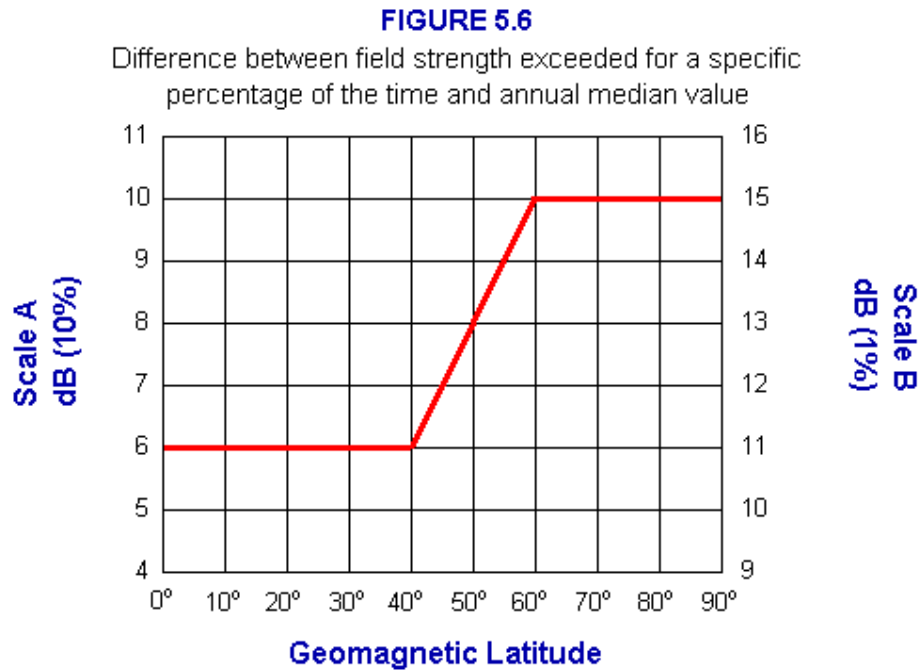


FIGURE 5.6
Difference between field strength exceeded for a specific percentage of the time and annual median value

A: 10%

B: 1%

5.3 Discussion on prediction methods

5.3.1 Sky-wave prediction methods in use at LF and MF

Several sky-wave field strength prediction methods have been proposed for various parts of the world. In all these methods the field strengths are expressed by their logarithms, in dB ($\mu\text{V}/\text{m}$), in order to simplify the introduction of local environmental factors.

The general form of a propagation formula where the field strength is expressed in dB ($\mu\text{V}/\text{m}$) is:

$$E = E_0 + P + \Delta_A - \Delta_t \quad (5.1)$$

where:

E : Annual median value of the field strength at a place and a given hour. The field strength E is that which would be measured by a loop antenna aligned in the vertical plane of the great circle path, at heights of less than 0.1λ . Thus, the field strength is the resultant of the downcoming wave and the ground-reflected wave.

E_0 : Value of E under standard conditions. These relate to an effective monopole radiated power (e.m.r.p.) of 1 kW which is equivalent to a cymomotive force (c.m.f.) of 300 V. E_0 also relates to a given reference time and to certain ground conductivities at the ends of the path. The reference time and the conductivities, may be different in different prediction methods. The way of calculating E_0 is different in each method.

P : Term accounting for the power actually fed to the antenna.

Δ_A : Term accounting for the gain of the transmitting antenna in the direction of propagation considered. It covers both the horizontal and vertical radiation pattern. In the case of an omnidirectional vertical transmitting antenna the correction factor Δ_A is identical to the transmitting antenna gain factor due to vertical directivity, G_V , given in Recommendation P.1147. The calculation of P and Δ_A is common to all methods.

Δ_t : Term accounting for the hour of the day. The computation of Δ_t may vary with the reference hour adopted; it may alternatively be replaced by the computation of a factor depending on the position of the Sun at the point of the propagation path under consideration.

The field strength value E_0 for standard conditions can be expressed in a general way by the following equation:

$$E_0 = C - f(d) + \Sigma\Delta_K \quad (5.2)$$

where:

C : Constant, different from one method to the other, which may vary, however, for a particular method with the region of the world.

$f(d)$: Represents the main influence of the length of the propagation path.

$\Sigma\Delta_K$: Sum of the correction factors accounting for the influence of the frequency or of spatial or temporal parameters depending on the propagation path and the time considered.

The computation of $f(d)$ and $\Sigma\Delta_K$ varies from one method to the other, but some of the elements may be common to several methods.

The various propagation formulae based on this general model permit the computation of the sky-wave field strength and do not take account of the ground-wave. In real cases, at short distances, the ground-wave is important and particular caution has to be exercised to take into account both the ground-wave and the sky-wave.

The expression "annual median of the field strength" requires some further explanation. It is, in principle, and by agreement, the annual median (i.e. the value exceeded during 50% of the nights of a year) of the half-hourly medians of the field strength recorded every night of the year during half an hour centred on the hour considered. A smaller number of nights may, in fact, be taken into account, provided this number remains sufficiently great and the nights are regularly distributed over the course of the year (e.g. every second or third night).

5.3.2 Comparison of predicted field strengths with measured data

A prediction method should be applicable for all populated areas of the world and comparisons with measured results should test the validity of various parameters included within the equations given in § 5.3.1. Of particular importance for comparisons are the effects of:

- polarization coupling loss at low latitudes (particularly on east-west paths);
- solar and magnetic activity (particularly at high latitudes), and
- the appropriate geomagnetic coordinate system.

5.3.2.1 Region 1

When compared with measured field strength values of one-hop intra-European paths, excellent and similar results have been obtained by using either the ITU-R method or the Wang method. In an overwhelming number of cases, the errors are less than 5 dB [Wang *et al.*, 1993].

When compared with measured field strength values of intra-African paths, satisfactory results have been obtained by using both methods. On the r.m.s. basis, the error of the ITU-R method is 9.3 dB and that of the Wang method is 8.9 dB.

When compared with measured field strength values of long intercontinental paths within Region 1 and inter-regional paths ending in Region 1, the ITU-R method shows a tendency to under-predict field strength levels by a large margin. This tendency becomes progressively stronger as path length increases. At distances between 5 000 and 10 000 km, the error of the ITU-R method is typically 10 dB. The Wang method shows no such tendency [Wang *et al.*, 1993].

5.3.2.2 Region 2

When compared with measured data from 87 paths, the r.m.s. errors of the ITU-R, the Region 2 and the Wang methods are 5.8 dB, 8.9 dB and 4.9 dB, respectively.

It should be mentioned that in Canada and northern United States, the accuracy of the ITU-R and the Wang methods can be improved if corrected geomagnetic latitudes are used.

5.3.2.3 Region 3

5.3.2.3.1 Asia

Pan [1981] has studied the Chinese data and reported that field strength values predicted by the ITU-R method and the Cairo curve are too low. When compared with data from 84 paths in Asia, the r.m.s. errors of the ITU-R method, the Cairo North-South curve, and the Wang method

are 4.9 dB, 4.6 dB and 3.5 dB, respectively. Again, when applied to long paths, the ITU-R method shows a tendency to underestimate field strength levels, typically by 8 dB. None of the other methods show such a tendency.

5.3.2.3.2 Australasia

Measured field strengths taken in Australia [Dixon, 1960] and New Zealand are somewhat higher than those observed elsewhere. For this reason, the 1974/1975 LF/MF Conference adopted the 1974 version of Recommendation PI.435 for applications in this area but some modifications were made. One of the modifications was that a correction factor of about 3 dB was added to the ITU-R formula. With such a correction factor included, the errors of the ITU-R and the Wang methods are both about 7 dB. It should be mentioned that measured field strengths of 11 long intercontinental (Asia-to-Australia) paths follow the predicted values by using the Wang method quite well (within 5 dB).

It should also be mentioned that the accuracy of both methods can be improved somewhat (less than 2 dB) if corrected geomagnetic latitudes are used instead of dipole latitudes.

5.3.2.3.3 Pacific

Japanese mobile experiments show that measured field strengths in many cases are about 10 dB stronger than predicted values by using the most conservative Cairo North-South curve. A study of the Japan-Antarctica experiment in western Pacific [Wang, 1989a] showed that when compared with measurements collected along this sailing course, the errors of the ITU-R method, the Cairo curve and the Wang methods are 7.5 dB, 6.5 dB, and 4.2 dB, respectively (sea gain factor has been included in all calculations).

5.3.3 Comparison of prediction methods

5.3.3.1 The Cairo North-South curve

The Cairo North-South curve, which is derived from low-latitude data and is latitude-independent, appears to be excellent for predicting field strength at low geomagnetic latitudes (e.g. 25° to 35°). When applied to higher (or lower) latitudes, predicted values are usually too high (or too low). Although it is well known for its simplicity, it should not be considered as a candidate for worldwide applications.

5.3.3.2 Region 2 method

Much the same can be said about the Region 2 method, which is derived from temperate-latitude data and is also latitude-independent. Excellent results can be expected when applied to average geomagnetic latitudes (e.g. 40° to 45°). This method should not be considered as a candidate for worldwide application either.

5.3.3.3 Recommendation ITU-R P.1147

The method described in Recommendation P.1147 was originally developed in 1974 for worldwide application. The sound treatment of the effects of geomagnetic latitudes of this method made it a very promising one. However, after years of extensive testing, some limitations have surfaced. For example, when applied to paths longer than, say, 4 000 km, the method has a strong tendency to underestimate field strength levels. Furthermore, Region 2 data do not seem to corroborate the frequency term of this method.

5.3.3.4 Modified FCC method

As in the method described in Recommendation P.1147, the Wang method (also known as the method proposed by ex-CCIR IWP 6/4 in 1985 or the modified FCC method), contains a latitude term. This method essentially has linked the Cairo curve and the FCC curve together and seems to work well for long paths as well as short paths.

5.4 LF/MF skywave propagation at daytime

Daytime sky-wave field strength data from 33 paths in Europe and North America have been studied [Wang 1995] and provide a simple procedure for estimating field strength and interference levels. Further measurements are needed especially at low latitudes.

5.4.1 Seasonal variation

Daytime field strengths display a consistent seasonal variation pattern with maximum occurring in winter months and minimum in summer months. This is true with both LF and MF cases. The winter-to-summer ratio is typically 10 to 20 dB. Many examples are available.

5.4.2 Effects of latitude

It is well known that latitude (throughout this paper, latitude means the geomagnetic latitude of the mid-point of a propagation path under study) is one of the most influential factors affecting night-time sky-wave propagation. Night-time signal levels decrease rapidly with increasing latitude. Both of the two most popular field strength prediction methods (the method described in Recommendation P.1147 and the new FCC method) contain similar latitude terms.

Daytime field strengths display a much lesser dependence on latitude. In fact, measured field strengths of several high-latitude paths are surprisingly strong.

Measurements of daytime field strengths are not as extensive as night-time measurements. Nevertheless, based on available data, it is safe to say that daytime signal levels at high latitudes can be strong. This applies to both LF and MF cases.

5.4.3 Effects of solar activity

Solar activity has a pronounced impact on night-time MF sky-wave propagation but has very little impact on LF propagation. Solar activity reduces MF night-time field strengths. The reduction is a function of sunspot number, latitude, distance and frequency. It has also been reported that daytime MF field strengths vary with solar activity in a similar manner as that of night-time [Wang *et al.* 1993; Wang 1983, 1989b; Hunsucker *et al.*, 1989].

5.4.4 Statistical distribution of field strengths

The distribution of sky-wave field strengths displays a tendency of skewness. That is, the median value is not always situated half way between the upper decile (10% of the time) and lower decile (90% of the time) values. Measurements taken in the United States of America show that the distribution of daytime field strength is usually skewed to the left (i.e., median value is closer to the lower decile value than to the upper decile value). The distribution of night-time field strengths is usually skewed to the right (i.e., median value is closer to the upper decile value than to the lower decile value). More recent measurements taken in Europe seem to corroborate this finding.

5.4.5 Daytime sky-wave field strength and interference levels

The concept of "annual median" value of field strengths was originally developed for purposes of estimating night-time coverage area of a given broadcasting station. For purposes of estimating interference levels, either from sky-wave to ground-wave or from sky-wave to sky-wave, the upper decile value is traditionally used. The upper decile value can be defined as the value that is exceeded for 10% of the nights (or days) of a year. Since daytime sky-wave is definitely a source of interference, not a source of service, annual median value has little usefulness. It does, however, serve as a stepping stone in calculating the upper decile value, which by far is a better and more meaningful indicator.

5.4.5.1 MF annual median value

Measurements made in Germany and Japan suggest that the annual median value of the sky-wave field strength at noon is about 45 dB lower than the corresponding value at six hours after sunset (SS+6) [see ITU-R Report P.431-5]. Based on more recent and somewhat more extensive data, we have reasons to believe that this figure is more accurate for higher frequencies than for lower frequencies in the MF broadcasting band. For lower frequencies, this figure appears to be slightly too high. It certainly is desirable to have one figure for the entire MF broadcasting band if at all possible. Having studied the latest data bank, it is believed that 42.5 dB is a more reasonable figure and can be used for the entire broadcasting band of 535 - 1 705 kHz.

5.4.5.2 MF upper decile value

Short-term fluctuations of daytime field strengths at higher frequencies are usually much larger than those at lower frequencies. Consequently, the difference between the upper decile and the median values vary with frequency. At 1 500 kHz, for example, the upper decile value is typically 10 to 15 dB greater than the median value. At 700 kHz, the difference is typically 5 to 10 dB. Again, if a single figure is desired, it is suggested that the figure of 12.5 dB be used for the entire MF band.

5.4.5.3 MF top-percentile value

On 1% of the days of the year, field strengths are expected to be 20 dB higher than the median value.

5.4.5.4 LF cases

When other factors are about the same, a night-time LF signal, say at 150 kHz, is about 3 dB stronger than that at 1 000 kHz. At daytime, this difference is expected to be much larger. The reason is that the D layer of the ionosphere, which exists only at daytime, can reflect LF waves but absorbs MF waves. Daytime LF field strength data are very difficult to collect, mainly due to the presence of the strong ground-wave component. Based on limited data available, the median value of the daytime field strength at LF appears to be 20 dB lower than its counterpart at night. The upper decile is about 12.5 dB stronger than the annual median value, similar to MF cases.

REFERENCES
FOR CHAPTER 5

- DIXON, J.M. [1960] - Some medium frequency sky-wave measurements. *Proc. IRE, Australia*, Vol. 21, 407-409.
- HAGG, E.L. [1982] - Reduction of MF sky-wave field strength at night due to magnetic-storm and winter-anomaly-related absorption. *AGARD Conf. Proc. No. 305*, Medium, Long and Very Long Wave Propagation (at frequencies less than 3 000 kHz), 29-1 to 29-9. Ed. J.S. Belrose. NASA Accession No. N82-27613. National Technical Information Service, Springfield, VA 22161, United States.
- HUNSUCKER, R.D., DELANA, B.S. and WANG, J.C.H. [1989] - Medium-frequency sky-wave propagation at high latitudes: results of a five-year study. *IEEE Trans. on broadcasting*, Vol. BC-35, No. 2, 218-222.
- ITU-R Report P.431-5 Analysis of sky-wave propagation measurements for the frequency range of 150 to 1600 kHz. Annex to Volume 6, 1990.
- ITU [1975] - Final Acts of the Regional Administrative LF/MF Broadcasting Conference (Regions 1 and 3), Geneva 1975.
- ITU [1988] - Final Acts of the Regional Administrative Radio Conference to Establish a Plan for the Broadcasting Service in the Band 1 605 - 1 705 kHz in Region 2 (Rio de Janeiro).
- KNIGHT, P. [1973] - MF propagation: a wave hop method for ionospheric field strength prediction. *BBC Eng.*, Vol. 100, 22-34.
- KNIGHT, P. [1977a] - LF and MF sky-wave propagation: the origin of the Cairo curves. BBC Research Dept. Report 1977/42.
- KNIGHT, P. [1977b] - LF and MF propagation: a study of sky-wave field strength variation. BBC Research Dept. Report 1977/12.
- PAN, Z. [1981] - MF night-time sky-wave field strength prediction. *Guangbo Yu Dianshi Jishu* (Broadcasting and Television Engineering), Vol. 28, 3, 1-6.
- PHILLIPS, G.J. and KNIGHT, P. [1965] - Effects of polarization on medium-frequency sky-wave service including the case of multihop paths. *Proc. IEE*, Vol. 112, 31-39.
- WANG, J.C.H. [1977] - Prediction of medium-frequency sky-wave field strength in North America. *IEEE Trans. Broadcasting*, Vol. BC-23, 43-49.
- WANG J. [1983] Interference and sharing at medium frequency, *AGARD Conf. Proc. No. 332*, Ed H. Soicher.
- WANG, J.C.H. [1985] - A sky-wave propagation study in preparation for the 1 605 - 1 705 kHz broadcasting conference. *IEEE Trans. on Broadcasting*, Vol. BC-31, 10-17.

- WANG, J.C.H. [1989a] - Prudent frequency management through accurate prediction of sky-wave field strengths. *IEEE Trans. on Broadcasting*, Vol. BC-35, No. 2, 208-217.
- WANG, J. [1989b] Solar activity and MF skywave propagation, *IEEE Trans.* **BC-35**, No. 2, pp 204-207.
- WANG, J.C.H. [1995] - LF/MF skywave propagation at day time, *IEEE Trans.* **BC-41**, No. 1, pp 23-27.
- WANG, J.C.H., KNIGHT, P. and LEHTORANTA, V.K. [1993] - A study of LF/MF sky-wave data collected in ITU Region 1. Proc. of IES93, Alexandria, VA-USA, 4-6 May 1993, J.M. Goodman, editor.

CHAPTER 6

HF PROPAGATION

This Chapter of the Handbook describes the ITU-R method for predicting the performance of radiowave communications systems in the high frequency band (3 - 30 MHz). It is a long-term prediction method that estimates values of the monthly medians of hourly smoothed sky-wave field strengths. The method may be used successfully for the design of HF systems, and for determining the appropriate frequency bands and frequencies to cope with normal diurnal and seasonal changes that may occur during operation of a system. It is not in general applicable to disturbed propagation conditions.

6.1 HF circuit design

An HF circuit is a link established for communications purposes between two terminals, by means of radio signals in the high frequency band. An HF radiocommunication system consists of one or more such circuits, and thus the design of a system is based on the design of the required circuit(s). In designing an HF circuit, the overall considerations are:

Factors determining the selection of the frequency band to be used:

- path length;
- time of year;
- number of consecutive days for which the circuit is required;
- time of day or night;
- number of hours within a 24 hour period for which the circuit is required;
- sunspot number;

If the circuit is to be used for an appreciable fraction of a year, it may not be possible to retain the same frequency throughout. In general, it will be desirable to use the highest frequency band possible, since this will minimize the path loss.

Factors determining the choice of antenna type are: type of service (point-to-point or point-to-area); if point-to-area service, size of area to be served; and path length.

Factors determining the minimum required field strength, and hence the required power are: level of man-made and other noise in target area; sensitivity of available receivers; type of modulation; for a point-to-point circuit, the gain of the receiving antenna; path loss; for a digital system, time and frequency dispersion; and gain of transmitting antenna.

Factors determining the exact choice of frequency within the selected band are: possible sources of interference (co-channel and adjacent channel); selectivity of available receivers and the required protection ratio. If a clear channel cannot be found, it may be necessary to use a band other than that originally selected.

Factors determining the choice of transmitter site are: availability of sites; and a site providing the best service to the target area, for example from the point of view of skip distance.

6.2 Requirement for predictions

The sky-wave signal strength and signal-to-noise ratio are dependent on the frequency of operation and on the characteristics of the ionosphere, which vary with time of day, season and sunspot number. A radiocommunication system operating in the HF band therefore has to cope with a varying transmission channel (for point-to-point communications) or channels (for broadcasting or area coverage). Long-term measurements of ionospheric characteristics have been made to establish the statistics of these variations, which are useful in both the design and operation of a system. The goal of predictions is to provide the channel characteristics to be used for planning a specified HF service. For this purpose, principal attention must be paid to median conditions, although some statistical considerations should also be given to day-to-day changes.

Worst-case conditions (e.g. sunspot minimum conditions) are often used in system design, so as to provide adequate signal at the receiver, usually at the expense of greater transmitter power. However, designing for the worst conditions has also led to frequency spectrum congestion, particularly in the broadcasting bands where high reliability is desirable but interference is very common. The judicious use of predictions promotes optimum use of spectrum resources.

Reliable HF performance predictions are needed for two main purposes:

- by the radio engineer in the design and construction of HF communications systems;
- by the operator of a HF communications system, usually for assistance in choosing the appropriate frequency band or frequency to be assigned under normal conditions.

HF propagation is dependent on the varying conditions of the ionosphere, which have slowly varying components (diurnal, seasonal and solar cycle) overlaid sporadically by short-term disturbances. In designing and operating radiocommunication services under normal conditions it is the slowly varying component that needs to be taken into account by long-term predictions.

Short-term predictions and real-time channel evaluation may be used by an HF operator to assist in day-to-day and hour-to-hour frequency management, especially in the presence of short-term disturbances. Information on the short-term forecasting of disturbances to radiocommunications will be found in Recommendation P.313.

6.3 Development of prediction techniques

To determine the performance of an ionospheric-dependent radio system, an ionospheric model and a propagation model are needed. These models make it possible to calculate path geometry and the noise environment, and may have provision to include power, antenna characteristics and required performance.

The ITU-R has developed a method for estimating the high frequency sky-wave field strength and transmission loss between ground-based terminals [Recommendation P.533]. This field strength model is a combination of a simplified version of ex-CCIR Report 252-2 (for path lengths less than 7 000 km) and the FTZ model developed by the Deutsche Bundespost for path lengths greater than 9 000 km, with interpolation in the interval.

This method has been refined in the light of experience gained in its implementation for the use of the HF Broadcast WARC (the HFBC-84 model), and of extensive testing within ITU-R Study Group 3. Although designed to be relatively simple and quick to use where large numbers of path computations are to be performed, it has proven to be sufficiently accurate for the prediction of HF circuit performance and system design.

6.4 Noise and interference

For the estimation of the performance to be expected in an HF communications circuit, it is insufficient to consider the signal level alone. Equally important are the characteristics of radio noise in the bandwidth of the receiving equipment and the level of unwanted interfering signals at the receiver. That is, signal-to-noise ratios (S/N) and signal-to-interference ratios (S/I) must also be considered.

The noise level at the receiver consists of the combined noise from three main sources:

- a) *the receiving system;*
- b) *atmospheric noise:* the source of atmospheric radio noise is lightning; the noise being propagated from all distances to the vicinity of the receiving system. Atmospheric noise data are given in Recommendation P.372 as a function of geographic location and season within 3-hour time blocks. The directional properties of atmospheric noise would be useful in the design of systems using directional antennas, but this information is currently unavailable.
- c) *man-made noise:* man-made noise is generally the result of human activity (industry, power lines, etc.) in the vicinity of the receiver. It may dominate the radio noise at the lower frequencies when there is no local atmospheric noise. It has been measured at many frequencies in the HF band for several typical locations.

Recommendation P.372 gives median man-made noise power as a function of frequency for business, residential and rural environments, together with the corresponding decile deviations from the hourly median field strength arising from within-the-hour variability at a fixed location. The upper and lower decile values in decibels, appropriate to HF, are given in Table 6.1. The median of all values is 10.0 dB. Values of the deviation for other percentages of locations may be obtained by assuming a log-normal half distribution each side of the median. Recommendation P.372 also gives the median value F_{am} for the three environmental categories at frequencies from 0.25 to 250 MHz.

TABLE 6.1

Upper and lower decile deviations from the hourly median field strengths for man-made noise (dB)

Frequency (MHz)	Environmental category					
	Business		Residential		Rural	
	D_u	D_l	D_u	D_l	D_u	D_l
1	9.8	4.0	10.0	4.4	9.2	6.6
2.5	11.9	9.5	10.1	6.2	10.1	5.1
5	11.0	6.2	10.0	5.7	5.9	7.5
10	10.9	4.2	8.4	5.0	9.0	4.0
20	10.5	7.6	10.6	6.5	7.8	5.5

Other sources of noise are the ionosphere, the magnetosphere, the Sun and the "Milky Way" galaxy. The noise levels from such sources are usually much less than atmospheric noise and can be ignored in terrestrial communications.

The unwanted signals from known interferers may be estimated in the same way as the wanted signal. Interference is often greater at night due to decreased absorption. The effect of unknown interferers is to increase the noise level, but is not easily quantified.

6.5 Variations of field strength and propagation features

6.5.1 HF signal characteristics - multipath

A feature of the propagation of signals on HF links is multipath, which results from the existence of more than one ray between transmitter and receiver. This is illustrated in Fig. 6.1, which shows two different ray paths or modes between the transmitter and receiver. Mode 2 has two F2-layer hops (2F mode), and so is said to have a higher *order* than mode 1, which has only one hop (1F mode). D is the distance between the path terminals, and $d = D/n$, where n is the number of hops. h' is the virtual reflection height, or mirror reflection height, for the F2 layer in this example.

Multipath propagation is one cause of distortion in communication signals. The multipath state is determined by propagation conditions along the circuit and also depends on the operating conditions used on the circuit. It is necessary for the communicator to have effective means of decreasing multipath. Such means may be the selection of an appropriate working frequency or of an appropriate ratio of working frequency to MUF, especially on one-hop circuits, i.e. where the propagation is single-mode F layer (1F mode). As an example, the extent of multipath and of signal distortion as a function of working frequency/MUF is given in Table 6.2.

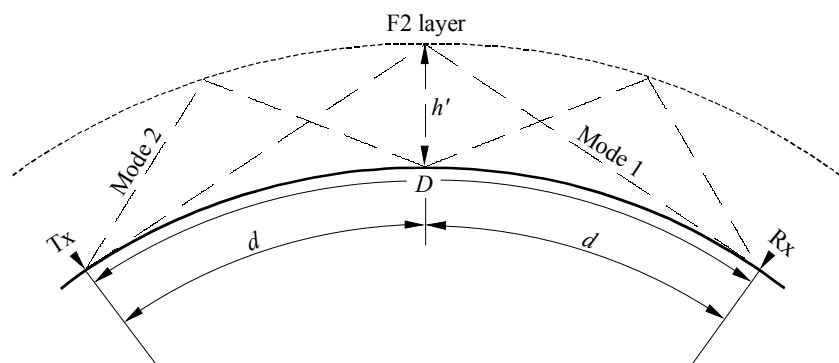


FIGURE 6.1
Propagation modes

TABLE 6.2

Fading characteristics of multipath signals

Mode	1F		1F + 2F	2F
	1 - 0.9	0.9 - 0.7	0.7	0.7
Working frequency/MUF	1 - 0.9	0.9 - 0.7	0.7	0.7
Number of rays	2 - 4	1	3 - 9	4 - 8
Spread in signal propagation time (ms)	0.3 - 0.6	-	0.8 - 1.2	0.6 - 0.8
Amplitude distribution	Rayleigh	Rice	Rayleigh	Rayleigh
Interval of temporal correlation (s)	4 - 6	15 - 25	2 - 4	2 - 4
Interval of frequency correlation (Hz)	2 500	30 000	0 - 1 000	1 250
Interval of space correlation (m)	300 - 500	1 000	300	300
Spread of angles in vertical plane (degrees)	10 - 20	1 - 2	8 - 30	8 - 25

6.5.1.1 Time delay

When a single mode (one-hop F) is operational, the propagation may comprise up to four multipath components as there can be both O and X (magneto-ionic polarization components) and high- and low-angle rays at frequencies near the MUF [Hall *et al.*, 1996]. When the ratio of working frequency/MUF exceeds 0.9 the magneto-ionic components are resolvable and there are 2-4 rays with equal relative powers and total time dispersion about 0.3 - 0.6 ms. As the ratio of working frequency/MUF decreases below 0.9 the O and X modes merge and the high-angle ray becomes defocused and disappears, limiting the total dispersion for the path. When the ratio decreases further to below 0.7, the time dispersion may increase up to a maximum of 4 ms.

The ray structure of the 2F mode alone consists of the resolvable magneto-ionic components and the low-angle and high-angle rays. For multi-hop links (2F and higher-order modes) the multipath does not depend so much on the ratio of working frequency/MUF as there are usually several groups of rays with a total time dispersion of about 0.6 - 0.8 ms.

The values of time dispersion are also dependent on the path length (§ 6.11.3.2).

6.5.1.2 Amplitude fading

Multipath can cause severe amplitude fading and a consequent reduction in communication quality.

When only one ray exists in a region of single-mode propagation (1F), the amplitude fading is the least severe and the most slow. The distribution of fading of such a signal is a Nakagami-Rice distribution with a small steady component, and the interval of temporal correlation of fading attains 15-25 s. The interval of frequency correlation of fading is sufficient and the fading of the spectral components of the signal are smooth within the frequency bandwidth of the channels used for HF communication. Spatial diversity is effective if the antennas are separated by 1 000 m or more. The angle of arrival in the vertical plane for such a signal has some spread, the standard deviation of this spread is 1-2°.

As the number of rays increases, the distribution of fading approaches a Rayleigh distribution, the intervals of temporal, frequency and spatial correlation decrease, the spread of angles in the vertical plane increases, the changes of signal phases become more rapid. Such deterioration of the signal is noticeable particularly when the 1F mode is replaced by a combination of the 1F and 2F modes. In this situation there are also selective fading and intersymbol distortion.

When only 2F mode propagation exists, the signal distortion is approximately the same as for combined modes 1F and 2F. The same applies to multi-hop links.

NOTE – It should be noted that the multipath features mentioned above are applicable to an undisturbed ionosphere. For a diffuse ionosphere multipath effects show less dependence on working frequency/MUF.

6.5.2 Absorption

For frequencies above LF, radiowaves are absorbed as they pass through the D region. The absorption is very frequency dependent: when its value at 30 MHz is 1 dB, it may be 10 dB or more at lower HF frequencies. The absorption will also be higher for signals at low elevation than for those at high, because the low angle rays have to travel for a longer distance through the D region.

6.5.3 Fading

Experience has shown that information concerning the mean value of the received signal is not sufficient for planning radiocommunication systems. The variations in time, space and frequency, collectively described as fading, also have to be taken into consideration. Fading has a decisive influence on the performance of radiocommunication systems and on the type of modulation that may be used effectively. It is essential to know the severity and rapidity of fading to be able to specify the power required for transmitters, the necessary protection ratio to guard against interference and, with additional knowledge of the correlation of signals at separate antennas or frequencies, to be able to determine the most efficient and economical diversity or coding systems. Similar considerations may also apply to the noise and interference at the receiving site.

6.5.3.1 Causes of fading

Fading may be caused by several different effects, such as:

- movement of the ionosphere, and multipath changes causing interference fading;
- rotation of the axes of the polarization ellipses;
- variations of the ionospheric absorption with time;
- focusing and temporary disappearance of the signal due to MUF failure.

Fading may appear either as amplitude fading or as a Doppler-frequency shift. Amplitude fading may cause dispersion in both time and frequency. Motion of the transmitter, receiver or ionospheric reflector causes Doppler shifts. In general multipath signals have differing amplitudes and frequency shifts.

6.5.3.1.1 Interference fading

Interference fading results from interference between two or more waves which travel by different paths to arrive at the receiving point. This type of fading may be caused by interference between: sky-wave and ground-wave, multiple reflected sky-waves, the ordinary (O) and extraordinary (X)

waves, and various scattered signals from irregularities. Interference fading may last for a period of a fraction of a second to a few seconds, during which time the resultant field intensity may vary over wide limits.

6.5.3.1.2 Polarization fading

Polarization fading occurs as a result of changes in the direction of polarization of the downcoming wave, relative to the orientation of the receiving antenna, due to random fluctuations in the electron density along the path of propagation. Polarization fading also lasts for a period of a fraction of a second to a few seconds.

6.5.3.1.3 Absorption fading

Absorption fading is caused by variation in the absorption due to changes in the densities of ionization and it may sometimes last longer than one hour.

6.5.3.1.4 Skip fading

Skip fading may be observed at receiving locations near the skip distance (the minimum range from the transmitter before the ray passes through the ionospheric layer rather than being refracted down from it) at about sunrise and sunset, when the basic MUF for the path may oscillate around the operating frequency. The signal may decrease abruptly when the skip distance increases past the receiving point or increase with a decrease in the skip distance.

6.5.3.1.5 Selective fading

Fading tends to be faster at high frequencies than at low frequencies, because for a given movement in the ionosphere, there is a greater phase-shift on the shorter wavelengths. Motion of the ionized regions causes selective fading (frequency-dependent fading) when, on a modulated carrier, the frequency components in the sidebands fade independently, giving rise to distortion of the modulation envelope. The motion produces changes in path length, and Doppler shifts of frequency on each of the individual contributing signal components. Selective fading may also be caused by multipath propagation at HF.

6.5.3.2 Characteristics of amplitude fading

6.5.3.2.1 Depth of fading

Depth of fading is measured by the amplitude distribution, or probability density function of the amplitude of the downcoming wave. The amplitude distributions normally conform to one of three standard statistical curves or distributions: Rayleigh, normal or Gaussian distribution, and log-normal. For a description of these distributions, see Recommendation P.1057.

6.5.3.2.2 Rapidity of fading

The rapidity or speed of fading can be characterized in different ways. One statistical property of the instant-to-instant variation of amplitude is given by the autocorrelation function. The rapidity or the speed of fading can be described in terms of the time auto-correlation function of the amplitude or in terms of the power spectrum of fading, which is the Fourier transform of the auto-correlation function. The frequency spectrum of the fading signal may be obtained with the aid of the auto-correlation function. The width of the fading power spectrum is related to the speed of fading.

Another definition of fading rate is the number of positive crossings per unit time through any specified level, or the number of maxima N of the amplitude of the signal envelope per unit time. It has been shown that if σ is the standard deviation of the power spectrum of the received signal, $N = 2.52 \sigma$.

6.5.3.3 Fading allowances for service planning

A service planning method which makes use of a compatibility analysis will require:

- comparison of the strength of wanted signals with noise to establish whether a desired reception quality is achieved in the absence of interference; and
- comparison with co-channel and adjacent-channel interfering signals to determine if these are harmful.

In addition to monthly median estimates, appropriate fading allowances are required. These have to be considered separately depending on whether the background is atmospheric noise, man-made noise or an interfering signal, but in each case they depend on both short- (within-the-hour) and long-term (day-to-day) fading of both the wanted signal and the background, the correlation between the wanted signal and background, and the fraction of the time for which the desired reception quality must be achieved.

With the monthly median wanted signal/background for satisfactory reception given, we may evaluate the fading allowance $F_{b,90}$ necessary to achieve the desired reception quality for 90% of the time in the presence of short- and long-term fading of both the signal and background. Fading allowances for other percentages of the time may then be expressed in terms of $F_{b,90}$.

On the assumption that both the within-the-hour and day-to-day fading of the wanted signals and the background are uncorrelated, $F_{b,90}$ (dB) is given by the root-sum-square of four deviations:

- S_{wh} : wanted signal lower decile deviation from the hourly median field strength arising from within-the-hour changes (dB)
- S_{dd} : wanted signal lower decile deviation from the monthly median field strength arising from day-to-day changes (dB)
- B_h : background upper decile deviation from the hourly median field strength arising from within-the-hour changes (dB)
- B_d : background upper decile deviation from the monthly median field strength arising from day-to-day changes (dB).

The World Administrative Radio Conference for Planning of HF Bands Allocated to the Broadcasting Service (WARC HFBC-87), adopted for short-term signal fading the upper decile deviation of 5 dB and the lower decile deviation of 8 dB. For long-term signal fading the decile deviations were taken as a function of the ratio of operating frequency to the basic MUF as given in Table 6.3. The fading allowance $F_{b,x}$ for $x\%$ of the time is given in terms of $F_{b,90}$ by:

$$F_{b,x} = c \cdot F_{b,90} \quad \text{dB} \quad (6.1)$$

Values of c for x in the range 50% to 90% are similar for all distributions, and are given in Table 6.4.

TABLE 6.3

90% and 10% deviations from the predicted monthly median value of signal strength (dB), arising from day-to-day variability

Corrected geomagnetic latitude*	< 60°		≥ 60°	
	90%	10%	90%	10%
≤ 0.8	8	6	11	9
1.0	12	8	16	11
1.2	13	12	17	12
1.4	10	13	13	13
1.6	8	12	11	12
1.8	8	9	11	9
2.0	8	9	11	9
3.0	7	8	9	8
4.0	6	7	8	7
≥ 5.0	5	7	7	7

* If any point on that part of the great circle which passes through the transmitter and the receiver and which lies between control points located 1 000 km from each end of the path reaches a corrected geomagnetic latitude of 60° or more, the values for ≥ 60° must be used.

TABLE 6.4

The value of *c* (for calculating fading allowance)

<i>x</i> (%)	50	60	70	80	90
<i>c</i>	0	0.18	0.36	0.63	1.0

6.5.4 Regional anomalies

6.5.4.1 Features of fading encountered in the Tropical Zone

Fading of signals in the tropics at low geomagnetic latitudes has special characteristics due to the regular daytime occurrence of sporadic E, and to irregularities in the night-time F layer (spread F).

6.5.4.1.1 Fading due to sporadic E

Fading observed during daytime in the equatorial zone is often attributed to sporadic E. In a narrow zone near the magnetic equator ($\pm 6^\circ$ magnetic dip), a special type of highly transparent sporadic E called equatorial sporadic E or Es-q appears regularly during daytime.

6.5.4.1.2 Flutter fading

Very rapid fading has been observed in the equatorial region after sunset, where it represents one of the most important factors in the degradation of communications, particularly for broadcast services. This flutter fading is caused by F-region irregularities, known as spread F. In the equatorial zone after local sunset, such irregularities develop in the F-region ionization between 30°N and 30°S geomagnetic latitude, their occurrence being particularly frequent within $\pm 20^\circ$ geomagnetic latitude. Under these conditions, the F region increases markedly in height and breaks up into patchy irregular plumes associated with plasma instabilities. The spread-F irregularities are seen normally after sunset and before midnight. The seasonal variations show maxima at the equinoxes near sunspot maximum.

Both north-south circuits and east-west circuits are affected. The time of start is well defined and sudden, but the time of disappearance is gradual. The fades are deep and the signal is almost completely drowned in noise, even though the mean signal strength remains high. The flutter fading rate is proportional to the wave frequency, ten fades per second being typical at 15 MHz.

6.5.4.1.3 Surge fading

Another type of fading in the Tropical Zone is surge fading, which is slower than flutter fading, but is deeper and accompanied by severe distortion. It is worst after sunset and more pronounced during autumn and winter. The recurrence rate is a few surges per minute.

6.5.4.1.4 Fading allowances

A discussion of the fading allowances required for planning broadcasting services in the Tropical Zone is given in ITU-R Report BS.304. Recommendation BS.411 proposes values of fading allowance to ensure that the steady-state ratio is attained for 90% of the time, under three conditions of reception, i.e., where the RF signal-to-noise ratio is as follows:

- ratio of wanted signal to interference: 16 dB;
- ratio of wanted signal to atmospheric noise: 17 dB;
- ratio of wanted signal to man-made noise: 12 dB.

6.5.4.2 High latitude effects

6.5.4.2.1 Frequency and time spreading

Irregularities in the polar cap ionosphere have motions up to 1.0 km/s, and therefore ionospherically reflected signals are subject to Doppler shifts. The roughness of the ionosphere also gives rise to multipath and time spreading. For great-circle paths, the frequency spread is 0.1 to 0.5 Hz. For non-great-circle paths it is 5 to 10 Hz. The time-delay spread is 100 to 200 ms for great circle paths, and 1 to 2 ms for non-great circle paths.

6.5.4.2.2 Polarization

At high latitudes, where the magnetic field is almost vertical, the extraordinary or X-mode waves have horizontal polarization for near grazing incidence. Since X-mode waves are strongly absorbed, a vertical HF antenna, receiving the ordinary or O-mode waves, should have an advantage over a horizontal antenna. However, horizontal dipoles are usually employed for convenience, and operate satisfactorily.

6.5.4.2.3 Two-hop modes

The ice caps of Greenland and Antarctica are particularly poor reflectors of radio energy. This results in greater path loss for multi-hop modes over the ice-caps than elsewhere. The irregular terrain and the large variation in ground electrical properties can also increase signal loss at the ground reflection point.

6.5.4.2.4 Scattering from electron density irregularities

Electron density irregularities in the ionosphere scatter radio waves over a wide range of frequencies from HF to UHF. In the case of oblique HF transmissions, backscatter is observed from all heights. Backscatter from E-region auroral and F-region irregularities is aspect angle sensitive; maximum reflectivity occurs when the propagation direction is normal to the magnetic field lines.

6.6 Reliability of HF radio systems

The communications reliability of an HF radio system may be estimated with some confidence when the underlying statistics of the propagation and noise are known. The statistics of the signal-to-noise ratio are used to estimate the basic reliability. Recommendation P.842 gives methods for estimating reliabilities and compatibilities for use in the planning and design of radio systems. Circuit reliability applies to a single frequency, considering all propagation modes; reception reliability to a single circuit, considering all frequencies; and service reliability to area coverage, considering a set of representative reception locations. For network applications, path reliability applies to circuits in series, and communications reliability to paths in parallel.

The terms *basic* and *overall* may be used in combination with the reliabilities mentioned above. Basic reliability is concerned with communications in the presence of noise alone, whereas overall reliability also includes the presence of known interference. A summary of the calculation procedure is given below.

Refinement of Recommendation P.842 is underway to extend the definitions and the methods of calculation of reliability to also include the treatment of dispersion.

6.6.1 Basic circuit, reception and service reliability (BCR, BRR, BSR)

For the computation of basic circuit reliability the method requires the following parameters: monthly median available receiver signal power (§ 6.8.1.7); monthly median atmospheric, man-made and galactic noise power; upper and lower decile deviations from the monthly median signal and noise powers, long-term (day-to-day) and short-term (within-the-hour); and required signal-to-noise ratio. Recommendation F.339 includes a table giving the required signal-to-noise protection ratios for various services. Recommendations F.240 and BS.560 also include information on radio frequency protection ratios in the fixed and broadcasting services respectively.

Basic reception reliability (BRR) is a function of BCR at all frequencies, while basic service reliability (BSR) concerns service to a required area, and its determination involves the use of test points within the service area. Basic service reliability is the value of BRR exceeded by a required percentage of the test points.

6.6.2 Overall circuit, reception and service reliability (OCR, ORR, OSR)

The computation of overall circuit reliability parallels the computation of basic circuit reliability except that the received powers from the potentially interfering transmitters are summed and compared with the available signal power to determine the within-the-hour and the day-to-day

distribution of hourly median signal-to-noise-plus-interference ratios. The required RF protection ratio may be obtained from Recommendation F.240 for the fixed service or from Recommendation BS.560 for the broadcasting service.

6.6.3 Basic path and communications reliabilities (BPR, R)

In networks, where a number of circuits are available between terminals, path reliability (BPR) and communications reliability (R) may be estimated from the BRR and BPR respectively.

6.6.4 Computation of compatibility

Compatibility is a measure of the degradation a wanted circuit or service will suffer in the presence of interference. In the case of a single point-to-point circuit the Circuit Compatibility (CC) is defined by the percentage of time during which a specified criterion of service quality is achieved at the receiver location in the presence of interference, relative to the value that would be obtained if only noise were present, i.e. it is the ratio of overall circuit reliability to basic circuit reliability.

If the wanted service applies to an area rather than a single reception point the compatibility can be defined either as Time Service Compatibility (TSC) or as Area Service Compatibility (ASC). TSC is the percentage of time during which a specified percentage of the target area can be served in the presence of interference, relative to the value that would be obtained if only the environmental noise would be present, i.e. it is the ratio of overall service reliability to basic service reliability. ASC is the percentage of the target area which can be served during a specified percentage of time in the presence of interference, relative to the value that would be obtained if only the environmental noise were present.

6.7 Service needs

Different types of radio services have different requirements. There are two major types of HF radio service: flow of information in one direction only (e.g. broadcasting); flow either one-way or two-way (e.g. fixed and mobile radio services).

TABLE 6.5

Radio services and their needs

	Fixed Service	Mobile Service	Broadcasting Service
Communication type	Point-to-point	Point-to-point and/or point-to-area	Point-to-area
Information flow	One- or two-way	Two-way	One-way
Frequency agility	Frequencies can be changed whenever required		Frequency continuity desirable
Reliability considered	Reception reliability	Communications or service reliability	Service reliability
Transmitter power	Medium	Medium or low	High
Receiver sensitivity / antenna gain	High	High sensitivity/ antenna limitations	Low
User	Technical	Technical	Non-technical
Minimum required audio quality	Intelligible	Intelligible	Good

6.8 The HF radio sky-wave propagation model

Recommendation P.533 provides estimates of the monthly median values of the maximum usable frequency (MUF), received signal strength, available receiver power, signal-to-noise ratio, reliability and lowest usable frequency (LUF) between two locations for any specified time and level of solar activity. This involves the following stages: i) determination of a representative model of the electron concentration over the propagation path, taken as being along the great circle between transmitter and receiver, ii) a ray assessment in order to estimate modes present and to determine median values of the MUF and related quantities, iii) calculation of the received signal intensity in terms of a) the various separate transmission-loss factors judged to be significant or b) from fitting empirical equations to measured data for different paths, times and frequencies, iv) estimation of the intensities of atmospheric noise and background man-made noise, and v) choice of some reference required signal-to-noise ratio to yield an acceptable grade of service.

Recommendation P.533 applies a ray-path analysis for paths up to 7 000 km, composite mode empirical formulations from the fit to measured data beyond 9 000 km, and a smooth transition between these approaches over the 7 000 - 9 000 km distance range. For all ranges the same numerical representations of the ionospheric characteristics foF2 and M(3000)F2 and for the noise intensities are employed.

Program REC533 is a computer implementation of Recommendation P.533. The antennas of Recommendation BS.705 have been incorporated in this program, permitting the computation of gain at both the transmitter and receiver. There is a wide selection of output options available ranging from the prediction of a single parameter such as field strength for a specified series of frequencies and times to a more sophisticated output involving the prediction of the parameters together with mode, elevation angle and system performance parameters. The program thus finds application for frequency planning, system design and for operational investigations.

Since at HF the active modes and their elevation angles depend markedly on ionospheric conditions, transmitted frequency and path length, a first requirement for accurate predictions must be a model of the vertical distribution of electron concentration in the E and F regions. This must take account of the known large geographic and temporal variations in the ionosphere. The most extensive ionospheric database is that derived from the world network of ionosondes. Hence models of the vertical distributions are produced with the parameters of the models given by empirical equations in terms of the ionospheric characteristics which are scaled on a routine basis at all ionosonde stations.

Numerical mapping of ionospheric characteristics is described in Recommendation P.1239. Recommendation P.533 uses the Oslo sets of foF2 and M(3000)F2 coefficients and foE is evaluated using empirical equations.

6.8.1 Path lengths up to 7 000 km

6.8.1.1 Monthly median path basic MUF and operational MUF

In Recommendation P.373 the term "basic MUF" is defined as the highest frequency at which a radiowave can propagate between given terminals on a specific occasion by ionospheric refraction alone. The "operational MUF" is the highest frequency that will give acceptable operation between two terminals on a specific occasion; under the same operational conditions it is greater than the basic MUF.

MUF (Maximum Usable Frequency) is a function of path length, geographic position and time. There are systematic variations with time-of-day, season and solar epoch, and also irregular day-to-day changes. Methods of prediction are restricted to determining smoothed monthly median values and to providing statistical parameters descriptive of the daily figures. The monthly median path basic MUF is taken as the highest monthly median basic MUF of any mode reflected from the different layers, so that it is necessary to first determine the separate E and F2 MUFs depending on path length.

The stages in the basic MUF (monthly median) determination process are:

- i) selection of procedures to define the positions of the control points along the propagation path at which ionospheric information should be sought;
- ii) evaluation of the critical frequencies of the E and F2 layers and M(3000)F2;
- iii) calculation of appropriate hop lengths;
- iv) determination of factor related to hop length (and other parameters);
- v) calculation of the path or mode basic MUFs in terms of the factors of (iv) above and the appropriate critical frequency.

6.8.1.2 E-layer basic MUF

The basic MUF of an n -hop E mode over a path length D is given in terms of the hop length, foE and the secant of the angle of incidence at a mid-hop mirror reflection height of 110 km for a hop length of $d = D/n$. The E-layer basic MUF for the path is that appropriate to the lowest-order E mode. The maximum length for a single-hop mode is 2 000 km and E modes are determined only for paths up to 4 000 km. The MUFs for higher-order modes are calculated using the same equation. The E-layer operational MUF is taken as equal to the basic E-layer MUF.

6.8.1.3 F2-layer basic MUF

The order, n_0 , of the lowest-order mode (minimum elevation of 3°) is initially determined from geometrical considerations, using an estimate for mirror reflection height h_r at the mid-path control point.

The parameter d_{max} , which is the maximum possible path length for a single-hop mode depends on the underlying ionization, indicated by the ratio $x = foF2/foE$, and the characteristic M(3000)F2.

For the lowest order mode, the F2-layer basic MUF is a function of factors including the hop length d , d_{max} and the critical frequency. For paths lengths of d_{max} and less, calculations are based on propagation via the ionosphere given at the mid-path position. The F2-layer basic MUF for an n -hop higher-order mode is calculated using the above equations for a hop length of $d = D/n$.

With greater distances the so-called two-control-point procedure is used in which the path MUF is taken as the lower of the two F2(d_{max})MUF values centred on locations $d_0/2$ km along the great circle from the transmitter and receiver, where d_0 is the hop length of the lowest-order mode. The F2-layer basic MUF for an n -hop higher-order mode is calculated in terms of F2(d_{max})MUF and a distance scaling factor dependent on the hop lengths of the mode in question.

The operational MUF depends, among other factors, upon the types of antenna used, the transmitter power, class of emission, information rate and required signal-to-noise ratio. The differences between the operational MUF and the basic MUF can be explained by various ionospheric phenomena, such as scattering in the E and F regions, off-great-circle propagation and propagation by unusual modes when ionization irregularities exist; also spread F may be an important factor. Values of the ratio of the operational MUF to the basic MUF given by Recommendation P.1240 for different conditions are contained in Table 6.6.

TABLE 6.6

Ratio of the operational MUF to the basic MUF

e.i.r.p., dBW	Summer		Equinox		Winter	
	Night	Day	Night	Day	Night	Day
< 30	1.20	1.10	1.25	1.15	1.30	1.20
> 30	1.25	1.15	1.30	1.20	1.35	1.25

The frequency of optimum traffic (FOT, Recommendation P.373), known alternatively as the optimum working frequency (OWF), is defined as the highest frequency that is likely to propagate at a given time between a specified pair of terminals via any ionospheric mode for 90% of the days. It is given in terms of the monthly median path operational MUF from a knowledge of day-to-day ionospheric variability. The E layer experiences relatively little variability from one day to another, and when the E layer controls the path MUF, the FOT is taken as 0.95 of the MUF. For F2 modes where the variation is larger, FOT is taken as a variable fraction of the operational MUF as indicated in Recommendation P.1240.

6.8.1.4 Oblique ray paths

Up to three E modes (for paths up to 4 000 km only) and up to six F2 modes are selected, each of which meets the following criteria:

- E modes – i) the lowest-order mode with a hop length of up to 2 000 km, and the next two higher-order modes;
- ii) having an elevation angle $\geq 3^\circ$;
- F2 modes – i) the lowest-order mode and the next five higher-order modes;
- ii) having an elevation angle $\geq 3^\circ$;
- iii) screening by the E layer does not occur.

Elevation angle is given in terms of hop length and mirror (i.e. apparent) reflection height for both E and F2 modes using a simple equation derived by geometrical considerations. In the case of E modes the mirroring height is 110 km.

For F2 modes the ITU-R has adopted empirical relationships giving mean mirror-reflection height as a function of time, location and path length. The values of the parameters of this model are given in terms of the average of the predicted ionospheric characteristics foE, foF2 and M(3000)F2 along the path. Where the level of the underlying ionization, indicated by the ratio $x = \text{foF2}/\text{foE}$, is average to low ($x > 3.33$) mirroring height is independent of this ionization but exhibits a frequency

dependence. In contrast, where the E region is well established no frequency dependence is apparent but the variation with x is significant. The two situations approximate to "night-time" and "daytime" conditions.

6.8.1.5 Field strength

Once all existing modes and their associated elevation angles are known, the next stage is to evaluate the corresponding signal intensities at the receiver. Monthly median values of field strength E_{tw} for each propagation mode w at frequency f are determined in terms of transmitter radiated power, transmitting antenna gain and the transmission losses.

$$E_{tw} = 136.6 + P_t + G_t + 20\log f - L \quad \text{dB (1}\mu\text{V/m)} \quad (6.2)$$

where:

- P_t = transmitter power (dB(1 kW))
- G_t = transmitting antenna gain (decibels relative to an isotropic antenna)
- L = summed transmission losses (dB)

The resultant equivalent median sky-wave field strength, E_{ts} , is taken as the root-sum-squares (RSS) for up to N modes where N encompasses the three strongest F2 modes and also, in the case of path lengths to 4 000 km, the two strongest E modes.

6.8.1.6 Transmission losses

Recommendation P.533-5 models the following loss mechanisms:

- i) basic free-space transmission loss (dB) which depends on the length of the raypath (slant range) and on the frequency;
- ii) absorption loss (dB), which occurs largely in the E and D regions and is expressed as a function of the solar zenith angle, χ ;
- iii) summed ground-reflection loss at intermediate reflection points (2 dB per point);
- iv) factor to allow for auroral and other (e.g. polarization) signal losses, dB;
- v) "above-the-MUF" loss: monthly-median field strength falls quickly above the basic MUF of a given mode as propagation is not possible on all individual days except by scatter mechanisms, dB;
- vi) term containing those effects not otherwise included in the method (the present recommended value is 9.9 dB) and has been determined by comparing predicted and measured values of field strength.

6.8.1.7 Median available receiver power

For each mode w the corresponding available signal power P_{rw} (dBW) from a lossless receiving antenna of gain G_{rw} (dB relative to an isotropic radiator) in the direction of signal incidence is:

$$P_{rw} = E_{tw} + G_{rw} - 20 \log_{10} f - 107.2 \quad \text{dBW} \quad (6.3)$$

From the above modes, the resultant root-sum-square (RSS) monthly median receiver power P_{sr} (dBW) is calculated by taking up to the three strongest F2 modes and additionally the two strongest E modes for ranges up to 4 000 km.

It should be noted that the strongest modes associated with the resultant RSS median receiver power may be different to those associated with the resultant RSS equivalent median sky-wave field strength as determined in § 6.8.1.5 because receiving antenna gain and directivity are allowed for.

6.8.2 Path lengths beyond 9 000 km

6.8.2.1 Introduction

Predictions are made by dividing the path into the minimum of equal length hops, none of which exceeds 4 000 km.

6.8.2.2 Monthly median path basic MUF

F2-layer basic MUF is evaluated by the method of § 6.8.1.3. It is not determined for higher-order F2 modes nor for E modes.

6.8.2.3 Field strength

Expressions are formulated giving the upper and lower reference frequencies, f_M and f_L respectively, where the RSS field strength E_{fl} is a low limiting value at frequency f_L . The field at any other frequency f is expressed in terms of the free-space field and is a function of these three frequencies.

The transmitter gain (dB) assumed is the largest value at the required azimuth in the elevation range 0° to 8° . The increase in field strength due to ray focusing at long distances is allowed together with a term containing those effects not otherwise included in the method (the present recommended value is -3.7 dB). This latter term is similar in concept to that of v_i in § 6.8.1.6.

6.8.2.4 Median available receiver power

The resultant RSS median receiver power P_{sr} is calculated in terms of the RSS field strength E_{fl} of § 6.8.2.3 above and equation (6.3) above and taking the largest receiving gain at the required azimuth in the elevation range 0° to 8° .

6.8.3 Paths between 7 000 and 9 000 km

In this distance range RSS field strength and RSS available receiver power are obtained by using a weighted interpolation procedure from the two values obtained respectively from the methods given in §§ 6.8.1 and 6.8.2 above for the required distance.

6.8.4 System performance parameters

The following system performance parameters are evaluated:

- i) Monthly median signal-to-noise ratio (S/N). The noise background is evaluated at the receiving site. Noise power P_n (dBW) at the receiver site for the frequency of interest and the quoted receiver bandwidth is taken as the largest of the median atmospheric, man-made and cosmic noise. The monthly median signal-to-noise ratio (dB) is deduced from the difference between this quantity and the RSS receiver power. Values of S/N for any other percentage of time are evaluated in terms of the variabilities of both signals and noise.
- ii) Lowest usable frequency (LUF) and basic circuit reliability (BCR). The LUF is defined as the lowest frequency at which a required S/N ratio is achieved by the monthly median S/N ratio, and BCR as the probability of achieving a required S/N ratio respectively. They are evaluated in terms of the variabilities of both signals and noise (thus BCR = 0.50 at the LUF).

6.9 Antenna considerations

The function of the antenna is to transmit or to receive radiowaves within its design frequency band. Recommendation F.162, for the fixed service, gives minimum and economic standards for directive antennas that help alleviate the frequency sharing problem by optimizing the transmitted energy and minimizing interference. These standards are given in terms of the directivity, the angular beamwidth of the wanted service and the ratio of the power-flux densities in the wanted and interfering directions. Recommendation BS.705 gives details of broadcasting antennas.

In terms of wavelength, HF antennas are usually located close to the ground. The conducting surface affects the characteristics of the antenna, and a real or artificial ground is usually considered part of an HF antenna system.

The distance of the receiver from the transmitter, or the distance, shape and size of the service area, are factors which influence the antenna selection. For short-range sky-wave communication to a few hundred kilometres, a relatively low-gain or omnidirectional antenna such as a horizontal dipole should be used, especially if the transmitting antenna is located within the area to be served. For longer ranges, a directional transmitting antenna such as a dipole array or log-periodic antenna should be used to provide maximum gain in the direction of the receiver or service area. A directional antenna may also be used to minimize interference to another user by orienting a minimum in its radiation pattern toward that user.

6.9.1 Antenna characteristics

The basic antenna current element is the Hertzian dipole, a thin linear conductor, short compared with a wavelength and carrying a constant current. The characteristics of more complicated antennas are computed by summation of the contributions of all current elements, taking account of the physical spacing, relative phasing and amplitudes of the currents.

6.9.2 Gain

The gain g of an antenna is the ratio of the input power required by a loss-free reference antenna and the input power supplied to the given antenna, to produce the same field strength at the same distance in a given direction. Gain may apply to a specified polarization.

There are three types of (directivity) gain corresponding to the choice of reference antenna - at HF, an isotropic antenna is usually the reference:

- g_i gain relative to an isotropic antenna in free space;
- g_d gain relative to a half-wavelength dipole in free space, whose equatorial plane contains the given direction;
- g_v gain relative to a very short vertical antenna normal to a perfectly conducting plane surface which contains the given direction,

where G (decibels) = $10 \log_{10} g$.

The half-wavelength or half-wave dipole in free space has a maximum gain in its equatorial plane of $G_i = 2.15$ dB, i.e. G_i and G_d are related by: $G_i = G_d + 2.15$ dB. This antenna is a straight wire or rod centre-fed by a transmission line. Its length, a little less than one-half wavelength, determines the resonant frequency, and its input impedance is about 73 ohms.

The directivity in a given direction is the ratio of the maximum radiation intensity to the radiation intensity of an isotropic source radiating the same power. It is given by:

$$D = \frac{4\pi}{W_0} |E(\theta, \varphi)|_{max}^2 \quad (6.4)$$

where:

- $E(\theta, \varphi)$: total field
- θ : elevation angle from the horizontal ($0 \leq \theta \leq 90^\circ$)
- φ : azimuthal angle from the axis of the antenna ($0 \leq \varphi \leq 360^\circ$)
- W_0 : radiation intensity of the isotropic source

D is equivalent to g_i , so the isotropic gain is also given by: $G_i = 10 \log_{10} D$ (dB).

The antenna efficiency is the ratio of the radiated power to the transmitter power, which takes into account the power lost due to currents induced in imperfectly conducting ground, in antenna conductors, insulators, terminating or series resistors, and the feeder line. In the above definition of directivity gain an antenna efficiency of 100% has been assumed. To take into account an antenna efficiency of less than 100%, the directivity has to be multiplied by this efficiency, which results in the power gain of the antenna.

Near 0° elevation angle above highly conducting ground or sea, the ground reflected wave tends to cancel the direct wave from a horizontal antenna element. However, the gain is reinforced at angles for which the path difference between these waves is a half wavelength, so the height of the antenna above ground is dominant in determining the gain with respect to elevation angle. Over poorly conducting ground, there is a loss in gain of 1 to 3 dB as the elevation angle is increased.

The gain of a vertical antenna above highly conducting ground is reinforced at small angles of elevation (in principle, by up to 3 dB over an infinite perfectly conducting surface). When the conductivity is less the ground reflection tends to cancel the direct wave at angles of elevation near 0° . Also, the reflection coefficient falls to a low value at the Brewster angle, about 5° - 12° over average ground, which is comparable to the angle of arrival of the sky-waves over long paths, so antenna performance is seriously affected, with gain reduced by up to 5 dB.

The gain of a vertical antenna is maximum when its height above ground is about 0.35 wavelengths, but over average ground there is little point in increasing its height further, since the elevation angle of maximum gain decreases below 10° and the antenna radiates poorly at low elevation angles because of the Brewster angle effect mentioned above.

6.9.3 Radiation pattern

The radiation pattern or directivity pattern shows the gain of the antenna in three dimensions. It may be illustrated in a number of ways, but is often represented simply by the projections at constant azimuth and constant elevation angle that include the maximum gain. The pattern is the same whether the antenna is transmitting or receiving.

It is possible to modify the vertical and horizontal radiation pattern of an antenna by using additional passive (reflecting) elements, or active (radiating) elements. By this means the pattern required for a particular service may be synthesized.

6.9.4 Polarization

The orientation of the electric field in the plane perpendicular to the direction of travel of an electromagnetic wave characterizes the polarization of the wave. The polarization of sky waves is generally elliptical after reflection in the ionosphere, and changing constantly. A receiving antenna responds mainly to the polarization for which it is designed when the signals arrive from the intended direction, but may be more sensitive to other polarizations when signals arrive from other directions. Similarly, the waves radiated by an antenna do not have the same polarization in all directions. For example, a horizontal dipole near the ground radiates signals that are essentially vertically polarized end-on, and horizontally polarized broadside. In other directions, it radiates waves having intermediate polarizations.

6.9.5 Ground effects

The ground affects the characteristics of an antenna near it.

At the antenna, the reflection of the incident or radiated wave by the ground depends on the Fresnel reflection coefficients, which are functions of ground conductivity, dielectric constant, frequency, polarization and angle of incidence. The reflected wave adds constructively or destructively to the direct wave, depending on its phase delay which is determined by the height of the antenna above ground. The superposition of the two waves can lead to a lobed structure of the radiation pattern.

The reflected wave is strongest if the antenna foreground terrain is flat within the first Fresnel zone. If the terrain has a slope relative to the horizontal, the reflection geometry and hence the positions of the maxima and minima in the vertical radiation pattern will be modified.

If the foreground terrain is irregular, the specular reflection will be weakened and a part of the incident energy may be scattered away from the antenna. In this situation the radiation minima will be filled up and the maxima reduced.

HF antennas are often supported by a vehicle or structure comparable in size to the wavelength. Nearby structures such as metal towers, other antennas, a building's electrical system or steel frame, and power lines, may be resonant at HF. Their presence can markedly affect the antenna pattern, so it is desirable to take their effect into account. Detailed numerical modelling using e.g. the method-of-moments technique is especially useful in such situations.

6.9.6 Radiated power

The total power radiated or received by an antenna near the Earth is that passing through the upper hemisphere centred on the antenna, having a radius large enough to enclose the first Fresnel zone.

The radiated power p_r of a transmitting antenna in a given direction is the product of the power p supplied to the antenna and the antenna gain g in that direction, or $P_r = P + G$ (dB), where $P = 10 \log p$, and G depends on the reference antenna, i.e.:

Equivalent Isotropically Radiated Power (e.i.r.p.), (G_i);

Effective Radiated Power (ERP), (G_d); and

Effective Monopole Radiated Power (e.m.r.p.), (G_v).

6.10 Application of prediction to HF system planning and design

Each radiocommunication service has its own unique requirements and may make significantly different use of predictions. The requirements of the service will therefore specify the reception site or area, as well as the proposed schedule and time of year for operation and possibly the transmitter location. These may be fixed parameters determined by the requirements of the service, which cannot be modified even if to do so would improve the performance. Because of this, it may well not be possible for the service to operate at the time when propagation for the path is optimum.

Further constraints result from environmental factors. It is the role of predictions to suggest optimum values for factors that are not otherwise specified, such as frequency, antenna pattern and transmitter power. Through iteration, the predictions can optimize these parameters and the reliability of communications.

6.11 Operational constraints

In setting up a service, it is also necessary to consider the constraints imposed by factors such as propagation, discussed in previous sections, and interference, both of which will influence the choice of frequency (band) to be used, and the times at which operation is possible.

6.11.1 Available frequencies (bands)

Available frequencies (bands) are defined as those frequencies on which a criterion for service quality is satisfied under given conditions.

For some applications it may be desirable to summarize the predictions in a suitable manner over the range of an important parameter. For example, if a service is operating during a period of hours or months, the frequencies (bands) available for the whole period may be obtained e.g. by averaging the hourly or monthly predictions over the period before deciding whether the quality criterion is satisfied. Alternatively, the summarizing process may include the evaluation of the minimum value (e.g. worst month), a decile or any other percentile, etc. The general procedure is shown in Fig. 6.2 in the case of area coverage involving calculations to a range of test points.

Fig. 6.3 shows an example of a computer calculation of the available broadcasting frequency bands for a reception area as a function of the hour of the day during a period of four months. The available bands are represented by their respective centre frequencies. Availabilities (reliabilities) of more than 80% and 50% of the time achieved at 80% of the locations are marked by different symbols. The upper diagram is based on reliabilities averaged over the specified four months, the lower one on the minimum reliability occurring during this period (worst case).

Fig. 6.4 shows a different output with the month as the variable parameter and the hour, or period of hours, held constant. This type of output may be used to study the variability of the usable frequencies (bands) with the month and sunspot number. In this example a frequency or frequency band is considered to be available if a required time percentage of satisfactory service over a required percentage of the service area (basic service reliability) is achieved for any hour within the specified time period.

If the reliability is chosen as the quality criterion the method may be extended to include not only single frequencies or frequency bands but also any possible combinations of preselected frequencies or frequency bands. In that case the circuit reliability is replaced by the reception reliability and the service reliability is determined from the reception reliability.

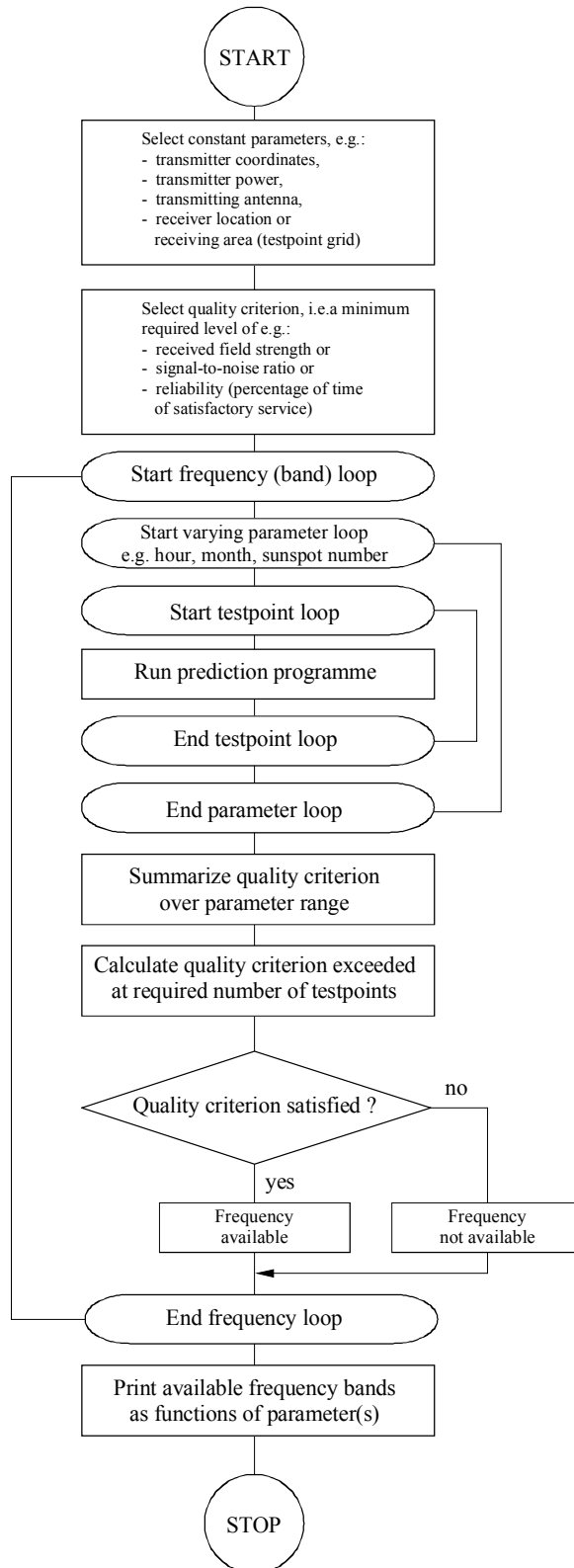


figure 6.2
**Determination of available frequency bands summarized
over a range of parameter values**

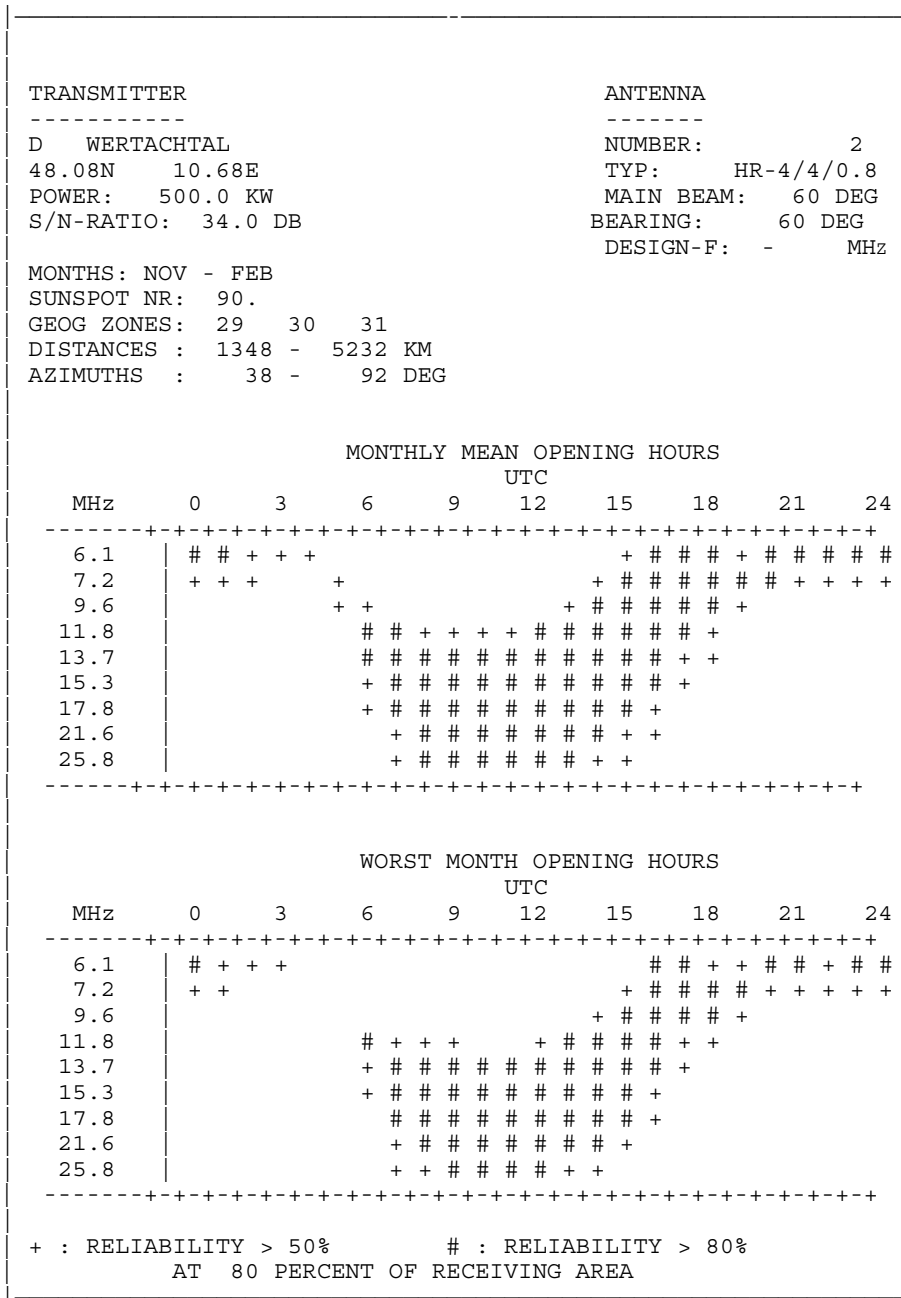


FIGURE 6.3
 Example of band availability calculation

<u>TRANSMITTER</u>				<u>ANTENNA</u>		
D	WERTACHTAL			NUMBER:	2	
48.08N	10.68E			TYP:	HR-4/4/0.8	
POWER:	500.0 KW			MAIN BEAM:	65 DEG	
REQ.S/N:	34.0 DB			BEARING:	65 DEG	
MIN.ANG:	3.0 DEG			DESIGN-F:	- MHz	
HOURS/UTC: 0600 - 0800						
GEOG ZONES : 29 30NW 30SW						
DISTANCES : 1348 - 3770 KM						
AZIMUTHS : 38 - 92 DEG						
BANDS USABLE 50% OF TIME FOR 80% OF AREA						
SSN	YEARS	MONTH		USABLE BANDS/MHZ		
14	1986	JAN	7			
13	1986	FEB		9		
13	1986	MAR		9	11	
14	1986	APR		9	11	13
15	1986	MAI			11	13
14	1986	JUN			11	13
14	1986	JUL			11	13
13	1986	AUG			11	13
12	1986	SEP		9	11	
13	1986	OCT		9	11	
16	1986	NOV	7	9		
16	1986	DEC	6	7		
17	1987	JAN	7			
19	1987	FEB		9		
23	1987	MAR		9	11	
25	1987	APR			11	13
27	1987	MAI			11	13
29	1987	JUN			11	13
31	1987	JUL			11	13
						15

FIGURE 6.4

Available frequency bands vs. Month

35	1987	AUG			11	13		
39	1987	SEP		9	11	13		
44	1987	OCT		9	11	13	15	
47	1987	NOV	7	9	11			
51	1987	DEC	7	9				
58	1988	JAN	7	9				
62	1988	FEB		9	11			
71	1988	MAR		9	11	13		
77	1988	APR			11	13	15	
83	1988	MAI			11	13	15	
94	1988	JUN			11	13	15	
100	1988	JUL			11	13	15	
114	1988	AUG			11	13	15	
119	1988	SEP			11	13	15	
125	1988	OCT			11	13	15	17
127	1988	NOV		9	11	13	15	
137	1988	DEC		9	11			
142	1989	JAN		9				
145	1989	FEB		9	11	13	15	
150	1989	MAR			11	13	15	17
153	1989	APR			11	13	15	17
157	1989	MAI			11	13	15	17
158	1989	JUN			11	13	15	17
159	1989	JUL			11	13	15	17
158	1989	AUG			11	13	15	17
157	1989	SEP			11	13	15	17
158	1989	OCT			11	13	15	17
158	1989	NOV		9	11	13	15	
154	1989	DEC		9	11			

FIGURE 6.4 (Continued)
Available frequency bands vs. Month

6.11.2 Interference

The effect of interference by unwanted emissions is to degrade the performance of a wanted service. The level beyond which interference is regarded as harmful in the case of broadcast transmissions is specified by the audio protection ratio which is the minimum required signal-to-interference ratio of the demodulated received signal to achieve a required service quality. The radio-frequency protection ratio is the value of the radio-frequency wanted-to-interfering signal ratio that enables, under specified conditions, the audio-frequency protection ratio to be obtained at the output of a receiver. The specified conditions include parameters like frequency spacing of wanted and interfering carrier, carrier offset, carrier-frequency tolerance, modulation characteristics (type of modulation, modulation depth, pre-emphasis, frequency deviations), characteristics of the demodulated signal (bandwidth, dynamic compression), receiver input level as well as the receiver characteristics (selectivity and susceptibility to cross-modulation etc.).

The compatibility of a wanted service with interference can be expressed by the percentage of time during which a specified criterion of service quality is achieved at the receiver location in the presence of interference relative to the value that would be obtained if only noise were present. If the wanted service applies to an area rather than a single reception point the compatibility can be defined in two ways:

- 1) by the percentage of the target area that can be served in the presence of interference during a specified percentage of time, relative to the situation where only noise is present (area service compatibility);
- 2) by the percentage of time during which a specified percentage of the target area can be served in the presence of interference, relative to the situation where only noise is present (time service compatibility).

The interference analysis [Hortenbach, 1988] described in the following applies to the more general case of a point-to-area circuit. In the case of a point-to-point link all operations relating to a reception area are, of course, reduced to a single reception point. In that case method 2 only is relevant, where the time service compatibility reduces to the percentage of time during which the receiving site can be served in the presence of interference, relative to the situation where only noise is present.

The percentage of the area which is satisfactorily served during $T\%$ of the time in the presence of only the environmental noise is given by

$$A_N = Z_N/Z_0 \cdot 100\% \quad (6.5)$$

and in the presence of noise and interferers by

$$A_I = Z_I/Z_0 \cdot 100\% \quad (6.6)$$

where

- Z_N is the number of all area test points where $E_W \geq E_{min}$,
 Z_I is the number of all area test points where $E_W \geq E_U$,

- Z_0 is the total number of test points representing the target area,
 E_W is the wanted field strength being exceeded during $T\%$ of the time,
 E_{min} is the "minimum usable field strength", i.e. the minimum value of the field strength necessary to permit a desired reception quality in the presence of natural and man-made noise in the absence of interference, during $T\%$ of the time,

$$E_{min} = a_N \cdot E_N$$

- E_U is the "usable field strength", i.e. the minimum value of the field strength necessary to permit a desired reception quality in the presence of natural and man-made noise and interference during $T\%$ of the time. It is defined by

$$E_U^2 = (a_N \cdot E_N)^2 + \sum (a_{I,i} \cdot E_{I,i})^2,$$

- $E_{I,i}$ is the field strength of the i -th interferer being exceeded during $T\%$ of the time,
 E_N is the noise field strength being exceeded during $T\%$ of the time,
 a_N is the minimum required signal-to-noise ratio and
 $a_{I,i}$ is the co- or adjacent-channel protection ratio.

The field strengths E_W and $E_{I,i}$ each are the larger ones of two values obtained for the short and the long great-circle paths between the respective transmitter and receiving locations.

The percentage loss of service area caused by an individual interferer i is determined from calculations for a series of test points by

$$L_i = (Z_N - Z_{I,i})/Z_N \cdot 100\% \quad (6.7)$$

where $Z_{I,i}$ is the number of those points where $E_W \geq a_{I,i} \cdot E_{I,i}$.

The area service compatibility according to the first definition is thus expressed by

$$ASC = A_I/A_N \cdot 100\% = Z_I/Z_N \cdot 100\%. \quad (6.8)$$

The concept may be extended for the case that more than one frequency is transmitted to the same area. In that case Z designates the number of points where the corresponding conditions are satisfied on any of the frequencies used.

Referring now to the second definition the percentage of time during which the wanted field strength at a receiving point p exceeds a specified minimum value in the presence of only noise (Basic Circuit Reliability) is given by the probability

$$R_{N,p} = \text{prob}(E_{W,p} \geq a_N \cdot E_N) \quad (6.9)$$

and in the presence of noise and interference (Overall Circuit Reliability) by

$$R_{I,p} = \text{prob}(E_{W,p} \geq E_U) \quad (6.10)$$

The value of R_N which satisfies the condition

$$\text{prob}(R_{N,p} \geq R_N) = P \quad (6.11)$$

i.e. which is exceeded at at least $P \cdot 100\%$ of the test points within the area is called Basic Service Reliability. It gives the percentage of time during which $P \cdot 100\%$ of the target area can be served in the presence of noise only. Replacing the index N by I (Overall Service Reliability) we find the corresponding magnitude R_I which applies in the presence of noise and interference.

The time percentage loss due to an individual interferer i is in analogy to the loss of service area given by

$$L_i = (R_N - R_{I,i})/R_N \cdot 100\% \quad (6.12)$$

and the time service compatibility

$$TSC = R_I/R_N \cdot 100\% \quad (6.13)$$

If more than one frequency is transmitted to the same service area the above reliabilities are replaced by the corresponding joint probability function of the different frequencies. Assuming independence, this may be written as the product of the individual probability functions

$$R_{X,p}(f_1, f_2, \dots, f_n) = 1 - \prod(1 - R_{X,p}(f_i)) \quad (6.14)$$

where the subscript X stands for the indices N or I . The respective probabilities are called "basic reception reliability" ($R_{N,p}$) and "overall reception reliability" ($R_{I,p}$).

Fig. 6.5 shows the results of a computer analysis of an interference situation. It contains the parameters hour, month, sunspot number, frequency, minimum required signal-to-noise ratio, protection ratio and relative (adjacent channel relative to co-channel) protection ratio. The transmitter list contains name and coordinates of the transmitting station, transmitter power, antenna number and type with the main beam direction and the channel separation in kHz between the interfering and the wanted transmitter.

The table contains from left to right the subdivisions of the required service area (geographical zones for broadcasting), the percentage of the area which is served by the wanted transmitter during the specified percentage (50%) of the time when environmental noise only is present (SAW), the corresponding percentage when all interferers are present (SAI) and the area service compatibility (ASC)). The columns show the losses of service area due to the presence of the individual interferers.

The last table shows the percentage of time during which the specified percentage (80%) of the total area will be served in the presence of only noise (BSR) and interference (OSR). It follows the time service compatibility (TSC) and the losses due to individual interferers, each for the individual geographical zones and the total service area.

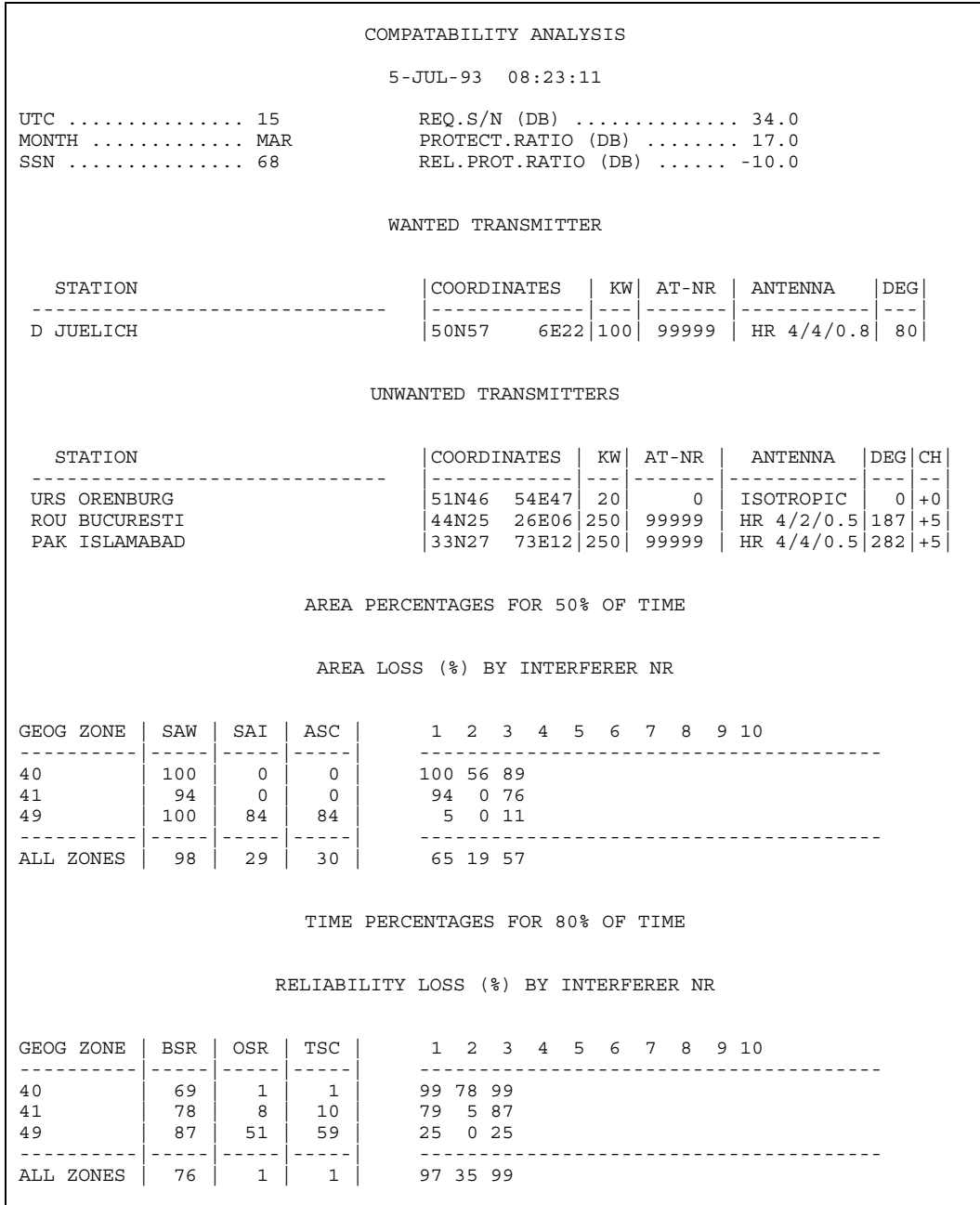


FIGURE 6.5

Interference analysis

- SAW = Percentage of target area served by wanted transmitter in the presence of only noise
- SAI = Percentage of target area served by wanted transmitter in the presence of interferers
- ASC = Area service compatibility
- BSR = Basic service reliability
- OSR = Overall service reliability
- TSC = Time service compatibility

6.11.3 Digital systems

The additional propagation factors affecting digital system performance at high S/N ratios are ionospheric variability and ionospheric dispersion. The performance of digital systems is characterized by the bit error ratio which is the probability that a transmitted binary digit is wrongly detected by the receiving discriminator. At high frequencies, transmission errors are usually not distributed stochastically in time, but periods with a high error density (error bursts) alternate with periods of low error density. Error bursts occur when a narrow transmission channel (e.g. 100 baud) is affected by selective fading and thus, the signal-to-noise ratio temporarily falls below a critical limit. Consequently, a particular fading distribution will give rise to a particular duration and frequency distribution of error bursts. As examples, Fig. 6.6 and Fig. 6.7 give the number and the duration and probability of fades measured on specific circuits.

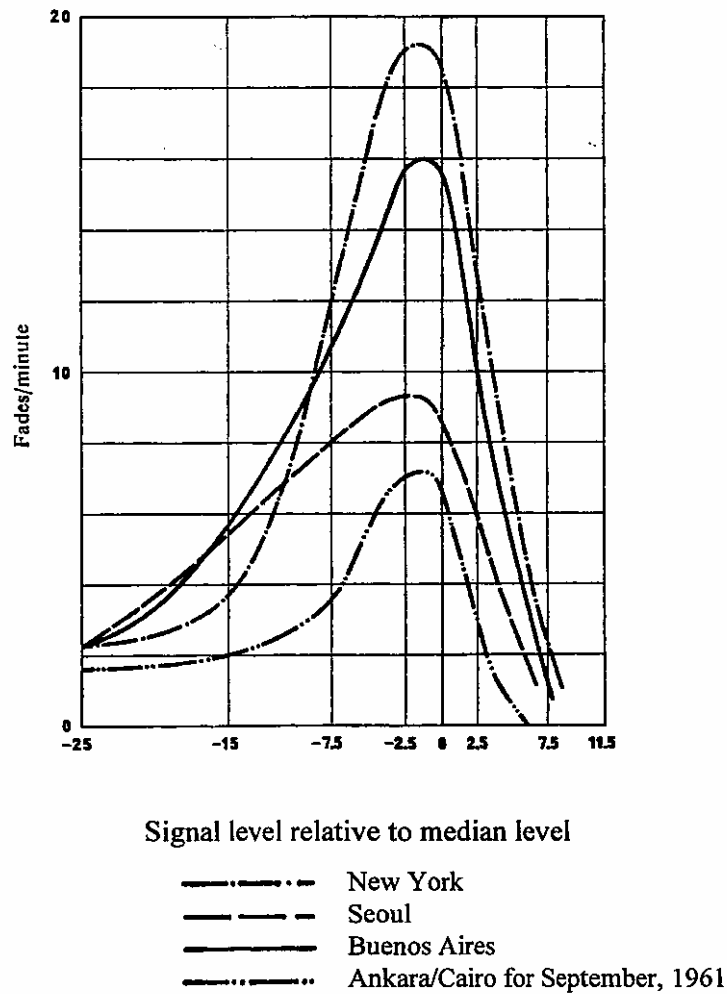


FIGURE 6.6

Number of fades per minute as a function of the measured signal level for various circuits (reception in Frankfurt)

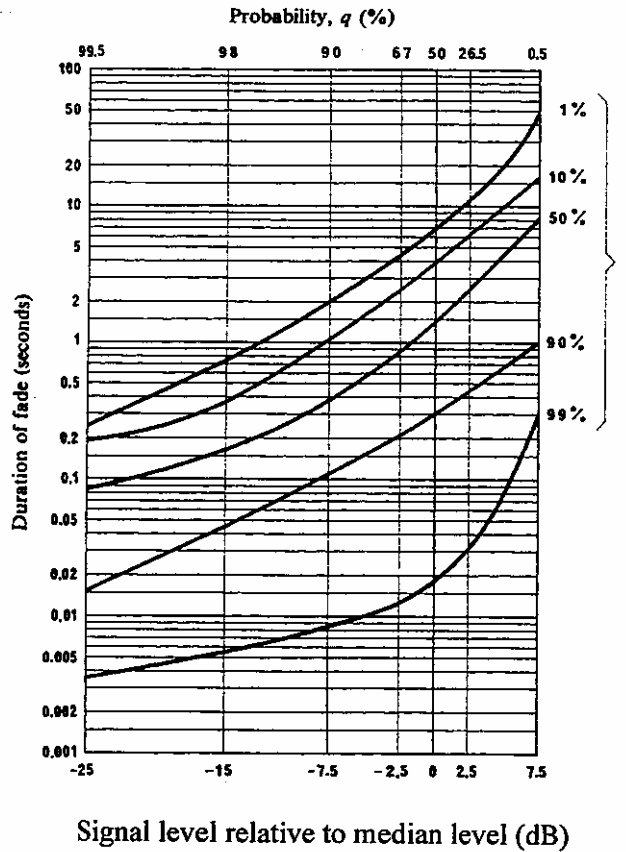


FIGURE 6.7

Duration of fades as a function of the measured signal level

Circuit: New York-Frankfurt-on-Main; 14 September 1961; 1100 hours Central European Time; frequency 13.79 MHz.

The figures on the right-hand side of the curves represent the percentage p of the number of fades for which a given duration of fade is exceeded. The measured values of signal levels are shown, together with the probability q that these levels will be exceeded

Amplitude fading is accompanied by associated fluctuations in group path and phase path, giving rise to time and frequency dispersion of modulated signals. The degree of time and frequency dispersion imposed by the ionosphere on the transmitted signal is an important factor affecting the choice of modulation technique as it dictates the minimum inter-symbol interval.

In a situation where time and/or frequency dispersion is significant, the detrimental effects at the receiver may normally be reduced by making use of one or more forms of diversity processing as e.g. space, polarization, frequency, time, multipath or geographical diversity.

6.11.3.1 Signal-to-noise ratio

The performance of digital systems expressed by the bit error probability depends also on the signal-to-noise ratio. Fig. 6.8 shows this dependence for different types of transmissions when the signal is disturbed by white Gaussian noise. A theoretical limit below which no transmission is possible is imposed by the Shannon limit which is 1.42 dB [Lüke, 1975].

In the absence of fading the signal-to-noise ratio is also the controlling parameter of digital transmission speed. The theoretical error-free channel capacity, C , is given by

$$C = B \cdot \log_2 (1 + S/N) \text{ bit/s} \quad (6.15)$$

where B is the channel bandwidth in Hz, S and N being respectively the total signal and noise power within the bandwidth B . In practice, the measured capacity of a channel may be lower due to a non-uniform distribution of signal and noise energy within the channel bandwidth, a non-ideal channel bandwidth profile and differing amplitude probability density functions for signals and noise.

FIGURE 05-07
Error probability with different transmission systems

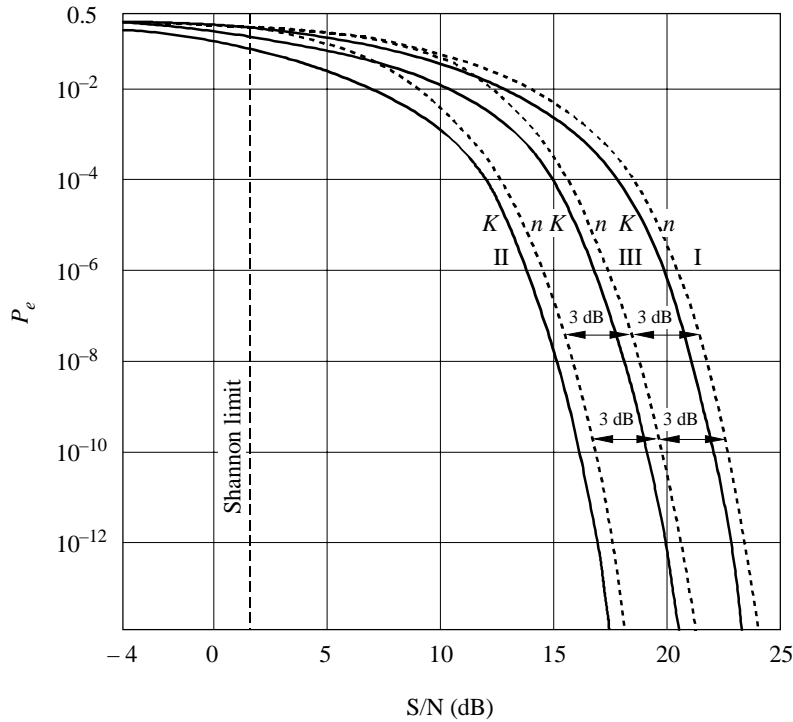


FIGURE 6.8

Error probability as a function of S/N in the presence of Gaussian noise for different transmission systems

- | | | | |
|------|--|----|------------------------|
| I: | Unipolar transmission | K: | Coherent reception |
| II: | Bipolar transmission | n: | Non-coherent reception |
| III: | Orthogonal transmission with two signals | | |

6.11.3.2 Time dispersion

In ionospheric propagation the main origin of time dispersion is multipath propagation arising from differences in transit time between different propagation paths. The multipath spread causes amplitude and phase variations in the signal spectrum due to interference of the multipath wave components. If these fluctuations are correlated within the signal bandwidth the fading is called non-selective or flat, because all spectral components of the signal are affected in nearly the same way. If the fluctuations are uncorrelated the fading is frequency selective. Time dispersion is characterized by its delay power spectrum or the frequency autocorrelation function in the frequency domain. A single parameter of these functions, the multipath delay spread or its inverse, the coherence or correlation bandwidth, is used to distinguish between selective and non-selective fading.

In digital transmissions time dispersion results in inter-symbol interference and in irreducible error rate, which are not improved by increasing the signal-to-noise ratio. This effect arises when the spread in propagation delays becomes comparable with the duration of the digital data frame period. Therefore, simple data transmission systems are limited to a relatively low bit rate. The maximum permissible values of delay for frequency telegraphy and double amplitude telegraphy with given modulation rate are shown in ITU-R Report 996. The error probability of binary signals can be calculated from the probability distribution of the amplitude fluctuations in a multipath channel [Fomin *et al.*, 1984]. Examples of the combined effect of signal-to-noise ratio and delay time on the bit error ratio of different modulation systems can be found in ITU-R Report 345.

The delay time between pulses corresponding to the individual propagation paths depends on the propagation conditions, the highest values occurring at night-time in winter. Fig. 6.9 shows the maximum delay as a function of radio circuit length for two sunspot activity levels given by idealised calculations for parabolic-layer models at median latitudes, in which the lowest order and next highest order F2-propagation modes are taken into account. The delay times range between 0.5 and 4 ms and almost double in the transition from minimum to maximum sunspot activity.

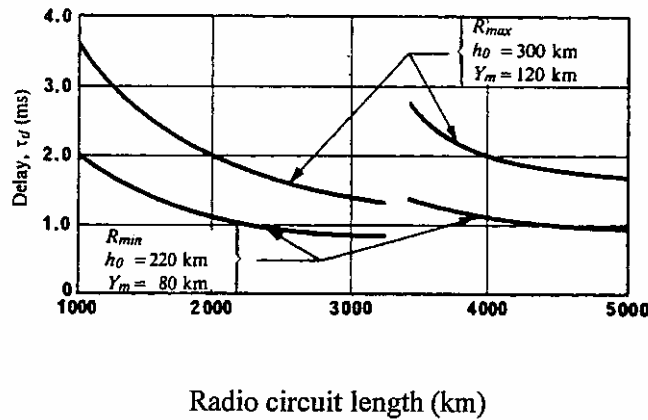


FIGURE 6.9

Delay as a function of radio circuit length

- R_{min} : Minimum sunspot activity
- R_{max} : Maximum sunspot activity
- h_0 : Height of lower limit of ionospheric layer
- Y_m : Half-thickness of ionospheric layer

The multipath delay time also depends strongly on the operating frequency and tends to zero when the frequency approaches the MUF. This is shown by the "multipath reduction factor" (Fig. 6.10) which is defined as the lowest percentage of the MUF for which the range of multipath propagation times is less than a specified value [Bailey, 1959]. It thus defines a frequency above which a specified minimum protection against multipath is provided.

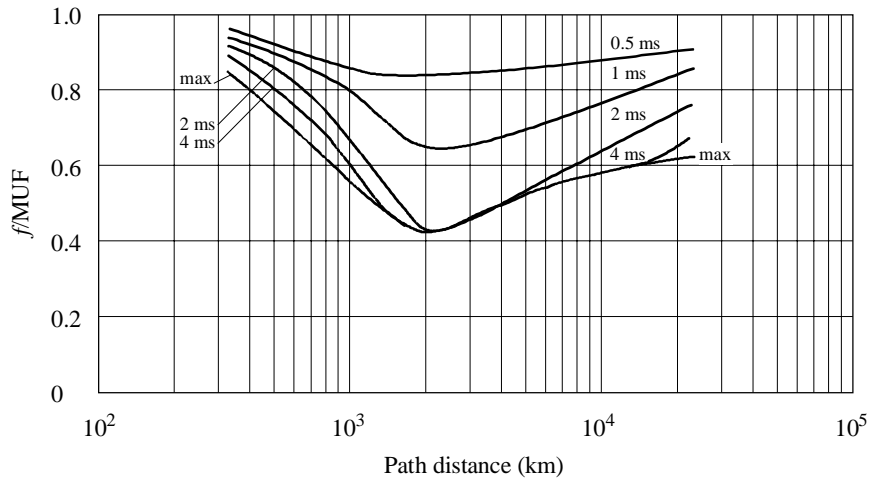


FIGURE 6.10

Dependence of delay time on frequency relative to the MUF and path length

In wideband (spread-spectrum) communication links the propagation effects differ with the modulation methods used. In direct sequence p.s.k. systems the group time delay instability of the individual modes deteriorates the correlation detection process while in frequency hopping systems it leads to a jitter of the arrival time of individual hops depending on the occupied spread bandwidth [Milsom and Slater, 1982]. Measurements with an experimental HF 2-p.s.k. spread-spectrum system indicate that the performance of the system in the presence of multipath depends on the bandwidth of the spread signal. The bandwidth should be chosen large enough to resolve the multipath components but sufficiently small to prevent the time spread of the individual components from becoming troublesome [Skaug, 1982].

6.11.3.3 Frequency dispersion

Frequency dispersion arises because the reflecting properties of the ionosphere are varying with time. This is due to changes in the electron density caused by the variations of the Sun's zenith angle with the time of the day but also by irregularities. The ionosphere may be thought of as an irregular reflecting surface that is drifting across the sky. Because of this drift, waves arriving at the receiving site are being reflected from moving elemental surfaces. Consequently, each reflected wave will be subject to different phase and Doppler frequency shifts. The interference of these phase- and frequency-shifted waves give rise to rapid fading, or, in digital transmissions, may affect the

performance of phase- and frequency-shift keying systems. The system will make an error if the transmitted frequency or phase is changed far enough to cross over into the wrong side of the discriminator and remains there for a period comparable to half the element length.

A reasonable model describing the fading signal is to assume it has the character of very narrow-band Gaussian noise. For this case the fading signal bandwidth or Doppler spread is proportional to the fading rate, i.e. the mean number of times per second the signal passes through the median signal level with positive slope. The proportionality factor depends on the type of filter assumed. A more comprehensive description of the fading signal is obtained by the probability distribution function of the instantaneous frequency deviation. Fig. 6.11 shows this function normalized to the fading rate. For a fading rate of 1 Hz, the instantaneous frequency will be within about 12 Hz of the carrier frequency for 99.9% of the time. The mean duration of the instantaneous frequency deviation is shown in Fig. 6.12 with the fading rate as a parameter. It is practically independent of the fading rate.

As is the case with multipath spread, the Doppler spread also depends on the frequency-to-MUF ratio. Correspondingly, a "Doppler reduction factor" can be calculated, defined as the fraction of the MUF below which one must operate in order to remain below a certain pre-specified Doppler spread [Pickering, 1975].

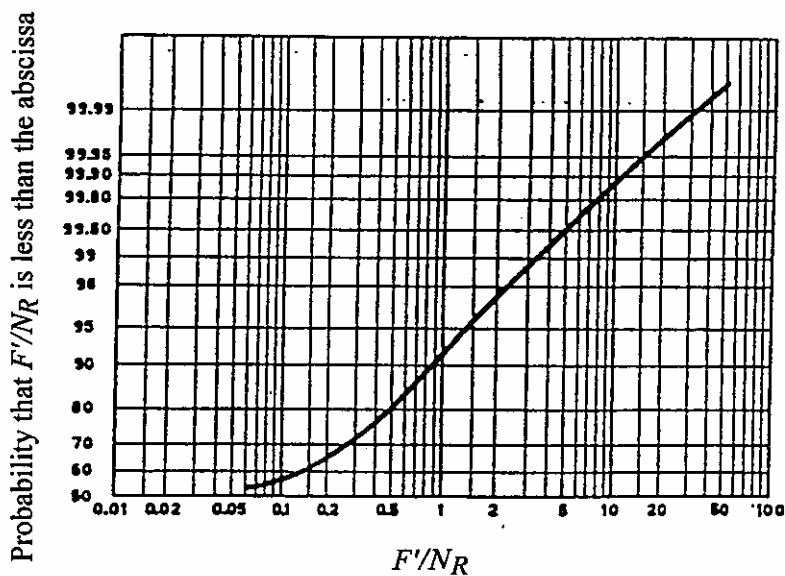


FIGURE 6.11

Cumulative probability distribution of instantaneous frequency change

- F' : Instantaneous departure from centre frequency (Hz)
- N_R : Fading rate (fades per second)

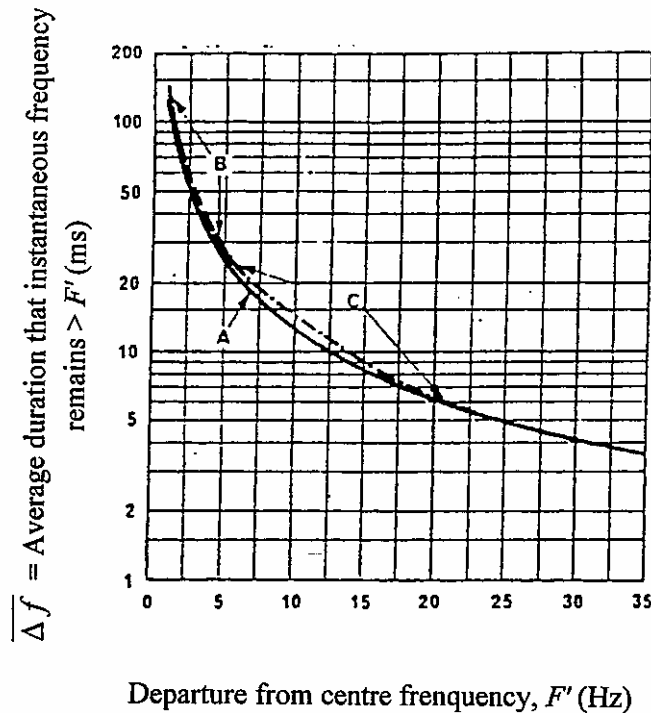


FIGURE 6.12

Average duration that instantaneous frequency change due to the ionosphere exceeds F' , with fading rates of 0.2, 1.0 and 5.0 fades per second (assuming a model of narrow-band Gaussian noise)

Curves A: 0.2 fade/second
B: 1 fade/second
C: 5 fades/second

6.12 Selection of system parameters

6.12.1 Selection of frequencies

The selection of frequencies for a service comprises the following steps:

- 1) Determine available frequencies (or bands) by calculating the reception reliabilities (or service reliabilities in the case of a service area) for all frequencies (bands) and suitable combinations of frequencies (bands), using the fixed parameters associated with the required service.
- 2) Rank the frequencies (bands) and frequency (band) combinations in terms of reception reliability (or service reliability for areas) and select that one which achieves the required reliability by use of the minimum number of frequencies (bands).

- 3) Determine the compatibility of the wanted transmission with the existing interference situation on the frequencies available (see § 6.11.2). Select those frequencies which satisfy a required minimum overall reception reliability (or service reliability for areas).
- 4) From amongst the frequencies with tolerable interference, select those which satisfy any other required conditions, e.g. which assure continuity of a service over a period of hours within a month, or a period of months at a given hour, without change of frequency or other parameters.

6.12.2 Selection of antennas

Omnidirectional antennas should be used only if the transmitter location is in the centre of a service area. Typical omnidirectional and nearly omnidirectional antennas are vertical monopoles, horizontal dipoles, quadrant antennas and tropical antennas. All omnidirectional antennas are relatively low gain, and because of this they are best suited for short range communication; for longer ranges a directional antenna should be used if possible.

Fig. 6.13 gives an example of the procedure followed in the choice of optimum antennas for the broadcasting service according to the distance range required. Two different categories are considered: short distance and medium/long distance services.

The direction of radiation of the main lobe of a short-wave antenna, its elevation angle and maximum gain are principally dependent upon the type of array and its height above ground.

A short distance service, up to about 2 000 km, can be covered with either a non-directional or a directional antenna whose beamwidth can be selected according to the sector to be served. In the case of directional antennas, both horizontal dipole curtain and logarithmic-periodic antennas can be employed. The latter type is a multiband array with a wide operating frequency range, a low-to-medium gain and a large horizontal beamwidth. Ideally, the main lobe elevation angle should be relatively high (15°-30°).

Distances greater than approximately 2 000 km can be covered by antennas whose main-lobe elevation angle is small (less than 15°) and whose horizontal beamwidth - depending on the area to be served - is either wide (between 65° and 95°) or narrow (between 30° and 45°).

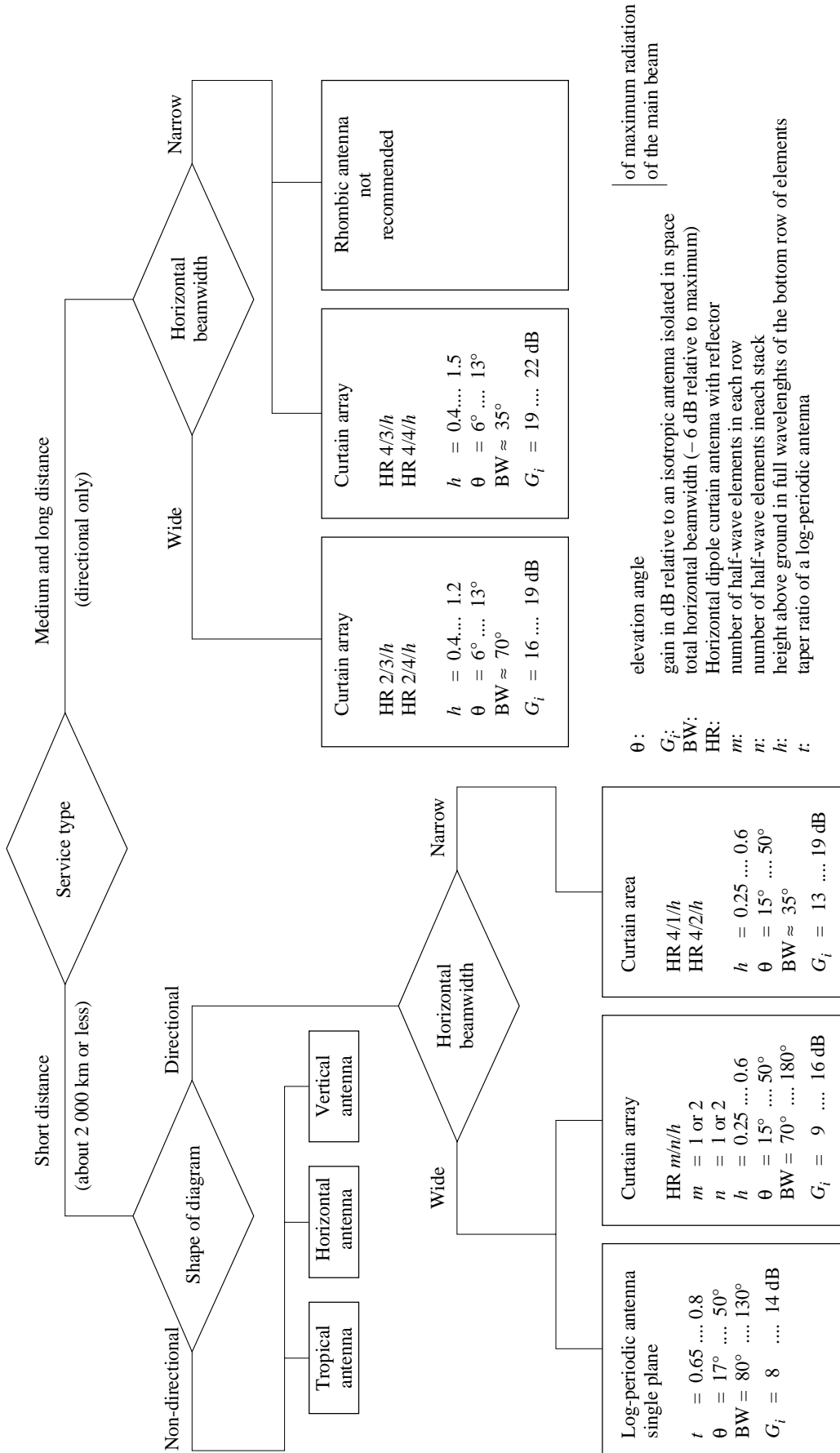


FIGURE 6.13

Procedure for antenna selection for the broadcast service

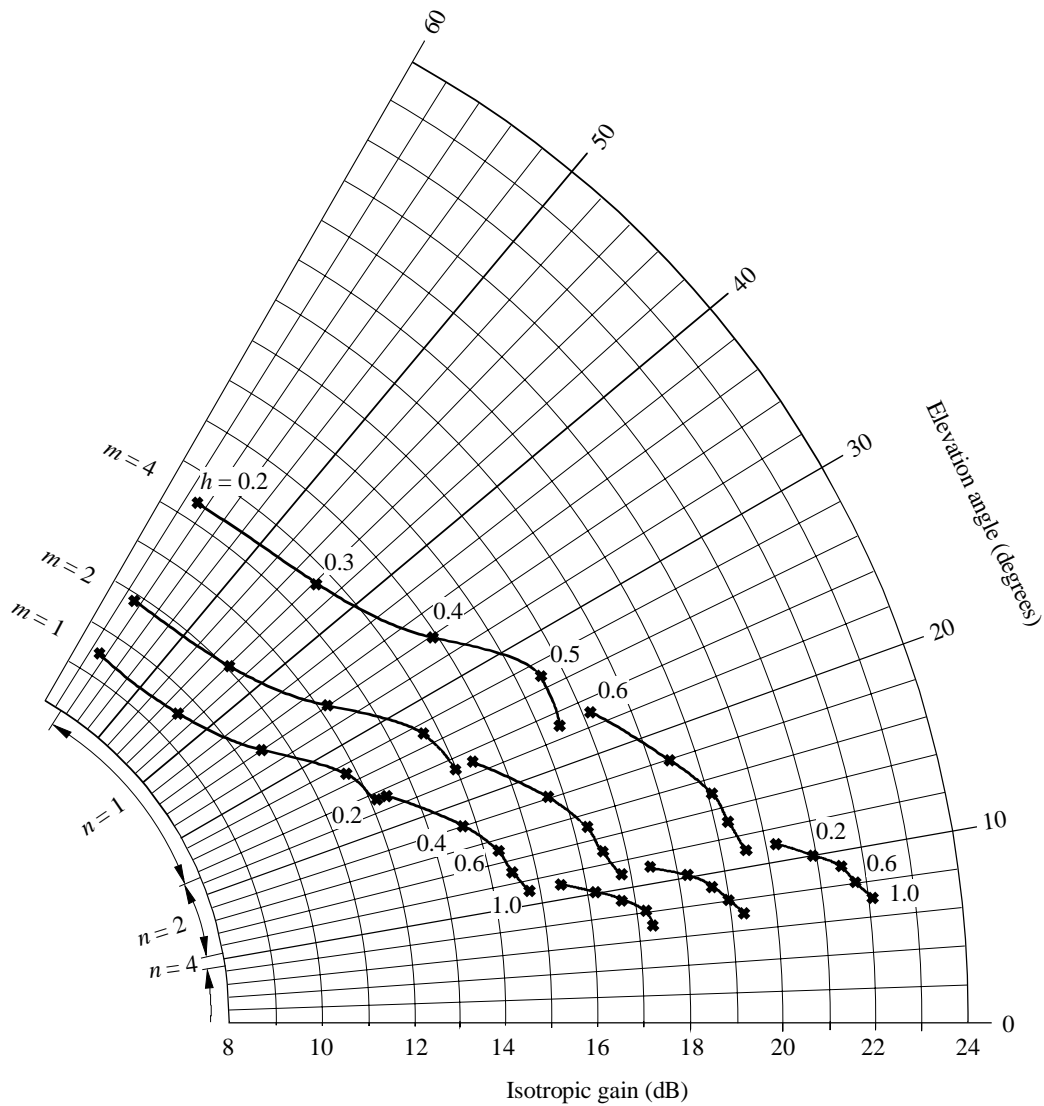


FIGURE 6.14

Variation of maximum gain and main lobe elevation with height for various dipole arrays of the type HR $m/n/h$

Fig. 6.14 illustrates the way in which maximum gain and the main-lobe elevation angle vary with height for the most commonly used forms of horizontal dipole curtain antennas fitted with reflectors when operated close to their design frequency. In the figure, m refers to the number of half-wave dipoles in each row, n is the number of dipoles in each stack and h is the height above ground in wavelengths of the bottom row of elements.

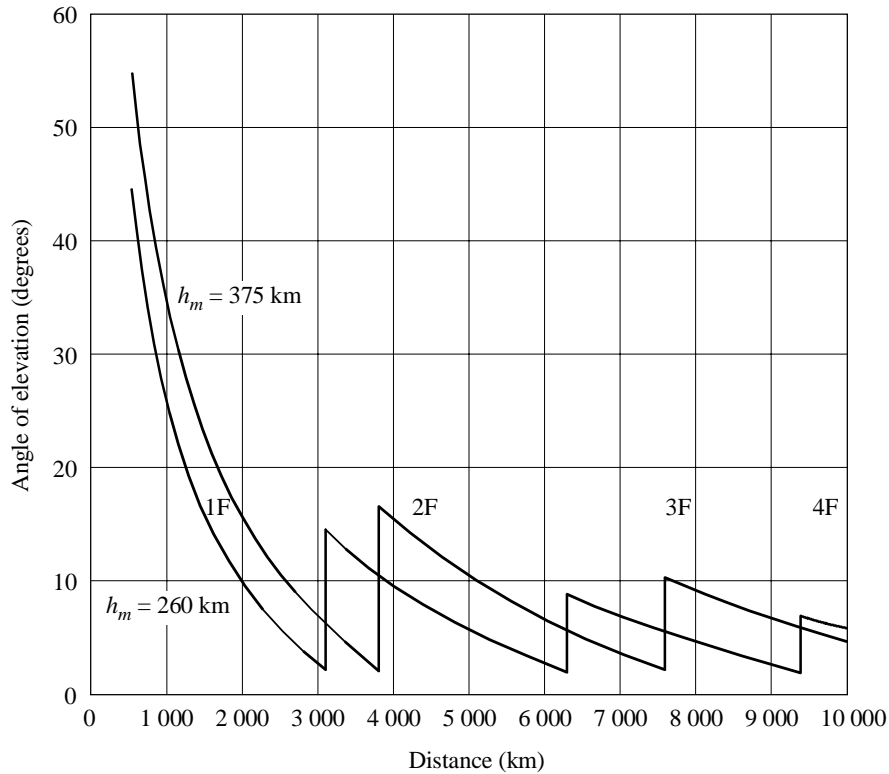


FIGURE 6.15

Variation of elevation angle with distance and ionospheric reflection height for F-layer propagation

Fig. 6.15 shows the angle of elevation involved in the propagation of short-wave signals via the F layer. Angles tend to be less than 10° for all distances beyond 5 000 km, angles above about 20° only being suitable for distances of less than 2 000 km. Fig. 6.14 shows that low-angle arrays whose maximum radiation is at angles of 10° or less tend to have the highest gains, and that low-gain antennas have their maximum radiation at the high angles most suitable for short-distance services.

Generally, an antenna can easily be selected according to its horizontal beamwidth from simple geometrical considerations. The selection according to its vertical pattern presents more difficulties, since the coverage depends on ionospheric parameters which will vary with time, e.g. the ionospheric reflection height. Frequently a detailed analysis of the elevation angles occurring during the required period of operation may be helpful. Fig. 6.16 shows the occurrence statistics for elevation angles of modes during a certain period of hours and months within the specified service area. By comparing the statistics with the vertical radiation patterns of different antennas an antenna type can usually be found which is sufficiently well adapted to the propagation and geographic conditions.

In Fig. 6.17 the predictions have been repeated with different antenna types so that the performance of each can be compared directly. This comparison may be done for any single hour and month, but may also include periods of hours and months.

COMPARISON OF ANTENNA PERFORMANCES													
=====													
TX STATION		: D WERTACHTAL		48.08N	10.68E	500 KW							
GEOG ZONES		: 29 30NW 30SW											
DISTANCES		: 1348 - 3770 KM											
AZIMUTHS		: 38 - 92 DEG											
UTC		: 6		4									
MONTH		: 11											
SSN		: 90											
FIELDSTRENGTHS (DBU) AT 80% OF AREA													
NR	ANTENNA			REF	BAND / MHz								
	TYPE	SLW			6	7	9	11	13	15	17	21	28

22212	HR	4/4/0.7	60	60	48	49	48	46					
22212	HRS	4/4/0.7	75	60	48	50	48	48					
22212	HRS	4/4/0.7	90	60	44	45	46	45					
12313	HRS	4/1/0.4	90	120			49	47	42				
72219	HR	2/2/0.7	45	45	50	52	59	56					
99999		HOR LP	80	80	49	52	57	57	54	50	31		
99999	HQ	1/0.3	-	-	40	44	51						
99999	HR	2/3/0.5	75	75	51	53	63	62					
99999	HR	4/4/0.8	90	90					44	26			
REF: Antenna bearing (degrees)													
SLW: Slewing direction (degrees)													

FIGURE 6.17

Comparison of antenna performances

6.12.3 Selection of transmitter power

The transmitter power necessary to provide a required service quality is interrelated with a large number of parameters like technical characteristics of the circuit, propagation conditions, number of frequencies used etc. and can therefore not be determined separately. The whole procedure of determining the circuit parameters described so far has to be repeated varying the transmitter power in suitable steps. The lowest possible power that enables a satisfactory service should be applied to avoid unnecessary congestion of the spectrum.

6.12.4 Location of terminals

When an HF communication link is to be established the normal task of planning is to determine the operating frequencies, antennas, transmitter powers and operating hours for given transmitter and receiver locations or receiving areas. However, it cannot be taken for granted that there will exist suitable operating conditions in any case. It may occur that propagation will be possible only during unsuitable times of the day or that the propagation path passes through frequently perturbed regions of the ionosphere, for example the auroral oval. In such cases it may be helpful to move, if possible, the transmitter location to more favourable geographical latitudes or closer to the receiving point or area. In some cases it may be necessary to establish relay stations as is often done in HF broadcasting.

In order to estimate the differences in service quality achieved from different transmitter locations the prediction program may be applied for two or more transmitter locations but the same receiving location or receiving area. The field strengths or reliabilities obtained can be compared and the location providing the best service performance be selected. Fig. 6.18 shows a computerized comparison of the field strengths obtained from two different transmitter locations. For each transmitter, the first table gives the field strengths which are achieved at the best of several given frequencies (broadcasting bands in this case), and the second table shows the frequencies (bands) at which these field strengths are obtained. The final table in Fig. 6.18 shows the difference between the optimum field strengths obtained at each of the stations involved.

COMPARISON OF COVERAGE BY DIFFERENT STATIONS												

SERVICE AREA (GEOG ZONES): 10SE 11SW 0 0 0 0 0 0												
STATION 1												
D WERTACTAL 10E41 48N05 500 KW												
ANTENNA-NR: 2 TYP: HR-2/2/0.5 BEAM: 270 BEARING: 270												
BANDS: 6 7 9 11 13 15 17 21 26 DESIGN-FREQUENCY: - MHz												
FIELD STRENGTH EXCEEDED AT 80% OF LOCATIONS ON BEST FREQUENCY BAND												
UTC	SSN= 10				SSN=100				SSN= 0			
	JUN	SEP	DEC	-	JUN	SEP	DEC	-	JUN	SEP	DEC	-
02	43	38	37	-	46	45	42	-	-	-	-	-
04	42	36	38	-	47	44	43	-	-	-	-	-
06	36	37	33	-	38	44	39	-	-	-	-	-
08	21	29	41	-	29	34	45	-	-	-	-	-
10	18	20	32	-	23	24	31	-	-	-	-	-
12	22	24	29	-	21	27	30	-	-	-	-	-
14	20	20	26	-	19	22	33	-	-	-	-	-
16	18	19	22	-	18	22	30	-	-	-	-	-
18	21	24	16	-	20	27	26	-	-	-	-	-
20	30	29	14	-	27	30	24	-	-	-	-	-
22	37	34	25	-	34	35	34	-	-	-	-	-
24	43	37	35	-	45	42	40	-	-	-	-	-

FIGURE 6.18
Comparison between transmitter locations

OPTIMUM FREQUENCY BAND												
SSN= 10				SSN=100				SSN= 0				
UTC	JUN	SEP	DEC	-	JUN	SEP	DEC	-	JUN	SEP	DEC	-
02	7	6	6	-	9	7	6	-	-	-	-	-
04	6	6	6	-	7	7	7	-	-	-	-	-
06	7	6	6	-	11	7	6	-	-	-	-	-
08	9	9	6	-	15	11	7	-	-	-	-	-
10	11	9	9	-	17	15	11	-	-	-	-	-
12	15	15	15	-	21	21	17	-	-	-	-	-
14	17	15	17	-	21	21	26	-	-	-	-	-
16	17	15	15	-	21	21	26	-	-	-	-	-
18	15	15	11	-	21	21	21	-	-	-	-	-
20	15	13	9	-	21	17	15	-	-	-	-	-
22	13	9	6	-	17	13	9	-	-	-	-	-
24	9	6	6	-	11	9	7	-	-	-	-	-

STATION 2

ANTIGUA 61W48 17N06 250 KW

ANTENNA-NR: 11 TYP: HR-2/2/0.5 BEAM: 270 BEARING: 270

BANDS: 6 7 9 11 13 15 17 21 26 DESIGN-FREQUENCY: - MHz

FIELD STRENGTH EXCEEDED AT 80% OF LOCATIONS ON BEST FREQUENCY BAND

OPTIMUM FREQUENCY BAND												
SSN= 10				SSN=100				SSN= 0				
UTC	JUN	SEP	DEC	-	JUN	SEP	DEC	-	JUN	SEP	DEC	-
02	61	59	57	-	62	62	60	-	-	-	-	-
04	60	58	57	-	62	62	60	-	-	-	-	-
06	59	58	58	-	62	61	59	-	-	-	-	-
08	57	58	58	-	61	61	59	-	-	-	-	-
10	57	57	57	-	61	60	58	-	-	-	-	-
12	58	58	58	-	58	58	59	-	-	-	-	-
14	55	57	57	-	55	57	58	-	-	-	-	-
16	54	57	56	-	54	58	57	-	-	-	-	-
18	56	58	56	-	56	58	58	-	-	-	-	-
20	57	57	56	-	57	58	57	-	-	-	-	-
22	59	59	58	-	59	60	59	-	-	-	-	-
24	61	61	58	-	61	62	61	-	-	-	-	-

OPTIMUM FREQUENCY BAND												
SSN= 10				SSN=100				SSN= 0				
UTC	JUN	SEP	DEC	-	JUN	SEP	DEC	-	JUN	SEP	DEC	-
02	11	9	7	-	17	15	11	-	-	-	-	-
04	9	7	7	-	17	15	9	-	-	-	-	-
06	9	9	9	-	15	13	9	-	-	-	-	-
08	7	7	7	-	13	11	9	-	-	-	-	-
10	7	7	7	-	13	9	9	-	-	-	-	-
12	13	13	13	-	17	17	15	-	-	-	-	-
14	15	15	21	-	17	26	26	-	-	-	-	-
16	17	17	26	-	21	26	26	-	-	-	-	-
18	17	21	17	-	21	26	26	-	-	-	-	-
20	17	21	17	-	21	26	21	-	-	-	-	-
22	21	21	15	-	21	26	21	-	-	-	-	-
24	15	13	7	-	21	17	13	-	-	-	-	-

FIGURE 6.18 (Continued)
Comparison between transmitter locations

DIFFERENCE OF FIELD STRENGTHS (STATION 1 - STATION 2) EXCEEDED AT 80% OF LOCATIONS ON BEST FREQUENCY BANDS												
	SSN= 10				SSN=100				SSN= 0			
UTC	JUN	SEP	DEC	-	JUN	SEP	DEC	-	JUN	SEP	DEC	-
02	-18	-21	-20	-	-16	-17	-18	-	-	-	-	-
04	-18	-22	-19	-	-15	-18	-17	-	-	-	-	-
06	-23	-21	-25	-	-24	-17	-20	-	-	-	-	-
08	-37	-28	-17	-	-33	-27	-14	-	-	-	-	-
10	-39	-36	-24	-	-38	-36	-28	-	-	-	-	-
12	-37	-34	-29	-	-38	-32	-29	-	-	-	-	-
14	-35	-37	-31	-	-36	-35	-26	-	-	-	-	-
16	-36	-38	-34	-	-37	-36	-26	-	-	-	-	-
18	-35	-33	-40	-	-35	-31	-31	-	-	-	-	-
20	-27	-28	-42	-	-31	-29	-34	-	-	-	-	-
22	-22	-26	-33	-	-25	-25	-25	-	-	-	-	-
24	-18	-24	-22	-	-16	-19	-21	-	-	-	-	-

FIGURE 6.18 (Continued)

Comparison between transmitter locations

6.13 Overview of computer programs

Program REC533:

REC533 is the ITU-R PC-based implementation of Recommendation P.533 for the estimation of HF sky-wave propagation and radio-circuit performance between 2 - 30 MHz. Antenna gain is modelled according to Recommendation BS.705.

This program has applications in areas of system planning, frequency management and performance diagnosis.

There are seven component outputs and a further set from a stand alone program for a particular point-to-point circuit covering different hours of the day in a given month. The field strengths shown are the root-sum-squared (RSS) values determined from up to the five strongest modes; mode and elevation angles refer to the strongest mode. Signal-to-noise ratios are derived from the RSS signal power and the noise power at the receiver. Antenna gain is evaluated at both the transmitter and the receiver for ten different types of antenna; an isotropic antenna may also be specified.

The component outputs are:

- 1 Root-sum-square (RSS) median field strength strongest mode at a set of user-specified frequencies, MUF, LUF, FOT and operational MUF.
- 2 Median signal-to-noise ratio, MUF, LUF, FOT and operational MUF.
- 3 Indication of those frequencies and times for which the median signal-to-noise ratio exceeds a required value.
- 4 Tabulation of the best frequency of those available, i.e. lying above the LUF, below the operational MUF and closest to the FOT.
- 5 Graphical presentation over 24 hours of the operational MUF, LUF and the hours for which up to three selected frequencies lie between these bounds (i.e. are usable).
- 6 An extended output providing mode, elevation angle, RSS field strength, signal-to-noise ratio, and probability of exceeding a required signal-to-noise ratio information.
- 7 An extended multi-mode output providing mode, elevation angle, field strength, signal-to-noise ratio and probability of exceeding a required signal-to-noise ratio for the RSS mode and the three strongest contributed modes.

The graphical presentation (Output 5) can give a clear indication of the times that these selected frequencies yield acceptable system performance. These frequencies are determined by an algorithm to be the optimum for use in the UT bands 0000 - 0400, 0400 - 08002400. This finds applications with non-specialist users who do not wish to have more detailed propagation information.

Using a file generated by program REC533 is a second and more sophisticated stand-alone graphics system. Options exist to display in colour i) circuit characteristics, ii) basic MUF, operational MUF, FOT and LUF, iii) RSS field strength, noise power and signal-to-noise ratio and iv) modes and angles of elevation.

Before running REC533 it may be necessary to call a program (DGCALC95) to configure an antenna used, by specifying its design parameters, and pre-calculate the time-consuming modelling components such as directivity gain. This task need be undertaken only once for each configuration prior to the antenna being used in multiple predictions. This program has a interface, similar to that for REC533, where full screen editing of antenna parameters is possible.

Binary object versions of the program suites for IBM PC (or compatible) host computers, running under MS-DOS, are available for systems with or without a maths co-processor and Hercules, CGA, EGA or VGA graphics cards. The source code is also available.

Examples of the output of REC533 can be found in the REC533 Program Users Guide [Dick *et al.*, 1996]. Examples of the output of REC533 are given in Figs. 6.19 to 6.22; further examples can be found in the REC533 program Users Guide.

PAGE 1		REC533 Vers 3 INPUT FILE DIRECTORY				
Transmitter	Receiver	Method	Month	R12		
1. NORFOLK,USA ISOTROPC	- LUECHOW	1	7	29.		
2. NORFOLK,USA ISOTROPC	- LUECHOW	2	7	29.		
3. NORFOLK,USA ISOTROPC	- LUECHOW	6	7	29.		
4. PARIS HR 4/4/0.5	- GUADELOUPE	5	6	10		
5. LONDON LOG. PER.	- ROME	1	6	148		
* 6. LONDON LOG. PER.	- ROME	2	6	148		
7. LONDON LOG. PER.	- ROME	3	6	148		
8. LONDON LOG. PER.	- ROME	4	6	148		
9. LONDON LOG. PER.	- ROME	5	6	148		
10. LONDON LOG. PER.	- ROME	6	6	148		
11. LONDON LOG. PER.	- ROME	1	12	106		
12. SLOUGH ISOTROPE	- DOORBES	1	6	10.		
13. SLOUGH ISOTROPE	- DOORBES	6	6	10.		
14. LONDON LPU	- E. USA	5	9	55.		
15. LONDON HR	- E. USA	5	9	55.		
16. SYDNEY LPH	- LONDON VM	6	10	140		
17. TUCUMAN LPU	- BUENOS AIRES	6	6	137		

More files on next page ...

F1 : RUN PRINTER O/P F2 : RUN VDU O/P F3 : RUN DISK O/P
 F4 (OR ENTER) : EDIT CIRCUIT F5 : SELECT MULTIPLE RUN F6 : DELETE CIRCUIT
 F7 : RENUMBER CIRCUITS F8 (OR ESC) : QUIT PROGRAM

FIGURE 6.19
 Example of REC533 input file display

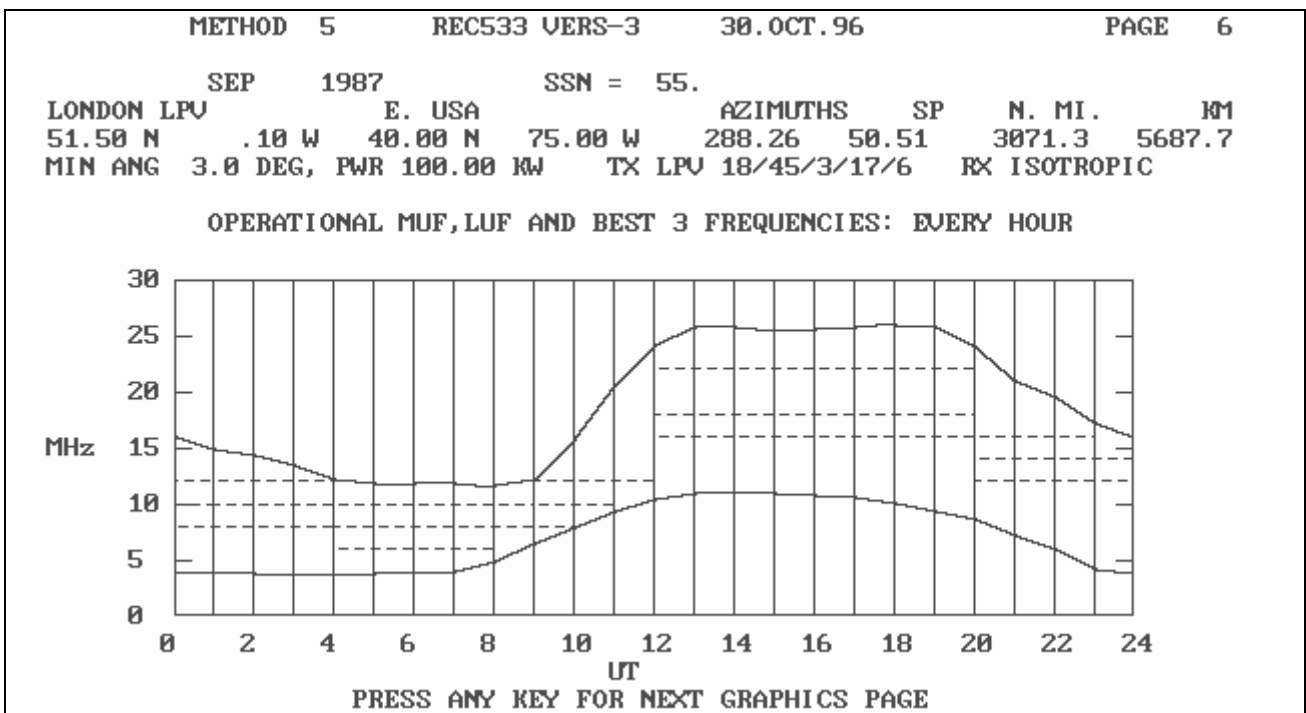


FIGURE 6.20
 Example of Method 5 output

METHOD 2		REC533 VERS-3		30.OCT.96		PAGE 3									
JAN 1990		SSN = 170.													
LONDON ANT=114		BRASILIA		AZIMUTHS		SP	N. MI KM								
51.00	N .10 W	16.00	S 48.00 W	226.61	28.41	4741.6	8780.8								
MIN ANG 3.0 DEG		TBEAR 225.0		RBEAR .0		PWR	10.00 KW								
TX AHR/2/2/0.3/S0/10		6.0- 14.0 MHz		RX ISOTROPIC		2.0- 30.0 MHz									
S/N% 50		-157 NOISE DBW		6000 HZ RX BDWTH		REQ	S/N 8 DB								
75% SIGNAL-TO-NOISE RATIO FOR STRONGEST MODE IN DB															
UT	MUF	DB	6.0	7.0	8.0	9.0	10.0	11.0	12.0	13.0	14.0	15.0	LUF	FOT	OPMUF
1	11.2	19	-89	18	19	20	20	19	17	14	11	-108	6.8	12.9	15.1
2	11.3	20	-87	20	21	21	21	20	18	15	12	-107	6.8	12.9	15.2
3	11.9	22	-84	23	24	24	24	23	21	18	15	-103	6.7	13.6	16.0
4	11.1	21	-81	25	25	24	23	21	18	15	11	-108	6.7	12.7	15.0
5	8.8	19	-82	23	21	18	14	9	5	-1	-7	-128	6.7	10.1	11.8
6	8.1	20	-82	23	20	15	11	6	0	-6	-14	-136	6.7	9.3	10.9
7	12.5	25	-75	32	32	32	31	29	27	24	20	-99	6.7	14.3	16.8
8	18.2	-82	-73	35	37	38	39	39	39	38	37	-78	6.6	19.9	23.5
9	22.0	-90	-204	-62	-38	-22	-9	-1	6	11	15	-96	10.4	22.5	26.4
10	30.7	-88	-287	-139	-95	-66	-45	-30	-18	-9	-2	-111	13.5	31.3	36.8
11	37.1	-90	-319	-182	-135	-101	-72	-51	-36	-24	-15	-122	44.6	37.9	44.6
12	37.2	-90	-332	-209	-157	-114	-85	-63	-46	-33	-23	-129	44.6	37.9	44.6
13	33.9	-92	-338	-220	-167	-127	-93	-69	-52	-38	-27	-132	40.7	34.6	40.7
14	32.1	-94	-341	-222	-169	-129	-94	-71	-53	-39	-28	-134	38.5	32.7	38.5
15	32.2	-94	-343	-219	-166	-128	-92	-69	-52	-38	-27	-133	38.6	32.8	38.6
16	32.7	-92	-338	-204	-154	-117	-82	-61	-44	-31	-21	-127	39.2	33.3	39.2
17	33.0	-91	-316	-168	-125	-87	-63	-45	-30	-19	-10	-117	36.7	33.7	39.7
18	28.6	-92	-276	-128	-93	-68	-43	-28	-16	-7	0	-109	13.4	29.2	34.3
19	23.4	-92	-209	-73	-50	-28	-15	-5	2	8	13	-98	11.2	24.1	28.3
20	19.5	-91	-150	-28	-10	0	7	12	17	20	22	-91	8.6	20.1	23.6
21	16.8	-91	-113	2	9	14	18	21	23	25	25	-89	6.9	17.3	20.4
22	14.9	-91	-104	9	13	17	20	22	23	24	24	-92	6.9	16.4	19.3
23	13.4	22	-98	12	16	19	20	22	22	22	20	-97	6.8	15.4	18.1
24	12.1	20	-93	16	18	19	20	20	20	18	15	-103	6.8	13.9	16.4

FIGURE 6.21
Example of REC533 Method 2

METHOD 6 REC533 VERS-3 30.OCT.96											PAGE 7				
JUL		1977		SSN = 29.											
NORFOLK ANT=103		LUECHOW		VM NO	SCREEN	AZIMUTHS		SP	N. MI.		KM				
36.80 N	76.50 W	52.98 N	11.22 E	43.91	292.73				3612.6	6690.0					
MIN ANG 3.0 DEG		TBEAR		53.0	RBEAR		.0	PWR		1.00 KW					
TX AHR/4/3/0.5/S0/10		6.0-		14.0	MHz	RX VM	8/0/0/0	2.0-		13.1 MHz					
S/N% 50		-157		NOISE	DBW	3000 Hz		RX	BDWTH		REQ S/N 8 DB				
UT MUF											LUF FOT OPMUF				
2	12.0	5.0	7.2	8.1	10.9	12.5	16.4	20.0	.0	.0	.0	FREQ	6.9	11.7	13.8
	3F2	3F2	4F2	3F2	3F2	3F2	3F2	3F2	0	0	0	MODE			
	14	5	15	9	13	15	16	17	0	0	0	ANGL			
	26	-91	26	27	28	18	-110	-118	-999	-999	-999	DBU			
	30	-99	21	23	29	22	-202	-208	-999	-999	-999	S/N			
	.93	.01	.87	.91	.92	.85	.01	.01	.00	.00	.00	FS/N			
6	9.9	5.0	7.2	8.1	10.9	12.5	16.4	20.0	.0	.0	.0	FREQ	6.9	10.6	12.4
	3F2	6F2	4F2	4F2	3F2	3F2	3F2	3F2	0	0	0	MODE			
	14	29	20	20	14	14	15	15	0	0	0	ANGL			
	22	-124	11	14	12	4	-119	-125	-999	-999	-999	DBU			
	25	-119	15	18	16	10	-211	-216	-999	-999	-999	S/N			
	.88	.01	.74	.77	.73	.57	.01	.01	.00	.00	.00	FS/N			
10	13.7	5.0	7.2	8.1	10.9	12.5	16.4	20.0	.0	.0	.0	FREQ	10.8	13.4	
15.8												MODE			
	3F2	3F2	6F2	5F2	4F2	3F2	3F2	3F2	0	0	0	ANGL			
	12	12	27	23	18	12	12	12	0	0	0	DBU			
	14	-245	-35	-21	2	11	-112	-118	-999	-999	-999	S/N			
	-79	-239	-28	-13	9	17	-204	-208	-999	-999	-999	FS/N			
	.01	.01	.01	.01	.53	.76	.01	.01	.00	.00	.00				
14	16.6	5.0	7.2	8.1	10.9	12.5	16.4	20.0	.0	.0	.0	FREQ	12.6	15.6	
18.3												MODE			
	3F2	2F2	6F2	5F2	4F2	3F2	3F2	2F2	0	0	0	ANGL			
	15	7	31	26	21	15	15	7	0	0	0	DBU			
	-97	-245	-59	-39	-10	3	-98	-109	-999	-999	-999	S/N			
	-191	-240	-53	-33	-5	8	-192	-200	-999	-999	-999	FS/N			
	.01	.01	.01	.01	.08	.48	.01	.01	.00	.00	.00				
18	16.5	5.0	7.2	8.1	10.9	12.5	16.4	20.0	.0	.0	.0	FREQ	12.4	15.4	
18.2												MODE			
	3F2	3F2	6F2	5F2	4F2	3F2	3F2	3F2	0	0	0	ANGL			
	14	14	30	26	20	14	14	14	0	0	0	DBU			
	-99	-245	-45	-28	-4	8	-99	-111	-999	-999	-999	S/N			
	-194	-246	-45	-29	-4	9	-194	-203	-999	-999	-999	FS/N			
	.01	.01	.01	.01	.10	.53	.01	.01	.00	.00	.00				
22	17.1	5.0	7.2	8.1	10.9	12.5	16.4	20.0	.0	.0	0	FREQ	8.7	16.0	
18.9												MODE			
	3F2	8F2	5F2	5F2	3F2	3F2	3F2	3F2	0	0	0	ANGL			
	12	31	20	21	10	11	12	12	0	0	0	DBU			
	-91	-152	1	6	20	23	-91	-104	-999	-999	-999	S/N			
	-184	-159	-4	2	19	24	-184	-195	-999	-999	-999	FS/N			
	.01	.01	.09	.23	.85	.92	.01	.01	.00	.00	.00				

FIGURE 6.22
Example of Method 6 Output

Program MUFFY:

Recommendations P.1239 and P.1240 give reference ionospheric data and algorithms that can be used to estimate the basic MUF, FOT (or OWF) and the operational MUF at integer hours UT over a fixed path between specified terminals in a given month for a quoted level of solar activity. Program MUFFY is a PC-based implementation of these Recommendations.

PROGRAM 'MUFFY' -MAR 95											
BASIC MUF, OPERATIONAL MUF AND FOT DETERMINATION - ITU-R PI.434											
OSLO FOF2 COEFFICIENTS											
MAY 1990 SUNSPOT NO. 152.0											
SYDNEY		TO ADELAIDE		AZIMUTHS				MILES		KM.	
33.93S	151.17E	34.92S	138.58E	261.01	88.14	720.4	1159.3				
SHORT PATH				TX PWR		1.0 KW					
UT	BMUF	MUF	FOT	UT	BMUF	MUF	FOT	UT	BMUF	MUF	FOT
01	20.1	24.1	20.5	09	12.7	16.5	14.0	17	7.6	9.9	8.4
02	20.2	24.2	20.6	10	10.8	14.0	11.9	18	6.8	8.8	7.5
03	20.2	24.2	20.6	11	9.3	12.1	10.3	19	6.0	7.7	6.6
04	19.9	23.9	20.3	12	8.2	10.7	9.1	20	6.5	8.5	7.2
05	19.7	23.6	20.1	13	7.8	10.1	8.6	21	9.7	11.7	9.9
06	19.2	23.1	19.6	14	7.8	10.1	8.6	22	14.6	17.6	14.9
07	17.7	21.3	18.1	15	7.9	10.3	8.8	23	18.4	22.1	18.8
08	15.3	18.3	15.6	16	7.9	10.3	8.7	4	19.8	23.8	20.2

FIGURE 6.23

Example of MUFFY output

Programs WOMAP and HRMNTH:

Recommendation P.1239 contains reference data defining monthly median values of the standard ionospheric characteristics scaled from a vertical-incidence ionogram. Orthogonal Fourier polynomial and associated numerical coefficients are used to represent the geographical and universal time variations. There are separate sets of coefficients for each month for reference low and high solar epochs (corresponding to smoothed sunspot number $R_{12} = 0$ and 100 respectively for the characteristics foF2 and M(3000)F2; for the other characteristics $R_{12} = 10$ and 150).

Programs WOMAP and HRMNTH provide a printout on a full or partial world map grid for a specified month and UT hour, and a printout of any of the following for a specified location and series of months and hours: monthly median, upper and lower decile foF2; monthly median M(3000)F2, h'F, h'-F2, foE and foF1; monthly median, upper and lower decile foEs

The characteristics foF1 and foE are evaluated in accordance with the empirical relations in Recommendation P.1239. Figs. 6.24 and 6.25 show HRMNTH and WOMAP examples respectively.

MEDIAN foF2 (MHz) USING ITU-R COEFFICIENTS (OSLO)												DISK SET B	
LATITUDE		51.5		LONGITUDE		- .6		SLOUGH, UK		1988			
	JAN	FEB	MAR	APR	MAY	JUNE	JULY	AUG	SEPT	OCT	NOV	DEC	
R12	55.0	59.0	63.0	69.0	75.0	81.0	88.0	94.0	101.0	108.0	114.0	120.0	
UT													
2.0	2.8	3.1	3.6	3.9	4.5	4.8	4.9	4.3	4.3	4.4	3.7	3.6	
4.0	2.5	2.6	3.0	3.6	4.5	4.9	4.6	4.1	3.6	3.4	3.0	3.3	
6.0	2.1	2.7	3.7	4.5	5.2	5.5	5.3	5.2	4.7	4.5	3.4	2.8	
8.0	4.7	5.3	5.8	5.7	6.2	6.1	6.0	6.4	6.5	7.9	7.4	6.7	
10.0	6.8	6.9	7.1	6.7	6.6	6.3	6.5	6.8	7.5	9.9	10.3	10.1	
12.0	7.5	7.6	7.7	7.1	6.7	6.3	6.4	6.7	7.9	10.7	11.4	11.3	
14.0	7.3	7.6	7.6	7.1	6.8	6.2	6.3	6.6	7.8	10.6	11.1	11.1	
16.0	6.0	7.1	7.5	7.1	6.6	6.0	6.1	6.5	7.7	10.0	9.5	9.2	
18.0	4.1	5.5	6.8	7.1	6.9	6.3	6.5	7.0	7.6	8.1	6.4	6.2	
20.0	3.0	3.9	5.3	6.3	6.8	6.6	6.7	7.0	6.4	5.7	4.2	4.2	
22.0	2.7	3.1	4.2	5.0	5.9	6.1	6.1	5.9	5.2	4.7	3.6	3.5	
24.0	2.8	3.1	3.7	4.4	5.2	5.4	5.6	5.1	4.7	4.5	3.6	3.5	
M3000-F2 USING ITU-R COEFFICIENTS												DISK SET B	
LATITUDE		51.5		LONGITUDE		-0.6		SLOUGH, UK		1988			
	JAN	FEB	MAR	APR	MAY	JUNE	JULY	AUG	SEPT	OCT	NOV	DEC	
R12	55.0	59.0	63.0	69.0	75.0	81.0	88.0	94.0	101.0	108.0	114.0	120.0	
UT													
2.0	2.95	2.85	2.70	2.70	2.75	2.80	2.80	2.70	2.65	2.65	2.75	2.75	
4.0	2.95	2.85	2.80	2.85	2.80	2.80	2.80	2.80	2.80	2.70	2.80	2.75	
6.0	3.05	3.05	3.05	3.00	2.95	2.90	2.90	2.95	3.00	2.95	2.90	2.85	
8.0	3.30	3.30	3.20	3.05	2.95	2.95	2.95	3.00	3.10	3.15	3.15	3.15	
10.0	3.45	3.40	3.15	2.95	2.90	2.90	2.90	2.95	3.00	3.10	3.25	3.25	
12.0	3.45	3.35	3.10	2.90	2.85	2.85	2.85	2.90	2.95	3.05	3.15	3.20	
14.0	3.40	3.35	3.10	2.90	2.80	2.80	2.85	2.85	2.90	3.00	3.15	3.15	
16.0	3.35	3.30	3.15	2.95	2.90	2.85	2.90	2.90	2.95	3.05	3.15	3.15	
18.0	3.25	3.25	3.15	3.05	3.00	2.95	3.00	3.00	3.00	3.05	3.05	3.05	
20.0	3.05	3.10	3.00	3.00	3.00	3.00	3.00	2.95	2.90	2.90	2.90	2.90	
22.0	2.95	2.90	2.80	2.80	2.90	2.90	2.90	2.85	2.75	2.75	2.75	2.75	
24.0	2.90	2.85	2.75	2.70	2.80	2.85	2.85	2.75	2.70	2.65	2.70	2.70	

FIGURE 6.24

Example of HRMNTH output

MEDIAN foF2 (MHz) ITU-R COEFF'S (OSLO) DEC R12 100.0 DATA SET B												
0600 U.T.												
LMT	6	8	10	12	14	16	18	20	22	0	2	4
LONG	0	30.0	60.0	90.0	120.0	150.0	180.0	210.0	240.0	270.0	300.0	330.0
LAT												
90.0	5.5	5.5	5.5	5.5	5.5	5.5	5.5	5.5	5.5	5.5	5.5	5.5
85.0	4.4	4.3	4.5	4.7	4.9	4.9	4.8	4.8	4.9	5.0	4.8	4.6
80.0	3.5	3.7	4.4	5.1	5.3	4.9	4.4	4.1	4.3	4.6	4.4	3.9
75.0	2.9	3.4	4.9	6.1	6.2	5.3	4.1	3.5	3.7	4.3	4.2	3.4
70.0	2.5	3.5	5.6	7.2	7.3	5.8	4.1	3.1	3.3	4.1	4.0	3.0
65.0	2.3	3.8	6.5	8.4	8.2	6.3	4.2	2.9	2.9	4.0	4.0	2.8
60.0	2.3	4.3	7.4	9.4	8.9	6.7	4.5	3.0	2.7	3.9	4.1	2.7
55.0	2.5	5.0	8.3	10.2	9.4	6.9	4.8	3.2	2.7	3.8	4.2	2.8
50.0	2.8	5.7	9.0	10.6	9.6	7.2	5.1	3.5	2.8	3.8	4.3	2.9
45.0	3.2	6.4	9.5	10.7	9.7	7.5	5.6	3.9	3.1	3.8	4.4	3.1
40.0	3.5	7.2	9.8	10.7	9.9	8.1	6.1	4.4	3.4	3.7	4.5	3.3
35.0	3.9	7.9	10.1	10.8	10.5	9.1	6.7	4.9	3.8	3.7	4.6	3.4
30.0	4.1	8.8	10.6	11.4	11.6	10.5	7.7	5.5	4.2	3.7	4.6	3.5
25.0	4.5	10.0	11.5	12.4	13.0	12.1	9.1	6.4	5.0	3.8	4.6	3.5
20.0	5.1	11.0	12.5	12.6	13.5	13.0	10.8	7.9	6.2	4.1	4.6	3.6
15.0	5.5	10.9	12.3	11.2	12.3	12.6	12.2	9.9	8.1	4.8	4.6	4.1
10.0	5.4	10.2	11.2	9.9	10.7	11.3	12.3	11.8	10.5	6.2	5.0	4.8
5.0	5.6	9.3	10.0	9.7	10.1	10.6	11.0	11.7	11.7	8.2	5.8	5.1
.0	5.8	8.9	9.5	11.0	11.1	10.9	10.2	9.5	10.0	9.1	6.9	5.2
-5.0	6.0	9.0	10.0	12.4	12.8	11.6	10.5	8.9	7.9	7.5	7.2	5.7
-10.0	6.3	8.9	10.4	12.5	13.4	12.0	10.5	9.9	8.8	6.2	6.4	6.2
-15.0	6.3	8.7	10.3	11.7	12.6	11.7	10.2	10.0	10.4	7.4	6.1	6.5
-20.0	6.4	8.4	9.8	10.5	11.0	10.8	9.9	9.3	10.4	8.7	6.8	6.8
-25.0	6.4	8.1	9.4	9.4	9.3	9.8	9.7	8.9	9.8	8.9	7.4	7.0
-30.0	6.5	7.8	8.9	8.4	7.9	8.8	9.3	8.8	9.3	8.8	7.6	7.1
-35.0	6.7	7.6	8.5	7.7	7.0	8.0	8.8	8.5	9.0	8.7	7.7	7.3
-40.0	6.8	7.5	8.1	7.2	6.4	7.4	8.2	8.0	8.5	8.6	7.9	7.4
-45.0	7.0	7.4	7.7	6.7	6.1	7.0	7.6	7.4	8.0	8.5	8.0	7.5
-50.0	7.1	7.2	7.3	6.4	6.0	6.7	7.1	6.7	7.3	8.2	8.1	7.7
-55.0	7.2	7.1	6.9	6.2	6.1	6.6	6.5	6.0	6.6	7.9	8.1	7.7
-60.0	7.2	6.9	6.5	6.0	6.1	6.5	6.1	5.5	6.0	7.4	8.0	7.7
-65.0	7.1	6.6	6.2	5.9	6.2	6.5	5.9	5.1	5.6	6.9	7.7	7.6
-70.0	6.8	6.2	5.9	5.8	6.2	6.4	5.7	5.0	5.3	6.4	7.3	7.3
-75.0	6.4	5.9	5.6	5.7	6.1	6.2	5.7	5.1	5.2	6.0	6.7	6.8
-80.0	5.8	5.5	5.4	5.6	5.9	5.9	5.6	5.3	5.2	5.6	6.0	6.1
-85.0	5.3	5.2	5.3	5.4	5.6	5.6	5.5	5.4	5.3	5.4	5.4	5.4
-90.0	5.1	5.1	5.1	5.1	5.1	5.1	5.1	5.1	5.1	5.1	5.1	5.1

FIGURE 6.25

Example of WOMAP output

REFERENCES AND BIBLIOGRAPHY
FOR CHAPTER 6

- BAILEY, D.K.[1959] The effect of multipath distortion on the choice of operating frequencies for high-frequency communication circuits, IRE Trans. Ant. Prop. AP-7, p.398.
- DICK, M.I., HARRISON, S.M. and SIZUN, H. [1996] Computer implementation of the propagation model of Recommendation ITU-R P.533, Users Guide, ITU-R Radiocommunications Bureau, Geneva
- FOMIN, A.I., SERDYUKOV, P.N. and MEZHEVICH, V.V.[1984] Evaluation of the error probability for optimal incoherent reception of binary signals in a multipath channel, Radiotekhnika, No. 8,48-50.
- HORTENBACH, K.J.[1988] A computer programme to calculate the coverage and compatibility of HF broadcasts in the presence of noise and interference, 4th Intern. Conf. on HF radio systems and techniques, IEE Conf. Publ. No. 284, London.
- LÜKE, H.D.[1975] Signalübertragung (signal transmission), Chapter 7, Springer Verlag (Berlin, Heidelberg, New York).
- MILSOM, J.D. and SLATER, T. [1982] Consideration of factors influencing the use of spread spectrum on HF sky-wave paths, in "HF communication systems and techniques", IEE Conf. Publ. Nr. 206,71-75.
- PICKERING, L.W. [1975] The calculation of ionospheric Doppler spread on HF communication channels, IEEE Trans. Comm., COM-23, 5, 526-537.
- SKAUG, R.[1982] An experiment with spread spectrum modulation on an HF channel, in "HF communication systems and techniques", IEE Conf. Publ. Nr. 206, 76-80.

BIBLIOGRAPHY

- DAVIES, K. - "Ionospheric radio", IEE electromagnetic waves series 31, Peter Peregrinus, 1990, ISBN 0 86341 186 X.
- HALL, M.P., BARCLAY, L. W. and HEWITT, M.T. (eds) [1996] Propagation of Radio Waves, Institution of Electrical Engineers, London.
- ITU [1997] Catalogue of Software for Radio Spectrum Management, ITU-R Radiocommunications Bureau, Geneva
- LIED, F. (ed) [1967] High frequency radiocommunications with emphasis on polar problems", AGARDograph No. 104, LCCC No. 67-22235.
- RICHTER, J. H.(ed) [1990] Radio wave propagation modelling, prediction and assessment: AGARDograph No. 326, ISBN 92-835-0598-0.

CHAPTER 7

PROPAGATION AT VHF AND ABOVE - EARTH-SPACE

7.1 Earth-space propagation

Radiowaves at frequencies at VHF and above are capable of penetrating the ionosphere, and therefore provide trans-ionospheric communications. For trans-ionospheric communications, the most significant degradations due to background ionization include Faraday Rotation and Group Delay. These degradations are all related to the Total Electron Content (TEC) along the propagation path. On the other hand, the leading degradation due to irregularities is a phenomenon commonly called scintillation. These will be the main subject matter of this chapter.

7.2 Total Electron Content (TEC)

Denoted as N_T , the total electron content (TEC) can be evaluated by

$$N_T = \int_s N_e(s) ds \quad \text{electrons/m}^2 \quad (7.1)$$

where N_e is the electron density (m^{-3}) along the path and s is the propagation path in metres. Typically N_T varies from 1 to 200 TEC units (1 TEC unit = 10^{16} electrons/ m^2). Even when the precise propagation path is known, the evaluation of N_T is difficult because N_e is highly variable in space and time [Davies, 1980; Soicher and Gorman, 1985].

For modelling purposes, the TEC value is usually quoted for a vertical path using the relationship $N_e(s) ds = N_e(h) \sec \phi dh$, where ϕ is the zenith angle of the ray at a mean ionospheric height (~ 400 km). From a knowledge of the TEC, Faraday rotation and group delay can be estimated for communications applications. The estimate is provided below.

7.3 Effects due to background ionizations

7.3.1 Faraday rotation

When propagating through the ionosphere, a linearly polarized wave will suffer a gradual rotation of its plane of polarization due to the presence of the geomagnetic field and the anisotropy of the plasma medium. The magnitude of Faraday rotation, Ω , will depend on the frequency of the radiowave, the geomagnetic field strength, and the electron density of the plasma as:

$$\Omega = \frac{KM}{f^2} N_T \quad (7.2)$$

where $K = 2.36 \times 10^4$ in MKS units, Ω is in radians, M is the value of $B_L \sec \phi$ at 420 km of height, B_L the longitudinal component of the Earth's magnetic induction, in Tesla, along the ray path, ϕ the zenith angle of the ray, and f the frequency in Hertz. Typical values of Ω as a function of frequency for representative TEC values are shown in Fig. 7.1.

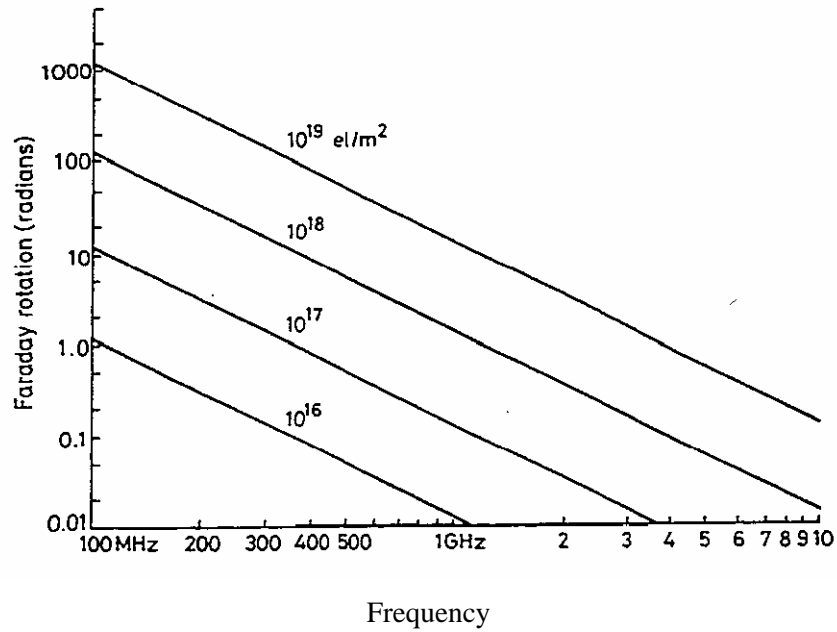


FIGURE 7.1

Faraday rotation as a function of TEC and frequency

Table 7.1 gives the Faraday rotation in degrees which would be exceeded for the stated percentages of time, at a frequency of 1 GHz, during a complete year of observation, at both sunspot maximum and near-minimum periods ($R_{12} = 42$).

TABLE 7.1

Faraday rotation at 1 GHz exceeded for given percentages of time

Time percentage	99	90	50	10	1	0.1	0.01	Period	R_{12}
Rotation (degrees)	3	7	23	43	64	75	82	1979-80	157
	1	2	7	14	30	41	47	1977-78	42

7.3.2 Group delay

The presence of charged particles in the ionosphere slows down the propagation of radio signals along the path and produces a phase advance. The time delay in excess of the propagation time in free space is called the group delay (t). It is an important factor to be considered for digital communication systems and navigational positioning systems. This quantity is given by:

$$t = 1.34 \times 10^{-7} N_T / f^2 \tag{7.3}$$

where

t = delay time in seconds in reference to propagation in a vacuum

f = frequency in Hz

N_T = TEC in electrons/m²

Fig. 7.2 is a plot of time delay (t) versus frequency f for several values of electron content along the ray path.

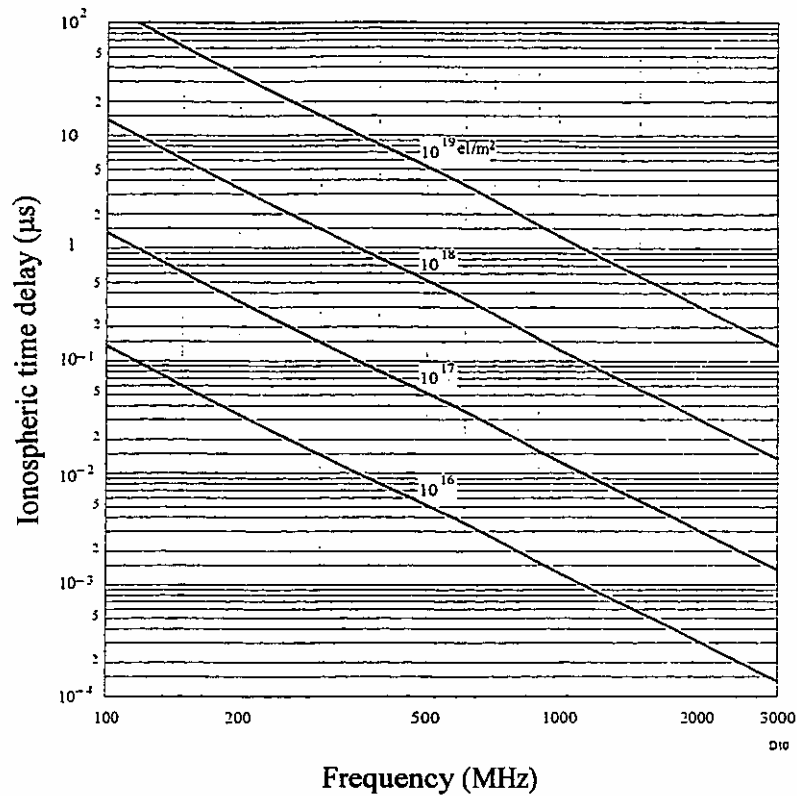


FIGURE 7.2
Ionospheric time delay versus frequency for various values of electron content

Fig. 7.3 shows the yearly percentage of daytime hours that the time delay will exceed 20 ns at a period of relatively high solar activity using a total electron content model developed by Bent *et al.*, [1981].

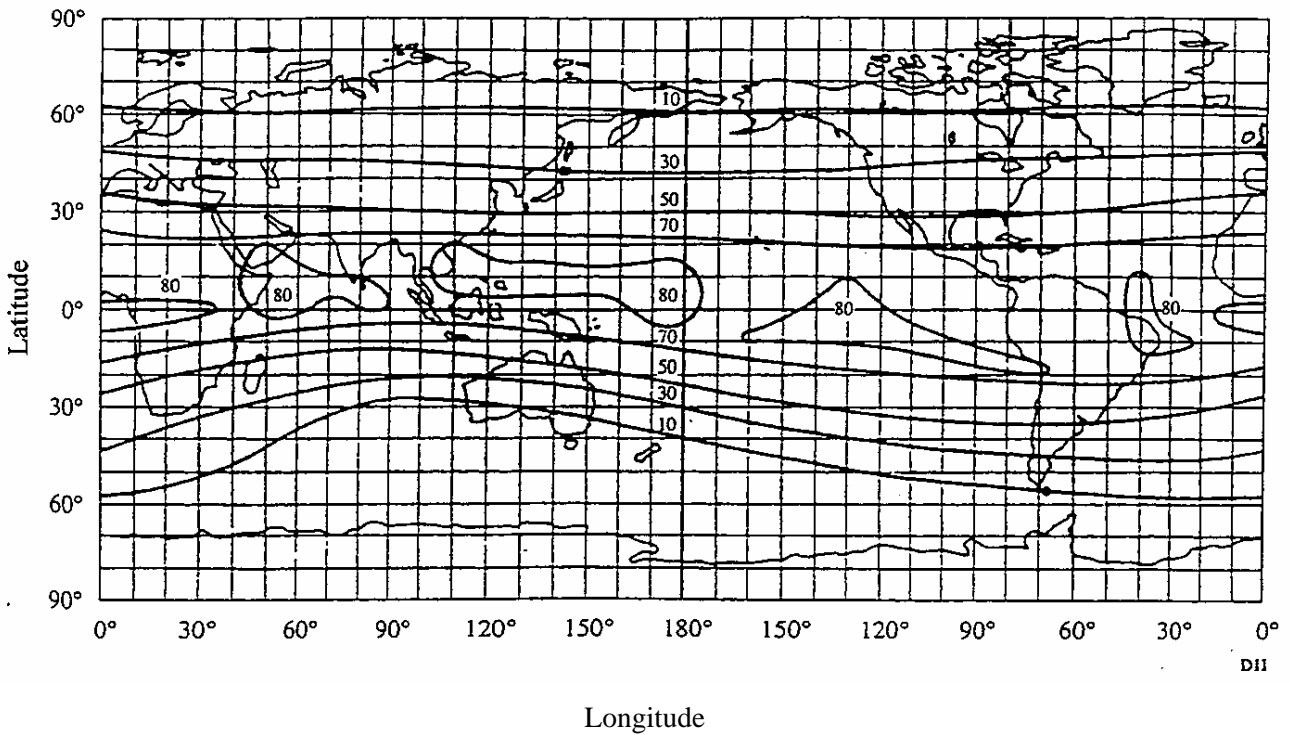


FIGURE 7.3

Contours of percentage of yearly average day time hours when time delay at vertical incidence at 1.6 GHz exceeds 20 ns (sunspot number = 140)

7.3.3 Dispersion

When trans-ionospheric signals occupy a significant bandwidth the propagation delay (being a function of frequency) introduces dispersion. The differential delay across the bandwidth is proportional to the integrated electron density along the ray path. For example, for an integrated electron content of 5×10^{17} electrons/m², a signal with a pulse length of 1 μ s will sustain a differential delay of 0.02 μ s at 200 MHz while at 600 MHz the delay would be only 0.00074 μ s (see Fig. 7.4) [Millman and Olsen, 1980; Mawira, 1990].

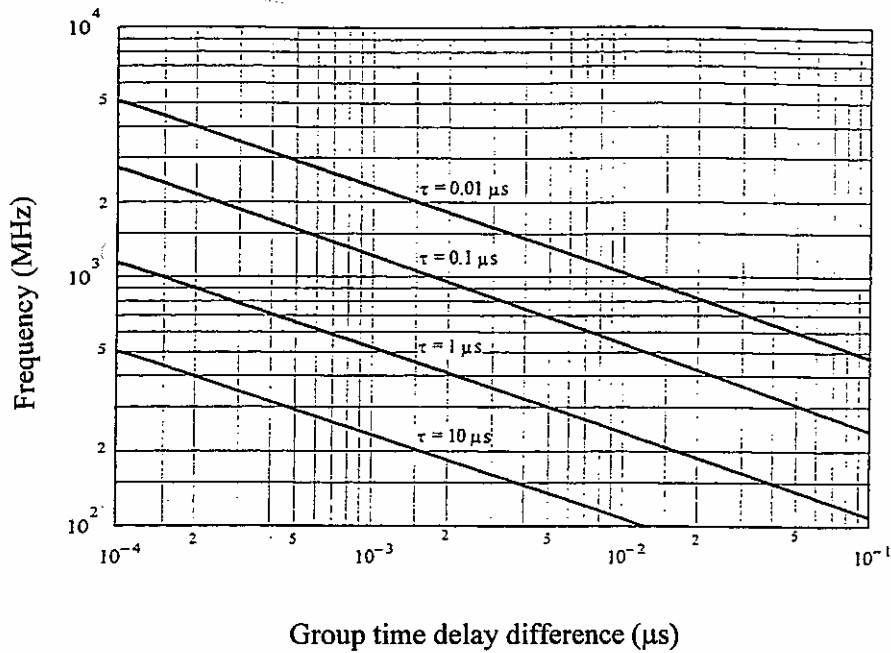


FIGURE 7.4

Difference in the time delay between the lower and upper frequencies of the spectrum of a pulse of width τ , transmitted through the ionosphere, one-way traversal

7.3.4 Doppler frequency shift

The effect of frequency change due to the temporal variability of the ionosphere upon the apparent frequency of the carrier, or the Doppler shifted carrier, is a second order effect. For example, at $f = 1.6$ GHz (GPS system), the observed frequency change Δf at high latitudes is:

$$\frac{\Delta f}{f} < 10^{-9} \quad (7.4)$$

7.3.5 Direction of arrival of the ray

When radiowaves propagate obliquely through the ionosphere, they undergo refraction which produces a change in the direction of arrival of the ray.

7.3.6 Absorption

When direct information is not available, ionospheric absorption loss can be estimated from available models according to the $(\sec \phi)/f^2$ relationship, for frequencies above 30 MHz where ϕ is the zenith angle of the propagation path in the ionosphere [Davies, 1990]. For equatorial and mid-latitude regions, radiowaves of frequencies above 70 MHz will assure penetration of the ionosphere without significant absorption.

Measurements at middle latitudes indicate that, for a one-way traverse of the ionosphere at vertical incidence, the absorption at 30 MHz under normal conditions is typically 0.2 to 0.5 dB. During a solar flare, the absorption will increase but will be less than 5 dB. Enhanced absorption can occur at

high latitudes due to polar cap and auroral events; these two phenomena occur at random intervals, last for different periods of time, and their effects are functions of the locations of the terminals and the elevation angle of the path. Therefore for the most effective system design these phenomena should be treated statistically bearing in mind that the durations for auroral absorption are of the order of hours and for polar cap absorption are of the order of days.

7.3.6.1 Auroral absorption

Auroral absorption results from increases of electron concentration in the D and E regions produced by incident energetic electrons. The absorption is observed over a range of 10° to 20° latitude close to the latitude of maximum occurrence of visual aurorae. It occurs as a series of discrete absorption enhancements each of relatively short duration, i.e. from minutes up to a few hours, with an average duration of about 30 minutes, and usually showing an irregular time structure [Hargreaves and Cowley, 1967]. Night enhancements tend to consist of smooth fast rises and slow decays. Typical magnitudes at 127 MHz are shown in Table 7.2.

TABLE 7.2
Auroral absorption at 127 MHz (dB)

Percentage of the time	Angle of elevation	
	20°	5°
0.1	1.5	2.9
1	0.9	1.7
2	0.7	1.4
5	0.6	1.1
50	0.2	0.4

7.3.6.2 Polar cap absorption

Polar cap absorption occurs on relatively rare occasions, at geomagnetic latitudes greater than 64° [Bailey, 1964]. The absorption is produced by ionization at heights greater than about 30 km. It usually occurs in discrete, though sometimes overlapping, events which are nearly always associated with discrete solar events. The absorption is long-lasting and is detectable over the sunlit polar caps. Polar cap absorption occurs most usually during the peak of the sunspot cycle, when there may be 10 to 12 events per year. Major events will produce absorption of 10 - 20 dB at 30 MHz. Such events may last up to a few days. This is in contrast to auroral absorption, which is frequently quite localized, with variations in periods of minutes.

A remarkable feature of polar cap absorption event is the great reduction in the absorption during hours of darkness for a given rate of electron production.

7.4 Effects due to ionization irregularities

7.4.1 Scintillation effects

One of the most severe disruptions along a trans-ionospheric propagation path for signals from VHF to C-band is caused by ionospheric scintillation. Principally through the mechanisms of forward scattering and diffraction, small-scale irregular structures in the ionization density produce the scintillation phenomenon in which the steady signal at the receiver is replaced by one which is fluctuating in amplitude, phase, and apparent direction of arrival. Depending on the modulation scheme of the system, various aspects of scintillation affect the system performance differently [Yeh and Liu, 1982]. The most commonly used parameter characterizing the intensity fluctuations is the scintillation index S_4 , defined by:

$$S_4 = \left[\frac{\langle I^2 \rangle - \langle I \rangle^2}{\langle I \rangle^2} \right]^{1/2} \quad (7.5)$$

where I is the intensity of the signal and $\langle \rangle$ denotes time averaging [Briggs and Parkin, 1963].

The scintillation index S_4 is related to the peak-to-peak fluctuations of the intensity. The exact relation depends on the distribution of the intensity. The intensity distribution is best described by the Nakagami distribution [Fang and Liu, 1987] for a wide range of S_4 values. As $S_4 \rightarrow 1.0$, it approaches the Rayleigh distribution. Occasionally, S_4 may exceed 1, reaching values as high as 1.5. This is due to focusing. For values less than 0.6, S_4 shows a consistent $f^{-1.5}$ frequency dependence for most multifrequency observations in the VHF and UHF bands. Recent equatorial observations at gigahertz frequencies, however, suggested values higher than 1.5 for the spectral index. As the scintillation becomes stronger such that S_4 exceeds 0.6, the spectral index decreases. This is due to the saturation of scintillation for Rayleigh fading under the strong influence of multiple scattering.

Empirically, Table 7.3 provides a convenient conversion between S_4 and the approximate peak-to-peak fluctuations P_{fluc} in decibels [Fang and Liu, 1987].

TABLE 7.3

Empirical conversion table for scintillation indices

S_4	P_{fluc}
0.1	1.5
0.2	3.5
0.3	6
0.4	8.5
0.5	11
0.6	14
0.7	17
0.8	20
0.9	24
1.0	27.5

7.4.2 Geographic, seasonal and solar dependence

Geographically, there are two intense zones of scintillations, one at high latitudes [Hoppe *et al.*, 1991] and the other within $\pm 20^\circ$ of the magnetic equator as shown in Fig. 7.5. Severe scintillations have been observed up to gigahertz frequencies in these two sectors, being most pronounced in the equatorial sector, while in the middle latitudes scintillations mainly affect VHF signals [Basu *et al.*, 1988]. In all sectors there is a pronounced night-time maximum of the activity [Aarons, 1982,1993].

At polar latitudes and at equatorial latitudes, the most dramatic changes occur over a sunspot cycle with sunspot maximum producing strong effects in the anomaly region of the equator (12-15° from the magnetic equator as shown in Fig. 7.5) and in the polar region. In the auroral region, magnetic storms play the dominant role in producing scintillations during any part of the sunspot cycle. During low sunspot years, the polar region and the anomaly region have, for the most part, low fading levels. For equatorial scintillation from 1.5 to 4 GHz, peak activity is as shown in Fig. 7.6. Peak-to-peak fluctuations at the magnetic equator are of the order of 5 - 6 dB in both high and low sunspot years for 1.5 GHz. At anomaly latitudes, peak-to-peak fluctuations can be over 20 dB for many hours during the years of sunspot maximum. At 4 GHz the peak-to-peak fluctuations of RF signal level exceed 10 dB in magnitude.

In terms of temporal characteristics, the fading rate of ionospheric scintillation is about 0.1 Hz to 1 Hz. A scintillation event has typically an on-set after local ionospheric sunset and can last from 30 minutes to hours. For an equatorial station at years of solar maximum, ionospheric scintillation occurs almost every evening after sunset.

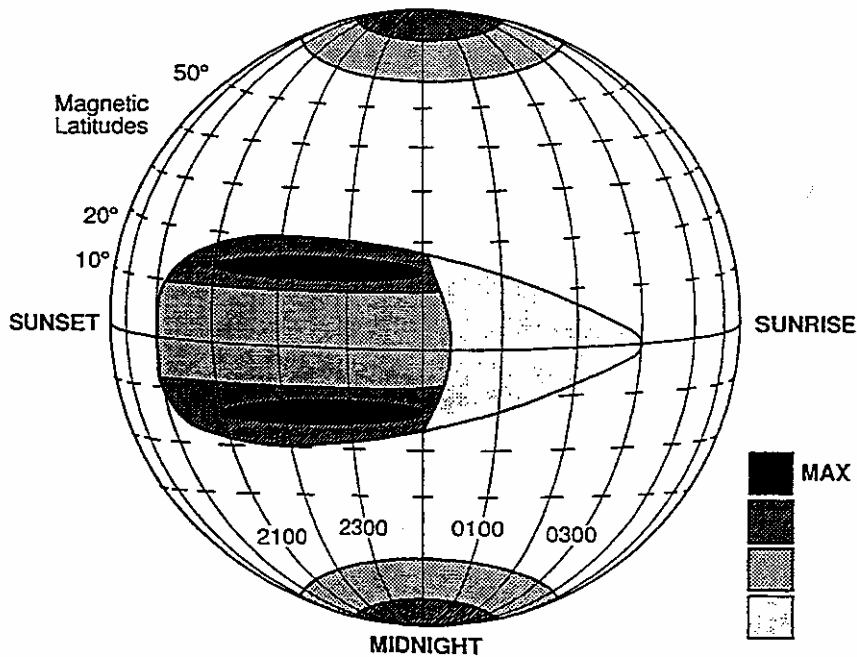


FIGURE 7.5

Illustrative picture of fading depths during high sunspot years

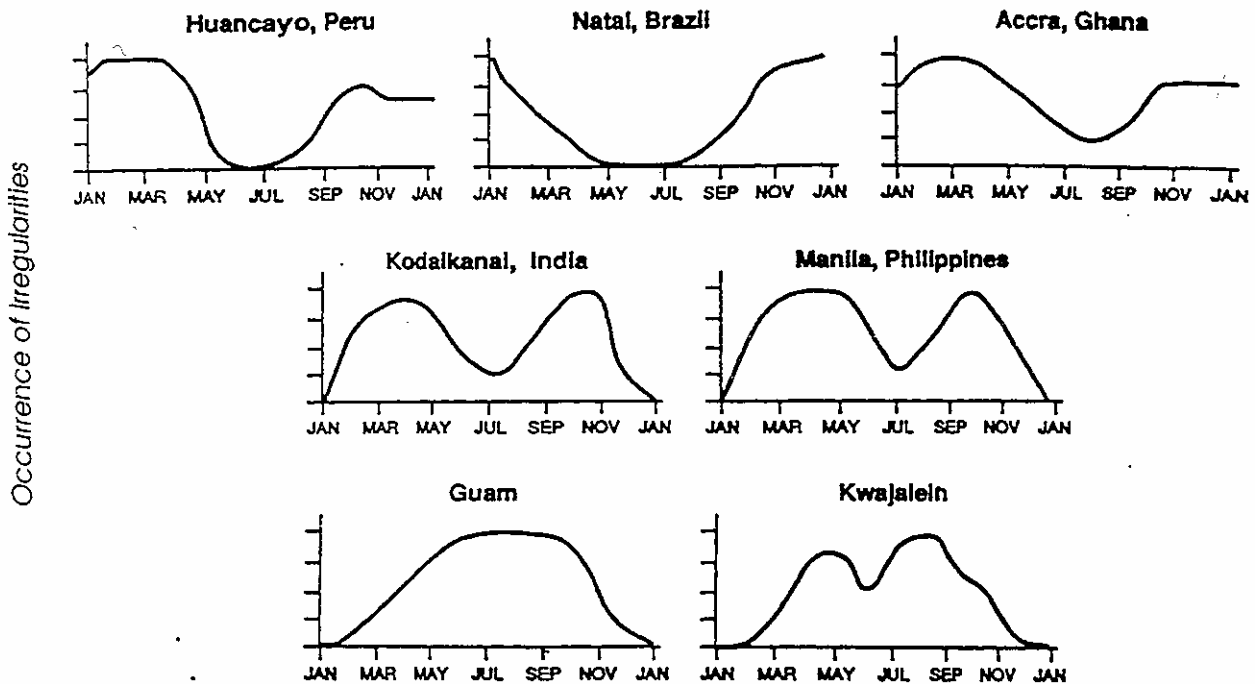
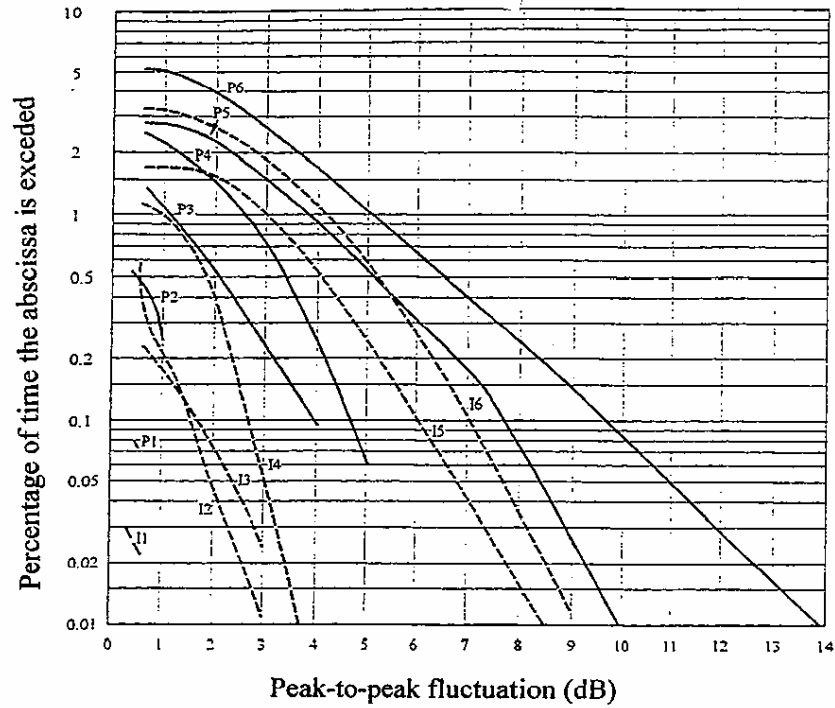


FIGURE 7.6

Schematic occurrence pattern of scintillation and ionospheric irregularities at the magnetic equator (maximum occurrence normalised to 4 units)

7.4.3 Scintillation models

To model the scintillation phenomenon one needs to understand the physical mechanisms that generate these irregularities [Goodman and Aarons, 1990]. Current knowledge about these irregularities, however, does not provide sufficient basis for the construction of a comprehensive model. It has been suggested that spread-F irregularities are responsible for scintillations. Spread-F irregularities are essentially evening and night-time events in the F region. Depending on latitudinal locations, the occurrence of spread F has distinctive patterns relating to seasonal variations and magnetic activities. Since spread F has been studied continuously from the early 1930s and enormous amounts of data are available, radio physicists have attempted to devise empirical models for predicting scintillations based on spread-F models. A more recent model has been constructed based on numerous satellite propagation observations, particularly on observations performed in the Wideband Satellite Experiment [Secan *et al.*, 1996]. With these inputs, models incorporate geographical, seasonal, diurnal, and solar activity as well as magnetic activity dependence. These models have been shown to be successful in predicting UHF scintillations. The most essential element of these models is provided below.



P curves refer to a 20° elevation angle pointing to an eastward synchronous satellite while *I* curves refer to a 30° elevation angle pointing to a westward synchronous satellite.

Curve	Period	SSN range
I1,P1	March 75-76	10-15
I2,P2	June 76-77	12-26
I3,P3	March 77-78	20-70
I4,P4	October 77-78	44-110
I5,P5	November 78-79	110-160
I6,P6	June 79-80	153-165

FIGURE 7.7

Annual statistics of 4 GHz ionospheric scintillation observed at Hong Kong earth station (Curves I1, P1, I3-I6, P3-P6) and Taipei earth station (Curves P2 and I2)

Available long-term observational data forms the basis for establishing these models. A typical example for an equatorial ionospheric path at 4 GHz is shown in Fig. 7.7 [Fang and Pontes, 1981]. The annual occurrence statistics of peak-to-peak amplitude fluctuations, P_{fluc} in decibels, are given for two links. Curves for different years when sunspot numbers (SSN) change from 10 to 165 are labelled. For link budget calculation, P_{fluc} is related to signal level loss L_p by:

$$L_p = \frac{1}{\sqrt{2}} P_{fluc} \quad (7.6)$$

7.5 Summary

To summarize, Table 7.4 estimates maximum values for the various ionospheric effects discussed above at a frequency of 1 GHz. It is assumed that the total zenith electron content of the ionosphere is 10^{18} electrons/m² column. An elevation angle of about 30° is also assumed. The values given are for the one-way traversal of the waves through the ionosphere.

TABLE 7.4

Estimated maximum ionospheric effects at 1 GHz for elevation angles of about 30° one-way traversal

Effect	Magnitude	Frequency dependence
Faraday rotation	108°	$1/f^2$
Propagation delay	0.25 μ s	$1/f^2$
Refraction	< 0.17 milliradians	$1/f^2$
Variation in the direction of arrival	0.2 min of arc	$1/f^2$
Absorption (polar cap absorption PCA)	0.04 dB	$\sim 1/f^2$
Absorption (auroral + PCA)	0.05 dB	$\sim 1/f^2$
Absorption (mid-latitude)	< 0.01 dB	$1/f^2$
Dispersion	0-4 ns/MHz	$1/f^3$
Scintillation	See § 7.4	See § 7.4

As communications and computer techniques rapidly advance the conventional approach of singling out propagation degradation as the physical effects, such as Faraday rotation, group delay, scintillations, is no longer adequate. Wave propagation in the ionosphere is a complicated phenomenon and manifests itself differently for different types of systems. For instance, fading level is a concern to a low-margin communications system in determining the link availability; excess time delay is a concern to a navigation system in determining the range and location; depolarization is a concern to a remote-sensing system which uses dual polarization returns to identify the target; nonstationarity is a concern to a tracking system which has a requirement of setting proper dwell time when sweeping through the space; and common volume scattering is a concern to a jamming/anti-jamming system which has to be able to control the level of wanted to unwanted interference. Consequently, propagation can only be adequately addressed with a proper reference to the communications and computer technology of the system to be used.

REFERENCES FOR CHAPTER 7

- AARONS J, [1982] Global morphology of ionospheric scintillations, *Proc. IEEE*, 70, pp 360-378.
- AARONS J, [1993] The longitudinal morphology of equatorial F-layer irregularities relevant to their occurrence, *Space Science Reviews*, 63, pp 209-243.
- BAILEY, D.K [1964] Polar cap absorption, *Planet. and Space Sci.*, 12, pp 495-541.
- BASU, S., MACKENZIE, E. and BASU, S. [1988] Ionospheric constraints on VHF/UHF communications links during solar maximum and minimum periods, *Radio Sci.*, 23, pp 363-378.
- BENT R.B. *et al.* [1981] The development of a highly-successful worldwide empirical ionospheric model and its use in certain aspects of space communications and worldwide total content investigation, *Effects of the Ionosphere on Space Systems and Communications*, ed. by J.M. Goodman, Naval Research Lab., Washington, D.C. 20375, United States Government Printing Office Stock No. 008-051-00064-0.
- BRIGGS, B.H. and PARKIN, L.A. [1963] On the variation of radio star and satellite scintillations with zenith angle, *J. Atmos. Terr. Phys.*, 25, pp 334-365.
- DAVIES, K. [1980] Recent progress in satellite radio beacon studies with particular emphasis on the ATS-6 radio beacon experiment, *Space Science Rev.*, 25, pp 357-430.
- DAVIES, K. [1990] *Ionospheric Radio*, IEE Electromagnetic Wave Series 31, Peter Peregrinus Ltd., London
- FANG D.J. and LIU C.H. [1987] Propagation, Chapter 29, in *Antenna Handbook*, Y.T. Lo and S.W. Lee, editors, Van Nostrand Reinhold, New York.
- FANG D.J. and PONTES, M.S. [1981] 4/6 GHz ionospheric scintillation measurements during the peak of the sunspot cycle, *COMSAT Tech. Rev.*, 11(2), pp 293-320.
- GOODMAN, J.M. and AARONS, J. [1990] Ionospheric effects on a modern electronic system, *Proc. IEEE*, 78, pp 512-528.
- HARGREAVES, J.K. and COWLEY, F.C. [1967] Studies of auroral radio absorption at three magnetic latitudes, *Planet. and Space Sci.*, 15 (10), pp 1571-1585.
- HOPPE, U. -P., OFSTAD, A.E. and VAN EYKEN, A.P. [1991] Scintillations in trans-ionospheric radio signals: studying their cause with EISCAT and the NAVSTAR GPS satellites, *1991 Nordic Society for Space Research Conf. Proc.*, Danish Met. Inst. Scientific Report 93-1, p 123.
- MAWIRA, A. [1990] Slant path 30 to 12.5 GHz copolar phase difference, first results from measurements using the OLYMPUS satellite, *Electronic Letters*, 26, 15, pp 1138-1139
- MILLMAN, G.H. and OLSEN, K.A. [1980] Ionospheric dispersion effects on wideband transmissions, *AGARD Conf. Proc.*, 284, Propagation Effects in Space/Earth Paths, pp 26-1 to 26-12.

- SECAN, J. A., BUSSEY, R. M., FREMOUW, E. J. and BASU, S. [1996] High-latitude upgrade to the WBMOD ionospheric scintillation model, Proc. Ionospheric Effects Symposium 7-9 May 1996, 5B-3-1 - 5B-3-8
- SOICHER, H. and GORMAN, F.J. [1985] Seasonal and day-to-day variability of total electron content at mid-latitudes near solar maximum, *Radio Science*, 20, pp 383-387
- YEH K.C. and LIU C.H. [1982] Radiowave scintillations in the ionosphere, *Proc. IEEE*, vol. 70, pp. 324-360.

CHAPTER 8

PROPAGATION AT VHF AND ABOVE - TERRESTRIAL

8.1 Ionized propagation at VHF and above

Radiowave propagation at VHF is mainly line-of-sight propagation controlled by physical objects, such as terrain and ground cover (clutter), and tropospheric factors, such as refraction. However, normal ionospheric (sky-wave) propagation over long distances at VHF can take place with relatively small loss at certain times and frequencies. Such propagation events may be significant in causing interference at VHF, particularly for systems requiring high reliability. Such propagation can also have radiocommunication applications.

At both VHF and above there are also several unusual propagation mechanisms, such as sporadic-E propagation, chordal trans-equatorial propagation, meteor forward scatter, and ionospheric scatter that can be useful, or harmful, depending on circumstances. The more important are described in the following sections. Recommendation P.844 gives information in planning radio systems in the VHF and UHF bands.

8.1.1 Normal F-region propagation at VHF

Near the peak of the solar cycle long-distance propagation via the F2 layer can occur for a significant fraction of the time above 30 MHz [Dyson *et al.*, 1992]. This effect extends to 70 MHz at low latitudes.

8.1.2 Trans-equatorial propagation (TEP)

Strong transmission can occur, particularly during high sunspot years, over long north-south paths spanning the geomagnetic equator. This propagation is characterised by low attenuation, high maximum observed frequencies (up to 100 MHz on paths of 4 500 km) and occurs towards solar cycle maximum in the late afternoon and evening hours, up to local midnight, between sites within about 3 000 to 4 000 km of the geomagnetic equator. The direction of propagation needs to be within about 30 degrees of a north-south line to be effective.

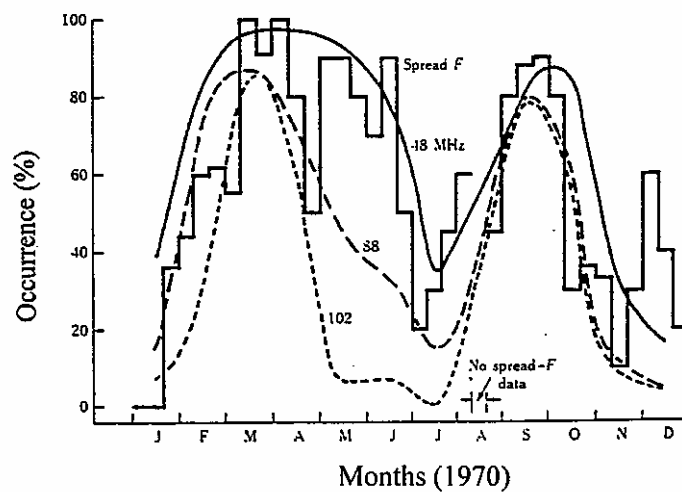


FIGURE 8.1

Occurrence rates of reception on the Darwin -Yamagawa TEP circuit and of spread F in the Australasian sector during 1970

There appear to be two types of trans-equatorial propagation defined by the times of peak occurrence, fading characteristics and modes of propagation [Heron and McNamara, 1979; Tanohata *et al.*, 1980].

The first type of TEP, which is called the afternoon type, has the characteristics:

- a peak occurrence around 1700-1900 LMT, the time being measured at the point where the circuit cuts the magnetic equator;
- normally strong steady signals with a low fading rate and a small Doppler spread (about $\pm 2-4$ Hz);
- path lengths of about 6 000-9 000 km and sometimes longer.

The second type of TEP, which is called the evening type, generally supports higher frequencies than the afternoon type and has very different characteristics:

- a peak occurrence around 2000-2300 LMT;
- high signal strengths but with deep and rapid fading at rates up to about 15 Hz and a large Doppler spread which sometimes exceeds 40 Hz;
- path lengths usually shorter than for the afternoon-type mode, being about 3 000-6 000 km.

Both TEP mechanisms depend on the gradients formed within ionospheric "bubbles" generated near the sunrise terminator and rising in height during the early night hours. The occurrence of the bubbles is solar cycle dependent and the existence of evening-type TEP is most easily identified by the presence of spread F on ionograms at sites near or along the path [Cole and McNamara, 1974]. The spread-F irregularities and evening-type TEP have their maximum occurrence at the equinoxes (Fig. 8.1).

8.1.3 Sporadic-E propagation

Intense sporadic-E ionization in the form of a horizontal sheet of about 1 km average thickness, a horizontal dimension of the order of 100 km and a height of about 100 to 120 km, can cause abnormal VHF propagation for periods lasting for several hours.

The occurrence of sporadic-E propagation decreases with increasing frequency, but can be a significant cause of interference at frequencies up to about 135 MHz.

The plane of polarization of VHF signals received via sporadic-E propagation tends to vary in two different ways. When the structure of the Es layer is dense and steady the plane of polarization has rapid fluctuations around a fixed direction. When the Es layer is weak and intermittent the polarization has slow variations.

Recommendation P.534 provides a method for calculating sporadic-E field strengths and probability of occurrence.

8.1.4 Meteor-trail ionization

Meteor-scatter propagation is independent of ionospheric variations (i.e. diurnal, seasonal, solar cycle). Because of this, only one frequency is required instead of a set of frequencies. Meteors vapourise when they reach the level of the E region of the ionosphere, about 90 to 120 km, forming tubular trails of positive ions and free electrons, about 0.5 m in diameter and some 15-30 km in length which expand and decay through diffusion. Propagation of radiowaves is by scattering from electrons in the trails when they exist.

Meteor scatter provides a means of propagation at VHF, both for communication and interference. Two-way radiocommunications circuits have been operated with frequencies between 30 and 100 MHz over ranges up to 1 300 km. The communication relies on bursts of propagation during the occurrence of meteor trails and supports data rates up to 100 bauds when averaged over several minutes.

Modern communication techniques, such as the use of computers to carry out interactive operations between transmitting and receiving terminals, have made meteor-burst communication relatively more attractive for special applications where time delays of possibly a few minutes can be tolerated. Among such applications are the intermittent transmission of information to a central station from a large number of remote stations, and transmissions to and from mobile terminals.

Scattering from ionization due to meteor trails can produce VHF interference over ranges up to approximately 2 000 km. Although individual meteor trails remain effective for periods measured in seconds, meteor bursts can support continuous or near-continuous propagation for much longer periods of time.

The effect of meteor trails on VHF propagation shows spatial, diurnal and seasonal variations. Information on estimating the useful burst rates for communication may be found in Recommendation P.843.

Meteor occurrence

At certain times of the year meteors occur in the form of showers (Table 8.1) and may be prolific over durations of a few hours. There is, however, a general background of meteors incident upon the Earth from all directions which provide the means for communication. At mid-latitudes there is a roughly sinusoidal diurnal variation of incidence of sporadic meteors (Fig. 8.2) with a maximum at 0600 h and a minimum at 1800 h local time owing to the daily motion of the Earth around the Sun sweeping in the meteors [Manning and Eshleman, 1959]. The ratio of maximum to minimum averages about four. There is a seasonal variation of similar magnitude (Fig. 8.2) with a minimum in February and maximum in July [Sites, 1978]. Considerable day-to-day variability exists in the incidence of both sporadic and shower meteors. Some combined statistics of the daily incidence of the two types are given by Millman [1978].

TABLE 8.1

Dates of meteor showers

Meteor shower	Date of maximum	Meteor shower	Date of maximum
Quadrantids	January 3	Orionids	Oct 21
Lyrids	April 21	Taurids	Nov 4
Eta Aquarids	May 4	Andromdids	Nov 10
Delta Aquarids	July 30	Leonids	Nov 16
Perseids	Aug 12	Geminids	Dec 13
Draconids	Oct 10	Ursids	Dec 22
<i>Permanent daytime streams</i>			
Arietids	June 8	Beta Taurids	June 30
Xi Perseids	June 9		

FIGURE 8.2
DAILY AND ANNUAL VARIATION OF METEOR RATES

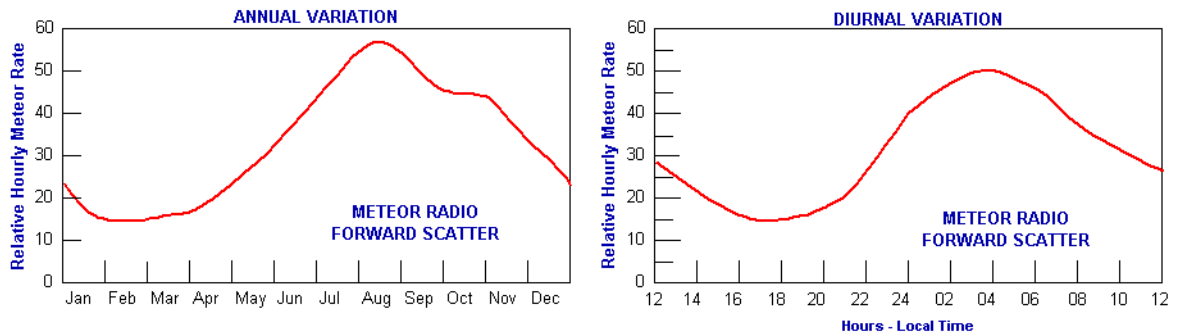


FIGURE 8.2

Daily and annual variation of meteor rates

The ionized trails caused by meteors are classified as underdense or overdense according to the intensity of the ionization. The division between the two cases occurs for line densities of approximately 2×10^{14} electrons/m. Underdense trails have an electron density sufficiently low that the incident wave passes through the trail. As the electron density increases, the trail appears less like a tubular cloud of independently scattering electrons and more like a plasma cloud and is referred to as overdense.

Overdense trails generally have a longer duration than underdense trails. As the frequency increases, the critical radius of a given trail decreases so that at higher frequencies more trails appear as overdense.

In both cases, the received power returned by a trail is a function of both the electron density and the length of the first Fresnel zone which is a function of trail orientation.

Transmission loss is given in Fig. 8.3 for typical electron densities and heights for underdense trails.

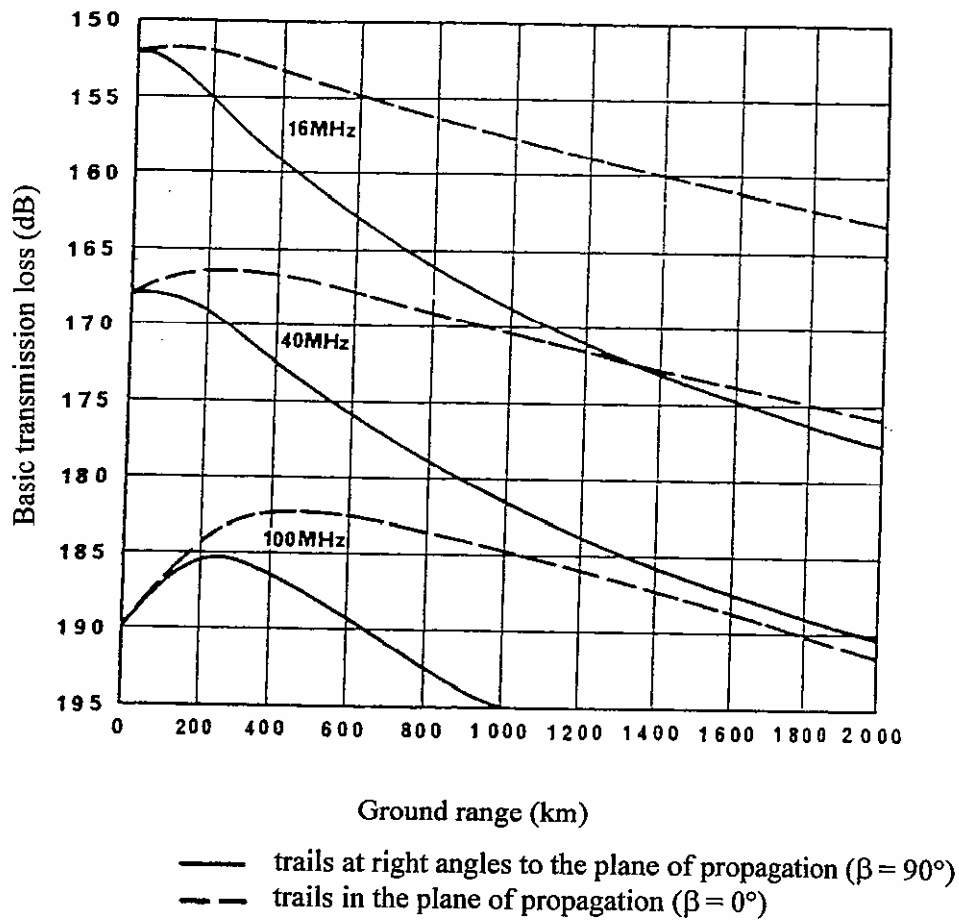


FIGURE 8.3
Basic transmission loss for underdense meteor trails for horizontal polarization

Practical considerations in the choice of frequency

The choice of frequency in a meteor-burst communications system is constrained by several factors. Firstly, the information duty cycle (i.e. the proportion of time that a given S/N is exceeded) is increased by reducing the frequency. Secondly, the high path loss associated with meteor-burst communication signals requires that the level of interfering signals be kept to a minimum. As a consequence, the operating frequency should be above that at which normal ionospheric modes propagate. Thirdly, absorption should be minimized, which also requires the use of as high a frequency as possible. This is particularly of concern for systems operated at high latitudes, where auroral and polar cap absorption can attenuate and even totally absorb the signal if the operating frequency is too low [Maynard, 1968]. Lastly, Cannon [1986] has shown that, at certain times, Faraday rotation of linearly polarized meteor-burst communication signals will severely reduce the communications link capacity for frequencies below about 40 MHz. Evidently, the first constraint is in conflict with the latter three, and when making his frequency choice the system designer must judge the appropriate weightings to be assigned to each.

Multipath and fading profile of the meteor channel

The meteor channel is for the most part a power limited channel as opposed to multipath limited channels [Wetzen and Ralston, 1988]. However, as data rates increase, multipath can become a significant limitation. Multipath mechanisms have been identified as the warping of a trail such that parts of the trail are in different Fresnel zones and scattered signals from them interfere destructively, and those occasions when there is more than one meteor trail on a circuit. The multipath spread resulting from the former mechanism is limited to several hundred nanoseconds at 40 - 50 MHz (Fig. 8.4 and 8.5 [Ellis *et al.*, 1996]), while the latter can cause multipath in excess of 1-2 ms although this phenomenon is observed on less than one or two percent of trails.

Doppler shifts

Large Doppler shifts are not generally observed owing to the specular nature of the scattering mechanism although trail drift in high altitude winds can account for Doppler shifts of some 2 - 20 Hz.

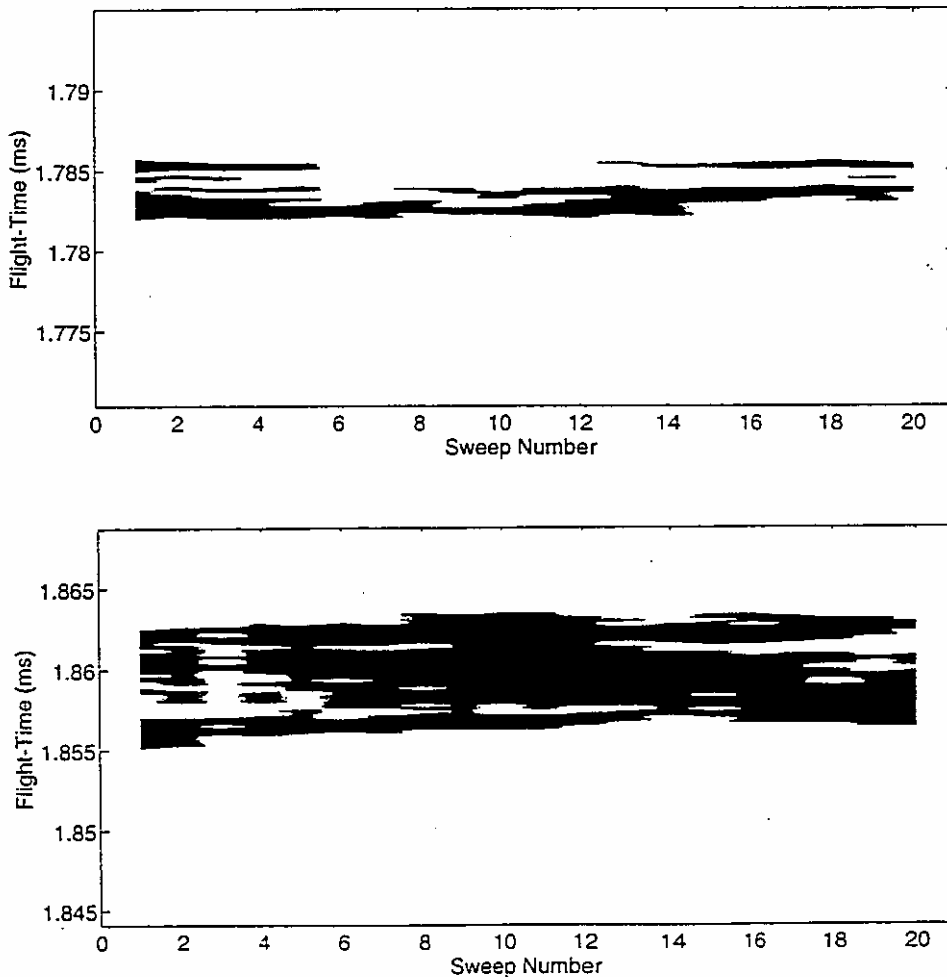


FIGURE 8.4
Impulse response profiles showing evidence of multipath
(swept soundings at 40 MHz over 500km)

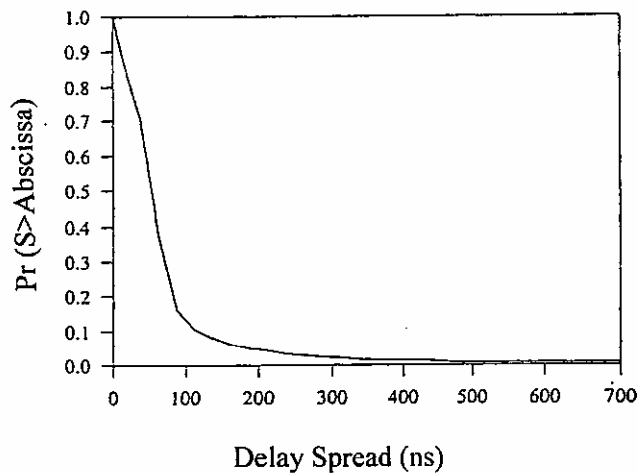


FIGURE 8.5

Delay spread distribution (40 MHz over 500 km circuit)

8.1.5 Auroral ionization

Field-aligned irregularities in the auroral zones appear during magnetically disturbed periods. Such ionization can produce significant reflections causing propagation which is normally off the great-circle path. This may cause interference at VHF frequencies, mainly in mid to high geomagnetic latitudes.

8.1.6 Ionospheric scatter propagation

Ionospheric scatter propagation refers to a propagation mode used to communicate over distances of 800 to 2000 km by means of scattering from ionospheric irregularities at a height of around 85 km. Operating frequencies are in the 30 to 60 MHz range. The lower frequency is set by absorption during sudden ionospheric disturbances (SIDs) and polar cap events and by the desirability of avoiding signals propagated by the F2-layer normal and side-scatter modes.

The upper limit of frequency is fixed by mainly economic considerations. Since, as a rough guide, the signal intensities may be taken as varying inversely as the 7.5 power of the frequency, for scaled antennas with equal input power, while the cosmic noise intensities vary inversely as about the 2.5 power of the frequency, the signal-to-noise ratio varies inversely as approximately the 5th power of the frequency. With this frequency dependence of the signal-to-noise ratio and using scaled antennas, 15 dB more transmitter power is required at 60 MHz than at 30 MHz to give the same signal-to-noise ratio.

The signal, while weak compared to the normal ionospheric modes, is persistent (in most areas of the world); and high-powered ionosphere scatter systems were used in the 1950s and 60s for high-reliability voice and data traffic. Communication systems employing ionospheric scatter propagation are rarely used today.

8.1.7 Summary

The propagation mechanisms that have been described above may be significant in causing interference at VHF. Table 8.1 provides a summary of such mechanisms of ionospheric origin.

TABLE 8.1
Main causes of ionospheric interference to stations working at frequencies between 30 and 300 MHz

Cause of interference	Latitude zone	Period of severe interference	Approximate highest frequency with severe interference (MHz)	Approximate frequency above which interference is negligible (MHz)	Approximate range of distances affected (km)	Principal distinguishing features
Regular F-layer reflections	Mid	Day, equinox and winter, solar-cycle maximum	50	60	E-W paths 3 000-6 000	Occurrence broadly in accordance with regular-layer morphology
	Low	Afternoon to late evening, solar-cycle maximum	60	70	or N-S paths 3 000-10 000	
Sporadic-E reflections	High	Night	70	90	500-4 000	Principally during summer months in mid latitudes. Sudden onset and conclusion, beginning later and ending earlier with increase of operating frequency. Area concerned relatively small and mobile. Duration minutes or hours. No associated signal enhancements at short range
	Mid	Day and evening, summer	60	83-135 (1)		
	Low	Day	60	90		
Sporadic-E scatter	Low	Evening to midnight	60	90	Up to 2 000	
Reflections from meteoric ionization	All	Particularly during showers	May be important anywhere in the range		Up to 2 000	Signal bursts with durations from a fraction of a second to several minutes. Marked diurnal variation, maximum 0600 h local time, minimum 1800 h. Some activity present at all times, but considerable increases during predictable shower periods
Reflections from magnetic field aligned columns of auroral ionization	High	Late afternoon and night				Associated with geomagnetic disturbances, typically when local K-index reaches 5 or more. Characteristic rasping note due to multiple Doppler shifting. Normal duration a few hours, often afternoon to midnight.
Scattering in the F region	Low	Evening to midnight, equinox	60	80	1 000-4 000	
Special transequatorial effects	Low	Evening to midnight	60	80	4 000-9 000	Paths generally aligned symmetrically across the dip equator. Generally around equinoctial periods with regular occurrences. Strong signals. Refer to main text for further details.

(1) For 0.1% of the time during the hours 0800-2300 LT for May to August (111 min total) the following frequencies may be derived from Annex 1 to Recommendation P.534 for a distance of 1 800 km and $\Gamma = 30$ dB for temperate zone: Region A (Europe and North Africa): 83 MHz; Region B (North America): 93 MHz; Region C (Asia): 135 MHz; Region D (Average for Northern Hemisphere): 115 MHz

REFERENCES FOR CHAPTER 8

- CANNON, P. S. [1986] Polarization rotation in meteor burst communication systems. *Radio Sci.*, Vol. 21, **3**, 500-510.
- COLE, D. G. and McNAMARA, L. F. [1974] Variations of Spread-F occurrence rates at near-equatorial stations in the Australasian zone, *Aust. J. Phys.*, 27, 249-257.
- DYSON, P. L., CHEN, J. and BENNETT, J. A. [1992] Single -hop F2 propagation above 30 MHz and over distances greater than 4000 km., *IEEE Trans-AP*, 40, No. 7, 841-843.
- ELLIS, K. J., WEBSTER, A. R., JONES, J. and CHOW, S. [1996] An impulse response measurement system and some experimental results from a forward scatter meteor burst link, *Digital Communications Systems: Propagation Effects, Technical Solutions, Systems Design*, AGARD Conf. Proc. CP-574.
- HERON, M.L. and McNAMARA, L.F. [1979] Transequatorial VHF propagation through equatorial plasma bubbles, *Radio Sci.*, 14, pp897-910.
- MANNING, L. A. and ESHLEMAN, V. R. [1959] Meteors in the ionosphere. *Proc. IRE*, Vol. 47, 186-199.
- MAYNARD, L. A. [1968] Meteor-burst communications in the Arctic. *Ionospheric Radio Propagation*, 165-173. Plenum Press, New York, NY, USA.
- MILLMAN, G. H. [1978] HF scatter from overdense meteor trails. *Aspects of Electromagnetic Wave Scattering in Radio Communications*. Ed. A. N. Ince. AGARD Conf. Proc. 244, 6-1 to 6-14.
- SITES, F. J. [1978] Communications via meteor trails. *Aspects of Electromagnetic Wave Scattering in Radio Communications*. Ed. A. N. Ince. AGARD Conf. Proc. 244, 25-1 to 25-21.
- TANOHATA, K., KURIKI, I., IGUCHI, M., YAMASHITA, K., and SAKAMOTO, T. [1980] The results of long-term experiment of transequatorial VHF wave propagation, *Rev. Radio Res. Labs. (Japan)*, 26, pp 885-897.
- WEITZEN, J. A. and RALSTON, W. T. [1988] Meteor scatter: an overview, *IEEE Trans. Ant. and Propagation*, Vol 36 (12), 1813-1819.

BIBLIOGRAPHY

- BAILEY, D. K. [1962] Ionospheric “forward” scattering. General survey to the XIIIth General Assembly of URSI, London, September 1960, in *Monograph on Ionospheric Radio*, 189-199. Elsevier, London, UK.
- BRAY, W. J., SAXTON, J. A., WHITE, R. W. and LUSCOMBE, G. W. [1956] VHF propagation by ionospheric scattering and its application to long-distance communications. *Proc. IEE*, Vol. 103, Part B, 236-260.
- Proc. IRE* [January, 1960] Vol. 48, 7-31. Report of JTAC on “Radio transmission by ionospheric and tropospheric scatter”.

CHAPTER 9

GLOSSARY

A number of definitions are given here to provide an understanding of terms used in this handbook. With few exceptions, they have been taken from ITU-R Recommendations P.341, P.373, V.573, BS.638 and P.842, and the ITU Radio Regulations. In many of the explanations or definitions of a term, another listed term is given in *italics*.

9.1 Ionosphere and waves

- Apparent reflection height;
Mirror reflection height, h': The virtual height in an ionospheric layer at which a radio wave appears to be reflected, as by a mirror or *specular surface* - e.g. h'F, h'F2.
- Auroral oval: An oval ring, at about 67° geomagnetic latitude, eccentric to the geomagnetic pole where visible and radio aurorae are caused by particle precipitation into the upper atmosphere. Its position is fixed relative to the Sun and its dimensions increase with geomagnetic activity.
- Brewster angle: The angle of incidence on a *specular surface* such that the magnitude of the reflection factor for vertical polarization is minimum.
- Collision frequency: The frequency with which an electron activated by a radiowave will collide with other particles and thereby lose its energy. The collision frequency depends on atmospheric density.
- Critical frequency: The highest frequency at which a *radiowave* undergoes reflection in an ionospheric layer on which it is incident vertically; there is usually one such frequency for each magneto-ionic component - e.g. foE, fxF2.
- Electromagnetic wave: A wave characterized by *propagation* of a time-varying electromagnetic field.
- Electron density; electron concentration: The number of free electrons per unit volume, in an ionized medium.
- Electron density profile: Vertical distribution of electrons with height above the Earth. The profile may be derived from ionosonde measurement
- Extraordinary wave (component); X wave: The *magneto-ionic component* which, at vertical incidence, is reflected at the altitude at which the electron density and the Earth's magnetic field are such that: $f_p^2 = f^2 - f \cdot f_B$, where f_B is the electron gyro-frequency and f_p is the plasma frequency.
- First Fresnel zone (of a reflective surface): For an *electromagnetic wave*, the locus of points on a reflective surface such that the sum of the distances from each of them to the transmitting and receiving antennas equals the phase path of the reflected wave, increased by a distance up to one-half wavelength.

<u>Index Φ:</u>	The monthly mean of the daily values of solar radio flux at 10 cm wavelength.
<u>Index K_p:</u>	Index of activity of the Earth's magnetic field.
<u>Ionosphere:</u>	The ionized regions of the Earth's upper atmosphere.
<u>Magnetosphere:</u>	The region around the Earth where the geomagnetic field is constrained by the <i>solar wind</i> .
<u>Magneto-ionic component:</u>	One of the separate <i>radiowaves</i> into which a radiowave entering the ionosphere is divided as a result of the action of the Earth's magnetic field.
<u>Ordinary wave (component); O wave:</u>	The <i>magneto-ionic component</i> which, at vertical incidence, is reflected at the altitude at which the electron density is such that the plasma frequency f_p is equal to the wave frequency f .
<u>Phase velocity v_p, and Group velocity v_g:</u>	Velocity of the carrier signal (group velocity is of the modulated signal envelope). The ionosphere is a dispersive medium, i.e. phase velocity varies with frequency, and v_p and v_g differ.
<u>Plasma frequency; f_p:</u>	The resonance frequency of a plasma (e.g. ionosphere) which is related to the electron density ($f_p(\text{Hz})=9N_e^{1/2}$ for N_e in electrons/m ³)
<u>Polar cap:</u>	The area within the <i>auroral oval</i> where the geomagnetic field lines are open to interplanetary space. Its extent varies from about 84° (quiet) to 65° (magstorm) geomagnetic latitude.
<u>Propagation:</u>	Energy transfer between two points without displacement of matter.
<u>Solar activity:</u>	The emission of electromagnetic <i>radiation</i> and particles from the Sun, including slowly variable components and transient components caused by phenomena such as <i>solar flares</i> .
<u>Solar cycle:</u>	A period of approximately 11 years characterizing the slowly variable components of <i>solar activity</i> .
<u>Solar effects:</u>	The effects of <i>solar activity</i> , usually on the <i>ionosphere</i> .
<u>Solar epoch:</u>	The location in time within the <i>solar cycle</i> .
<u>Solar flare:</u>	Sudden intense release of energy, across the spectrum, originating in an active region on the Sun
<u>Solar wind:</u>	The stream of particles, mainly protons and electrons, flowing outwards from the Sun at speeds up to 900 km/h.
<u>Solar zenith angle:</u>	The angular distance between the Sun and the zenith (i.e. directly overhead) at a given geographical location.
<u>Specular surface:</u>	A surface separating two media which is large, and the irregularities of which are very small, compared to the wavelength of an incident wave.

<u>Sunspot number, Wolf number, <i>R</i>:</u>	A number, following a daily count of sunspots and groups of sunspots, used for evaluating <i>solar activity</i> .
<u>Total Electron Content; TEC:</u>	Number of electrons along a wave path measured in electrons/m ² . TEC is used in determining propagation delays
<u>Wave polarization:</u>	The orientation of the electric field of an <i>electromagnetic wave</i> in the plane perpendicular to the direction of travel of the wave.

9.2 Signals, noise and interference

<u>Acceptable performance:</u>	Subjective evaluation of the minimum acceptable performance of a <i>radio circuit</i> under <i>specified working conditions</i> ; it may be given in terms of a maximum acceptable <i>error ratio</i> or a <i>required signal-to-noise ratio</i> .
<u>Atmospheric noise:</u>	<i>Radio noise</i> produced by natural electric discharges below the <i>ionosphere</i> and reaching the receiving point along the normal propagation paths between the Earth and the lower limit of the ionosphere.
<u>Available frequencies (available frequency bands):</u>	Those frequencies (bands) on which a criterion for service quality is satisfied under given conditions.
<u>Bit-error probability; bit-error ratio; error rate:</u>	The probability that a transmitted binary digit is wrongly detected by the receiving discriminator.
<u>Galactic noise; cosmic noise:</u>	<i>Radio noise</i> arising from natural phenomena outside the Earth's atmosphere.
<u>Interference; radio-frequency interference; RFI:</u>	Degradation of the reception of a <i>wanted signal</i> due to the effect of <i>unwanted</i> or <i>interfering signals</i> .
<u>Interfering signal:</u>	Signal that impairs the reception of a <i>wanted signal</i> .
<u>Lowest usable frequency, LUF:</u>	The minimum operating frequency or the lowest frequency that permits <i>acceptable performance</i> of a <i>radio circuit</i> between given terminals at a given time under <i>specified working conditions</i> . The LUF is determined by the <i>absorption</i> , by the <i>radio noise</i> background, by <i>interference</i> , and by system parameters such as transmitted power and antenna gains.
<u>Man-made noise:</u>	<i>Radio noise</i> having its source in man-made devices.
<u>Monthly median:</u>	The median of daily values for the month, usually for a given hour.
<u>Power spectrum:</u>	Distribution as a function of frequency of the power of the spectral components of a <i>signal</i> or <i>noise</i> .
<u>Radio-frequency noise, RF noise, radio noise, noise:</u>	Time-varying electromagnetic phenomenon having components in the radio-frequency range, apparently not conveying information and which may be superimposed on, or combined with, a <i>wanted signal</i> .

<u>Radio-frequency protection ratio; RF protection ratio; protection ratio:</u>	The minimum value of the <i>wanted-to-unwanted signal</i> ratio, usually expressed in decibels, at the receiver input, determined under specified conditions such that a specified reception quality of the <i>wanted signal</i> is achieved at the receiver output.
<u>Radio-frequency signal-to-interference ratio; RF signal-to-interference ratio:</u>	The <i>signal-to-interference ratio</i> evaluated in specified conditions at the input of a radio receiver.
<u>Radio-frequency signal-to-noise ratio; signal-to-noise ratio; S/N:</u>	The ratio, generally expressed in decibels, of the power of the <i>wanted signal</i> to that of the coexistent <i>radio noise</i> at a specified point in a transmission channel.
<u>Required signal-to-noise ratio:</u>	The value of the <i>radio-frequency signal-to-noise ratio</i> that is required for <i>acceptable performance</i> of a <i>radio circuit</i> between given terminals at a given time under <i>specified working conditions</i> .
<u>Signal:</u>	A physical phenomenon, e.g. an <i>electromagnetic wave</i> , one or more of whose characteristics may vary to represent information.
<u>Signal-to-interference ratio; S/I:</u>	The ratio, generally expressed in decibels, of the power of the <i>wanted signal</i> to the total power of <i>interfering signals</i> and <i>radio-frequency noise</i> , evaluated in specified conditions at a specified point of a transmission channel.
<u>Specified working conditions:</u>	Include such factors as antenna types, transmitter power, class of <i>emission</i> , required information rate and <i>required signal-to-noise ratio</i> .
<u>Unwanted signal; undesired signal:</u>	Signal without interest for the user or equipment that receives it, but which may impair the reception of a <i>wanted signal</i> .
<u>Wanted signal; desired signal:</u>	Signal conveying information sought by a user.

9.3 Antennas and radiation

<u>Absolute gain (of an antenna); isotropic gain (of an antenna):</u>	The ratio, generally expressed in decibels, of the <i>radiation intensity</i> produced by an antenna in a given direction to the radiation intensity that would be obtained if the power accepted by the antenna were radiated equally in all directions.
<u>Directivity; directivity gain; g:</u>	The ratio of the <i>radiation intensity</i> in a given direction (usually the maximum radiation intensity), to the radiation intensity of an isotropic source radiating the same power.
<u>Effective radiated power; ERP:</u>	The product of the power supplied to an antenna and its <i>gain relative to a half-wave dipole</i> in a given direction.
<u>Effective monopole radiated power; EMRP:</u>	The product of the power supplied to an antenna and its <i>gain relative to a short vertical antenna</i> in a given direction.

<u>Emission:</u>	<i>Radiation</i> produced, or the production of radiation, by a radio transmitting station.
<u>Equivalent isotropically radiated power; e.i.r.p.:</u>	The product of the power supplied by a radio transmitter to an antenna and the <i>absolute gain</i> of the antenna in a given direction.
<u>Gain relative to a half-wave dipole:</u>	The ratio, generally expressed in decibels of the <i>partial gain</i> of an antenna, in a given direction and for a specified linear polarization, to the maximum <i>absolute gain</i> of a half-wave dipole isolated in free space and oriented in a direction parallel to the electric flux density vector characterizing the specified <i>polarization</i> in the given direction.
<u>Gain relative to a short antenna:</u>	The ratio, generally expressed in decibels, of the <i>partial gain</i> of an antenna, in a given direction and for a specified linear polarization, to the maximum <i>absolute gain</i> of an antenna consisting of a linear conductor, much shorter than one quarter of the wavelength, normal to the surface of a perfectly conducting plane, and oriented in a direction parallel to the electric flux density vector characterizing the specified <i>polarization</i> in the given direction.
<u>Partial gain (of an antenna):</u>	The ratio, generally expressed in decibels, of that part of the <i>radiation intensity</i> in a given direction, corresponding to a given <i>polarization</i> , to the radiation intensity that would be obtained if the power accepted by the antenna were radiated equally in all directions.
<u>Polarization of an antenna (in a given direction):</u>	<ul style="list-style-type: none">– In transmission, that <i>wave polarization</i> radiated by an antenna in the far field region in the given direction.– In reception, that <i>wave polarization</i> incident from the given direction which results in maximum available received power.
<u>Radiation:</u>	The outward flow of energy from any source in the form of <i>radiowaves</i> .
<u>Radiation diagram:</u>	A graphical representation of a <i>radiation pattern</i> of an antenna.
<u>Radiation intensity:</u>	In a given direction and in the far-field region, the power radiated per unit solid angle by an antenna.
<u>Radiation pattern, antenna pattern, pattern:</u>	The distribution (usually in the far-field region) in space of a quantity characterizing the <i>radiation</i> from an antenna.

9.4 Radiowave propagation

<u>Basic MUF:</u>	The highest frequency by which a <i>radiowave</i> can propagate between given terminals, on a specified occasion, by ionospheric refraction alone, and may apply to a particular mode - e.g. the E-layer basic MUF.
-------------------	---

<u>Control points:</u>	For a particular <i>propagation mode</i> , the points in the ionospheric layer at which the properties of the ionosphere are used to determine the <i>basic MUF</i> of the layer - e.g. the E-layer control points.
<u>E mode, F2 mode:</u>	A <i>propagation mode</i> reflected by the E (F2) layer.
<u>Frequency band:</u>	Continuous set of frequencies in the <i>radio-frequency spectrum</i> lying between two specified limiting frequencies; generally includes many channels.
<u>HF propagation; Short-wave propagation:</u>	<i>Radiowave propagation</i> in the <i>high-frequency band</i> .
<u>High-frequency band, HF band:</u>	The part of the <i>radio-frequency spectrum</i> between 3 and 30 MHz.
<u>High frequency; HF; Short-wave:</u>	Relating to the <i>high-frequency band</i> .
<u>High frequency sky-wave; HF Sky wave; Sky wave:</u>	A <i>radiowave</i> in the <i>high frequency band</i> propagated by ionospheric reflection.
<u>M(3000)F2:</u>	<i>Transmission factor</i> for a distance of 3 000 km, for an F2-layer hop.
<u>Maximum observed frequency; MOF:</u>	The highest frequency at which reflection occurs during oblique incidence sounding between two given points.
<u>Mode; Propagation mode; Mode of propagation:</u>	Representation of a ray path by the number of hops between the end points of the path, the ionospheric layers producing the reflections being indicated for each hop. For example, a 1F + 1E mode represents a hop with reflection in the F region followed by reflection at the ground, followed by a hop with reflection from the E region.
<u>Mode basic MUF:</u>	The <i>basic MUF</i> of a particular <i>propagation mode</i> .
<u>MUF:</u>	Maximum usable frequency
<u>Operational MUF:</u>	The highest frequency that would permit acceptable performance of a <i>radio circuit</i> between given terminals at a given time under <i>specified working conditions</i> .
<u>Optimum working frequency; OWF; Frequency of optimum traffic; FOT:</u>	The frequency that is exceeded by the <i>operational MUF</i> , at a given time, between a specified pair of terminals via any ionospheric <i>propagation mode</i> , during 90% of a specified period, usually a month.
<u>Path; Ray path; Propagation path:</u>	See <i>mode</i> .
<u>Path basic MUF:</u>	The <i>basic MUF</i> of a particular <i>propagation path</i> , based on the <i>mode basic MUFs</i> .

<u>Radio circuit; Circuit:</u>	A <i>radio link</i> from one transmitter to one receiving location with or without diversity.
<u>Radiocommunication:</u>	Telecommunication by means of <i>radiowaves</i> .
<u>Radiocommunication service;</u> <u>Radio service:</u>	A service involving the transmission, <i>emission</i> , and/or reception of <i>radiowaves</i> for specific telecommunication purposes.
<u>Radio frequency; RF; Radio:</u>	A general term applied to the use of <i>radiowaves</i> .
<u>Radio-frequency channel; RF channel; Channel:</u>	Continuous part of the <i>radio-frequency spectrum</i> to be used for a specified <i>emission</i> or transmission.
<u>Radio-frequency spectrum; RF spectrum; radio spectrum:</u>	The part of the electromagnetic spectrum occupied by <i>radiowaves</i> .
<u>Radio link; Link:</u>	A transmission link provided by means of <i>radiowaves</i> .
<u>Radiowave; Hertzian wave:</u>	<i>Electromagnetic wave</i> of frequency arbitrarily lower than 3 000 GHz, propagated in space without artificial guide.
<u>Radiowave propagation; RF propagation:</u>	<i>Propagation</i> of <i>radiowaves</i> .
<u>Skip distance:</u>	The minimum distance from a transmission point and in a given direction at which a <i>radiowave</i> of given frequency can be received following ionospheric reflection.
<u>Transmission factor; Distance factor; M factor:</u>	In the case of a hop comprising only one ionospheric reflection at a given ionospheric layer and for a given distance, the ratio of the basic MUF to the critical frequency at the reflection point.

9.5 Fading and loss

<u>Above-the-MUF loss:</u>	That part of the attenuation of an <i>electromagnetic wave</i> due to losses at frequencies above the <i>basic MUF</i> .
<u>Absorption:</u>	The conversion of the energy of an <i>electromagnetic wave</i> into heat or another form of energy by interaction with the propagation medium.
<u>Absorption loss:</u>	That part of the attenuation of an <i>electromagnetic wave</i> due only to <i>absorption</i> .
<u>Basic free-space transmission loss; L_{bf}; A_0:</u>	The <i>transmission loss</i> that would occur if the antennas were replaced by isotropic antennas located in a perfectly dielectric, homogeneous, isotropic and unlimited environment, the distance between the antennas being retained.
<u>E-layer screening:</u>	Screening of the F2-layer reflected <i>radiowave</i> by the E layer, so that the radiowave is reflected back to the F2 layer, instead of reaching the Earth's surface.

<u>Fading:</u>	The temporary and significant decrease of the magnitude of the electromagnetic field or of the power of the <i>signal</i> due to time variations of the <i>propagation conditions</i> .
<u>Fade out; Blackout:</u>	Deep <i>fading</i> of long duration, often due to polar cap absorption (PCA).
<u>Fading rate; Fading frequency:</u>	The rate at which <i>fading</i> occurs, characterized for instance by a mean frequency or a mean period determined under specified <i>propagation conditions</i> .
<u>Frequency dispersion; Dispersion:</u>	The relatively significant variation with frequency, in a given <i>frequency band</i> , of certain properties of an <i>electromagnetic wave</i> , such as the phase velocity.
<u>Frequency selective fading; Selective fading:</u>	<i>Fading</i> which affects unequally the different spectral components of a modulated radiowave.
<u>Interference fading:</u>	<i>Fading</i> due to the interference of radiowaves with varying relative phases.
<u>Propagation conditions; Conditions:</u>	The environment along the propagation path in which a <i>radiocommunication service</i> is operated.
<u>Rapidity of fading:</u>	The slope of the curve of signal level versus time in the presence of <i>fading</i> , generally expressed in decibels per second.
<u>Spread:</u>	Refers to varying time delays for waves arriving by different <i>modes</i> or paths.
<u>Spread F:</u>	<i>Spread</i> of reflections from the F region, caused by irregularities of the <i>electron density</i> , and observable as a diffuse trace on certain ionograms.
<u>Transmission loss (of a radio link); <i>L</i>; <i>A</i>:</u>	The ratio, usually expressed in decibels, for a <i>radio link</i> , between the power radiated by the transmitting antenna and the power that would be available at the receiving antenna output if there were no loss in the radio frequency circuits.

9.6 Reliability and compatibility

<u>Basic . . . reliability:</u>	Signifies the reliability of communications in the presence of background <i>noise</i> alone.
<u>Overall . . . reliability:</u>	Signifies the reliability of communications in the presence of background noise and of known interference.
<u>Reliability:</u>	Probability that a specified performance is achieved.
<i>Terms relevant to the operation and design of HF radio systems</i>	
<i>Service to one receiver</i>	
<u>Circuit reliability:</u>	Probability for a <i>circuit</i> that a specified performance is achieved at a single frequency.

Communications reliability: Probability for a pair of terminals that a specified performance is achieved by taking into account all the paths between them and all frequencies associated with the desired signals.

Circuit compatibility; CC: The percentage of time during which a specified criterion of service quality is achieved at the receiver location in the presence of interference relative to the value that would be obtained if only noise were present.

Path reliability: Probability for a pair of terminals that a specified performance is achieved over a single path between the terminals consisting of one or more contiguous circuits, by taking into account all transmitted frequencies.

Reception reliability: Probability for a *circuit* that a specified performance is achieved by taking into account all transmitted frequencies associated with the desired signal.

Service to an area

Area of service; Service area;
Target area: Area associated with a transmitting station for a given *radiocommunication service*, within which reception or the operation of *radio links* is protected against *interference* by agreements in accordance with international regulations.

Area reliability: The percentage of test points in a *service area* for which the basic reception reliability is greater than a specified required value.

Area service compatibility;
ASC: The percentage of the *target area* which can be served during a specified percentage of time in the presence of interference, relative to the value that would be obtained if only the environmental noise were present.

Service reliability: Probability for a *service area* that a specified performance is achieved by taking into account all transmitted frequencies.

Time service compatibility;
TSC: The percentage of time during which a specified percentage of the *target area* can be served in the presence of interference, relative to the value that would be obtained if only the environmental noise were present.

Terms relevant to prediction techniques

Mode availability: Probability for a single *circuit* that a single *mode* at a single frequency can propagate by ionospheric refraction alone.

Mode performance achievement: Probability for a single *circuit* that a specified performance is achieved by single *mode* at a single frequency given that the mode can propagate by ionospheric refraction alone.

Mode reliability: Probability for a *circuit* that a specified performance is achieved by a single *mode* at a single frequency.



* 1 1 1 0 6 *

Printed in Switzerland
Geneva, 1998
ISBN 92-61-06671-2